Carbon Cycling at a Site of Present-Day Serpentinization:-

The Tablelands, Gros Morne National Park

by

© Natalie Szponar, B.Sc. (Hons)

A Thesis submitted to the

School of Graduate Studies

in partial fulfillment of the requirements for the degree of

Master of Science

Department of Earth Sciences

Memorial University of Newfoundland

September 2012

St. John's Newfoundland

ABSTRACT

This study addresses the origin of methane on Mars. A possible source of methane on Mars has been attributed to serpentinization. Active serpentinization is occurring in the subsurface at The Tablelands Ophiolite, in Gros Morne National Park, Newfoundland. Active serpentinization is evidenced by the highly reducing (Eh~ -700mV), ultra-basic (pH 10-12) groundwater springs containing dissolved methane and other lower molecular weight hydrocarbon gases, and the presence of travertine deposits.

The source of methane in the springs was determined to be non-microbial and attributed to either thermogenic or possible abiogenic synthesis. Despite this finding, the ultra-basic springs are an extreme environment for an extant microbial community. Phospholipid fatty acid (PLFA) analysis determined an abundance of gram-negative bacteria as well as the presence algae and fungal biomarkers; and carbon isotopic analysis of PLFA suggests both heterotrophic and autotrophic metabolisms.

ACKNOWLEDGEMENTS

First and foremost, I would like to thank my supervisor Penny Morrill for introducing me to our own Mars site in Newfoundland- the Tablelands. The discussions, enthusiasm, many ideas, and advice that you have provided me during these past few years have been invaluable. Your passion for science is contagious, and I am so glad that I was able to be part of "the building blocks" for your lab. You have been both a mentor and a companion, and for that I am deeply grateful.

I wish to also express my sincere gratitude to my current and past committee members, Richard Rivkin, and Mark Wilson for their feedback and guidance during the course of my thesis. To Richard Rivkin, in seminars and in discussions about my project you have challenged me to think on a deeper scale as a researcher in both critically analyzing problems and developing hypotheses, for which I believe has made me a better scientist.

To Mark Wilson, your passion for teaching has rubbed off on me. Your endless willingness to share your knowledge, discuss different ideas, and explore the terrains of the Tablelands in search for more springs is something that I admire and truly appreciate. Furthermore, I am glad to have had my own personal geology tour guide, with a similar sweet tooth for pie- on the many memorable trips to Gros Morne

I would like to thank my external reviewers Dr. Chris Romanek and Dr. Paul Sylvester for their valuable comments and recommendations for this thesis. I also gratefully acknowledge the financial support from the Natural Sciences and Engineering

Research Council of Canada, The Canadian Space Agency, and Memorial University of Newfoundland.

I would also like to thank laboratory managers Alison Pye, and Geert Van Biesen for all of all of your patience and teaching me everything there is to know about the many laboratory instruments. Post doctoral fellows Chad Lane, and Billy Brazelton for your willingness to share your knowledge, be of assistance without hesitation, and constant positive attitude has really helped me through these past years and is greatly appreciated.

I extend my gratitude to the Ziegler/Morrill lab group past and present and wish you all every success. Especially to Nicole, Amanda, Doreen, Heidi, Chris, and Dr Ziegler, - thank you for welcoming me into the lab and providing valuable help through discussions, fieldwork, and your overall support.

A special thanks goes to my family for supporting me through this journey, for always encouraging me to pursue my interests. Finally I would like to thank my best friend Matt, for joining me on this journey. You have helped me by providing encouragement and companionship both in and out of school. I will forever remember the many adventures we have had making my time in Newfoundland that much more enjoyable.

Table of Contents

ABSTRACT ii

ACKNOWLEDGEMENTS iii

List of Tables vii

List of Figures viii

List of Symbols, Nomenclature or Abbreviations x

List of Appendices xi

Chapter 1 : Introduction and Overview 12
1.1 Context and Objectives 12
1.2 Background 16
1.2.1 Sites of Serpentinization and The Tablelands, Gros Morne National Park 16
1.2.2 Mechanisms of Organic Synthesis (Biogenic and Abiogenic) 18
1.2.3 Distinguishing between Abiogenic and Biogenic Sources 19
1.2.4 Possible Microbial Carbon Cycling Pathways. at Sites of Serpentinization 20
1.3 Contributions to Field of Science 22
1.4 Co-authorship Statement 23
1.5 References 24

Chapter 2 : Geochemistry of a Continental Site of Serpentinization in the Tablelands Ophiolite, Gros Morne National Park: a Mars Analogue 31
2.1 Abstract 31
2.2 Introduction 32
2.3 Material and Methods 37
2.3.1 Site Description 37
2.3.2 Aqueous geochemistry sampling and analysis 38
2.3.3 Carbonate mineralogy and isotope analysis 40
2.3.4 Dissolved gas sampling 41
2.3.5 Analysis of dissolved gases 41
2.4 Results and Discussion 43
2.4.1 Origin of spring water 43
2.4.2 Mixing of freshwater and ultra-basic fluids at springs 44
2.4.3 Geochemical evidence of present-day serpentinization 46
2.4.4 Carbonate mineralogy and deposition 47
2.4.5 Source of CH_4 and low molecular weight hydrocarbons in spring fluids 51
2.5 Implications and Conclusions 55
2.6 Figures and Tables 58
2.7 References 70

Chapter 3 : Microbial Community Composition and Cycling of Carbon in the Ultra-basic and Reducing Springs at a Site of Serpentinization in the Tablelands- Gros Morne National Park 78
3.1 Abstract 78
3.2 Introduction 79
3.3 Sampling and Analytical Methods 82
3.3.1 Site Description 82

3.3.2 LAL Assay 83
3.3.3 Microscopic Cell Abundance 84
3.3.4 Dissolved organic matter and total inorganic carbon 85
3.3.5 C/N ratios and $\delta^{13}C$ of bulk organic matter 86
3.3.6 Phospholipid Fatty Acid identification and quantification 88
3.3.7 Phospholipid fatty acid stable isotope analysis 89
3.3.8 Data Analysis 90
3.4 Results 91
3.4.1 Life detection in ultra-basic springs 91
3.4.2 Organic matter analysis and carbon isotope composition 92
3.4.3 DOC and TIC analysis 93
3.4.4 Phospholipid fatty acids analysis 94
3.4.5 Isotopic composition of PLFA 95
3.5 Discussion 96
3.5.1 Evidence for life in the ultra-basic reducing springs 96
3.5.2 Microbial community composition 97
3.5.3 Source of bulk organic matter 98
3.5.4 Isotopic analysis of microbial community 99
3.5.5 Possible autotrophic and heterotrophic metabolism 101
3.5.6 Linking phospholipid fatty acid analysis to previous microbial studies 104
3.6 Conclusion 106
3.7 Figures and Tables 109
3.8 References 119
Chapter 4 : Summary 125
4.1 Summary and Future Work 125
4.2 References 131
APPENDIX A: RAW DATA 134
APPENDIX B: STATISTICS 144

List of Tables

Table 2.1 A comparison of average (± std, 1σ) aqueous geochemical parameters of spring waters. 67
Table 2.2 Gaseous composition of spring waters 68
Table 2.3 Isotopic composition of total inorganic carbon, water, and carbonates 69
Table 3.1Cell abundance and endotoxins detected from the Tablelands ultra-basic fluids as evidence for life 109
Table 3.2 Geochemical analyses of possible carbon substrates in ultra-basic springs for microbial metabolism including bulk organic matter (OM), dissolved organic carbon (DOC), and total inorganic carbon (TIC) 110
Table 3.3 Distribution of mol% and $\delta^{13}C$ of PLFA as detected in June, August 2010, and June 2011 111
Table 3.4 PLFA detected in this study and their interpretation for the Tablelands ultra-basic springs 112
Table 3.5 Enrichment factors of microbial., fungal., and algal groups as determined in this study 113

List of Figures

Figure 2.1 Geologic map, modified from (Berger et al., 1992), showing the Tablelands massif and approximate sampling locations (star symbols): Wallace Brook (WB), Tablelands East (TLE), Winterhouse Creek (WHC1, 2a, b, c); and Winterhouse Brook (WHB). The Tablelands is located in Gros Morne National Park in Newfoundland, Eastern Canada. 58
Figure 2.2 Images of springs and travertine deposits at sampling locations: Winterhouse Creek 1 (2.2a, human for scale ~1.70m); Winterhouse Creek 2 (2.2b, human for scale ~1.70m), Tablelands East (2.2c, human for scale ~1.70m); and Wallace Brook (2.2d, spatula for scale ~22cm)..... 59
Figure 2.3 $\delta^{18}O$ and δD of fluids sampled from all sites including rainwater, snowmelt, and pond water collected from the top of the Tablelands. $\delta^{18}O$ and δD of fluids are plotted with the GMWL (solid line) and the linear regression for collected freshwater (i.e. WHB, pond water, rain, snowmelt) as a proxy for the LMWL (dashed line). Error on $\delta^{18}O$ and δD represent ±0.1 ‰ and ±0.6‰ respectively. Note that error bars are smaller than the plotted symbol. 60
Figure 2.4 $\delta^{18}O$ and δD of waters sampled from WHC2b and WHB during different seasons: July and September 2009, and June 2010. Error on $\delta^{18}O$ and δD represent ±0.1 ‰ and ±0.6‰ respectively. Note that error bars are smaller than the plotted symbol..... 61
Figure 2.5 Dissolved ion concentrations of Br^- and Cl^- as conservative tracers to determine mixing of freshwater and ultra basic water. Samples plotted are from WHC1, WHC2a, WHC2b, WHC2c, TLE, WB, and WHB collected in September 2009 and June 2010. The solid line represents conservative mixing between the freshwater (WHB) and ultra basic (WHC01) end member. Note that TLE and WB do not plot on the conservative mixing line. Error bars are ±10% for Br^- and Cl^- and may appear smaller than the plotted symbol. 62
Figure 2.6 Ca^{2+}/Mg^{2+} plotted versus the fraction of ultra basic water mixing with the conservative mixing line. Ca^{2+}/Mg^{2+} ratios increase with greater fraction of ultra basic water. Ca^{2+}/Mg^{2+} of waters from the Tablelands are plotted against Ca^{2+}/Mg^{2+} ratios of spring (Ca^{2+}/Mg^{2+}= 177) and meteoric water (Ca^{2+}/Mg^{2+}= 0.14) from another continental site of present-day serpentinization in Cazadero, California (Barnes et al., 1967). Error bars of Ca^{2+}/Mg^{2+} are ±10% and may appear smaller than the plotted symbol..... 63
Figure 2.7 $\delta^{18}O$ and $\delta^{13}C$ of travertine (filled symbols) and carbonate sediment (open symbols) from serpentinization sites plotted with the equilibrium field for $^{18}O_{CaCO3}$ (17.9 to 21.0‰) determined by (O'Neil, 1969) corrected in (Friedman and O'Neil, 1977) assuming chemical precipitation of calcium carbonate in equilibrium with Tableland source waters. Error bars represent ±0.1 ‰ and ±0.5‰ for ^{18}O and ^{13}C respectively. Note that $\delta^{18}O$ bars are smaller than the plotted symbol. 64
Figure 2.8 Modified Bernard plot of $CH_4/[C_{2+}= C_2+C_3+nC_4]$ versus $\delta^{13}C$ of methane from serpentinization springs. Two distinct fields for microbially and thermogenically

produced methane are plotted. Data points for methane gas collected at the Tablelands fall within the thermogenic field.....65
Figure 2.9 Natural gas plot of $\delta^{13}C$ of hydrocarbon gases sampled at WHC2a, and WHC2b in June 2010, June 201. Error bars represent ±0.5‰ for $\delta^{13}C$. The block arrows represent general abiogenic and thermogenic isotopic trends. The solid line shows the predicted $\delta^{13}C$ values using an abiogenic polymerization model developed by Sherwood Lollar et al. (2008) using the following equations: $\delta^{13}C_{C2} = 1000\ln\alpha + \delta^{13}C_{CH4}$ (eq. 7), $\delta^{13}C_{C3} = 0.33\ \delta^{13}C_{CH4} + 0.66\ \delta^{13}C_{C2}$ (eq. 8), $\delta^{13}C_{nC4} = 0.25\ \delta^{13}C_{CH4} + 0.75\ \delta^{13}C_{C3}$ (eq. 9), and $\delta^{13}C_{nC54} = 0.2\ \delta^{13}C_{CH4} + 0.8\ \delta^{13}C_{C4}$ (eq. 10), where $\alpha = (1000 + \delta^{13}C_{C2})/(1000 + \delta^{13}C_{CH4})$ (eq. 11). The initial input data ($\delta^{13}C_{CH4}$ and $\delta^{13}C_{C2}$) for the abiogenic polymerization model were the average carbon isotope values of methane and ethane measured at the Tablelands. 66
Figure 3.1 Spatial and temporal changes in microbial mol% (bars) and $\delta^{13}C$ (circles) of PLFA in ultra-basic spring **WHC2a**. Error bars associated with PLFA mol % are ± 10% RSD, and error bars associated with $\delta^{13}C$ represents standard deviations on replicate samples. Error bars may be smaller than the plotted point. Please note that not all PLFA have $\delta^{13}C$ values because they were either not detected or below detection limits. Please note the different scales for the y-axis.....114
Figure 3.2 Spatial and temporal changes in microbial mol% (bars) and $\delta^{13}C$ (diamonds) of PLFA in ultra-basic spring **WHC2b** Error bars associated with PLFA mol % are ± 10% RSD, and error bars associated with $\delta^{13}C$ represents standard deviations on replicate samples. Error bars may be smaller than the plotted point. Please note that not all PLFA have $\delta^{13}C$ values because they were either not detected or below detection limits. Please note the different scales for the y-axis.....115
Figure 3.3 Spatial and temporal changes in microbial mol% (bars) and $\delta^{13}C$ (triangles) of PLFA in ultra-basic spring **WHC2c** Error bars associated with PLFA mol % are ± 10% RSD, and error bars associated with $\delta^{13}C$ represents standard deviations on replicate samples. Error bars may be smaller than the plotted point. Please note that not all PLFA have $\delta^{13}C$ values because they were either not detected or below detection limits. Please note the different scales for the y-axis.....116
Figure 3.4 Comparing the mol% of PLFA from the Tablelands ultra-basic springs by group type. Microeukaryotes include polyunsaturated fatty acids and fatty acids with carbon # greater than 20 and can include algae and some diatoms. Gram-positive bacteria include branched fatty acids. Gram-negative bacteria include monounsaturated fatty acids and cyclic fatty acids. Bacteria (non-specific) are saturated single chained fatty acids with carbon # less than 20. See Table 3.4 for list of PLFA signatures and their corresponding group. Note WHC2c from June 2010 represents average mol% for a duplicate sample.....117
Figure 3.5 Plot of fractionation between fatty acids and total inorganic carbon ($\varepsilon_{FA\text{-}TIC}$) versus the fractionation between fatty acids and dissolved organic matter ($\varepsilon_{FA\text{-}DOC}$). Errors on enrichment factors are smaller than the plotted point.....118

List of Symbols, Nomenclature or Abbreviations

‰ - parts per thousand
C:N - Carbon to Nitrogen Ratio
C_3 - type of photosynthesis, which incorporates CO_2 (carbon dioxide) into a 3-Carbon compound
C_4 - type photosynthesis, which incorporates CO_2 into a 4-Carbon compound
DAPI - 4'6-diamidino-2-phenylindole
DOC - dissolved organic carbon
DOM - dissolved organic matter
EA - elemental analyzer
Eh- reduction potential measurementl (also Redox potential)
EU - endotoxin units
FA - Fatty acids
FID- Flame Ionization Detector
f_{UB} - fraction of ultra-basic water
GC- Gas Chromatograph
GC-C-IRMS- gas chromatography-combustion-isotope ratio mass spectrometer
IRMS- Isotope Ratio Mass Spectrometer
LAL- Limulus Amoebocyte Lysate
mol- mole, unit of measurement used to express amounts of a chemical substance
OM - Organic matter
org - Organic matter
PFA:PBS- paraformaldehyde/phosphate buffered saline solution
pH –power of hydrogen, a measure of hydrogen ion concentration
PLFA- Phospholipid Fatty Acids
RLU- relative light units
RSD – relative standard deviation, expressed as per cent (%)
TCD- Thermal Conductivity Detector
TIC - Total Inorganic Carbon
TLE- Tablelands East
TOC - Total Organic Carbon
V-PDB – Vienna – Pee Dee Belemnite, international isotope ratio standard for carbon
V-SMOW – Vienna -Standard Mean Ocean Water, international isotope ratio standard for hydrogen and oxygen
WB- Wallace Brook
WHB- Winter House Brook
WHC- Winter House Creek
XRD- X-Ray Diffraction

List of Appendices

Appendix A

A.1. Hydrogen and oxygen isotopes of fluids from Chapter 2, Figure 2.3 and 2.4..... 135
A.2 Ion data from Chapter 2 and Figures 2.5 and 2.6 and extra Ion data from ICPMS..... 136
A.3. Raw Total Inorganic Carbon (TIC) concentration (mg/L) and stable carbon isotope values (‰) from Chapter 2 and 3 and Figure 3.5..... 137
A.4. Raw Dissolved Organic Carbon (DOC) concentration (mg/L) and stable carbon isotope values (‰) from Chapter 2,3, Figure 3.5..... 138
A.5. $\delta^{13}C$ and $\delta^{18}O$ of carbonates from Chapter 2, Figure 2.7..... 139
A.6. Hydrogen and hydrocarbon gas concentrations from Figure 2.8..... 140
A.7. Stable carbon isotope data of hydrocarbon gases from Figure 2.8, and 2.9..... 141
A.8. Phospholipid mol% from Figures 3.1, 3.2, 3.3 and 3.4..... 142
A.9. Stable carbon isotope values of phospholipid fatty acids from Figure 3.1, 3.2, and 3.3..... 143

Appendix B

B.1. $\delta^{13}C$ of organic matter (OM) statistical tests..... 145
B.2. C:N ratios on organic matter statistical tests..... 146
B.3. Dissolved organic matter concentration statistical tests..... 147
B.4. $\delta^{13}C$ of dissolved organic matter (DOM) statistical tests..... 149
B.5. Total inorganic carbon concentration statistical tests..... 150
B.6. $\delta^{13}C$ of total inorganic carbon (TIC) statistical tests..... 152
B.7. Phospholipid fatty acid (PLFA) mol% statistical tests..... 154
B.8. Phospholipid fatty acid (PLFA) $d^{13}C$ statistical tests..... 155
B.9. Model II regression for determining relationship between fractionation of PLFA to TIC and PLFA to DOM..... 156

Chapter 1: Introduction and Overview

1.1 CONTEXT AND OBJECTIVES

Abiogenic hydrocarbons (produced geologically by the reduction of oxidized forms of carbon) have been hypothesized to be possible precursor compounds from which life originated. Apart from being geologically synthesized, hydrocarbons can also form through microbial processes or by thermally induced decomposition of once living organic matter; both types of hydrocarbons are classified as biogenic (Schoell, 1988). The potential for the production of hydrocarbons not associated with biological processes has far reaching implications to the study of past and present life on Earth, and potentially life on other planets. Despite the intense focus on the discovery of abiogenic hydrocarbons in natural settings, only a handful of sites have reported abiogenic organic synthesis on Earth (Barnes et al., 1978; Neal and Stanger, 1983; Abrajano et al., 1988; Sherwood Lollar et al., 1993; Kelley and Frueh-Green, 1999; Sherwood Lollar et al., 2002; Proskurowski et al., 2008; Etiope et al., 2011b). These sites are considered to be important analogues for organic synthesis on early Earth and potentially other planets, such as Mars (Schulte et al., 2006). Of these studied sites, there has also been an emphasis on the geochemistry rather than the microbiology to determine how hydrocarbons are formed. Furthermore, the extent of abiogenic hydrocarbon production in natural settings has yet to be defined.

Perhaps the strongest evidence for abiogenic organic synthesis in natural settings is associated with the aqueous alteration of the mineral olivine in ultramafic rocks (originating from the Earth's mantle, e.g., peridotite) producing an abundance of

hydrogen gas (H_2), through a reaction referred to as "serpentinization". Serpentinization is highly exothermic and can produce high amounts of heat energy. The reaction of ultramafic rocks (olivine + pyroxene) with water can generally be described by the following half reactions (Reactions 1a, 1b and 1c):

Fayalite + water → magnetite + aqueous silica + hydrogen [1a]

$3Fe_2SiO_4 + 2H_2O \rightarrow 2Fe_3O_4 + 3SiO_2 + 2H_2$

Forsterite + aqueous silica → serpentine [1b]

$3Mg_3Si_2O_4 + SiO_2 + 4H_2O \rightarrow 2Mg_3Si_2O_5(OH)_4$

Forsterite + water → serpentine + bructite [1c]

$2Mg_3Si_2O_4 + 3H_2O \rightarrow Mg_3Si_2O_5(OH)_4 + Mg(OH)_2$

In the first half reaction, the Fe-endmember (fayalite) in olivine reacts with water to produce magnetite, aqueous silica and hydrogen gas. In the second half reaction the Mg-endmember (forsterite) in olivine reacts with aqueous silica to produce serpentine. The third reaction describes forsterite reacting with water only to produce serpentine and bructite. The production of bructite contributes hydroxide ions resulting in high pH fluids (Janecky and Seyfried, 1986). In general., the mineral alteration during serpentinization generates an extreme environment containing high concentrations of H_2 gas, and fluids with high pH.

The production of H_2 is important in that it creates highly reducing conditions (low Eh), which are favourable for synthesizing abiogenic methane (CH_4) (Horita and Berndt, 1999; Foustoukos and Seyfried, 2004; McCollom and Seewald, 2006; Fu et al., 2007; Taran et al., 2007; McCollom et al., 2010).Under reducing conditions, hydrogen can react with dissolved carbon oxides to produce CH_4 (Reactions 2 and 3).

$$CO_2 + 4\ H_2 \rightarrow CH_4 + 2H_2O \quad [2]$$

$$CO + 3\ H_2 \rightarrow CH_4 + H_2O \quad [3]$$

Moreover, it is widely suggested that higher molecular weight hydrocarbons (e.g., ethane, propane, butane) can be further synthesized from methane by the reduction of CO_2 with H_2 in the presence of water and catalyst via a Fischer-Tropsch Type (FTT) reaction (Horita and Berndt, 1999; McCollom and Seewald, 2006; Fu et al., 2007).

The production of H_2 is also important in that it is very energy rich and can serve as an electron donor to carry out metabolic processes by chemolithoautotrophic microorganisms including methanogenesis (i.e., microbial formation of CH_4). Therefore, understanding the microbial processes that may also be occurring at sites of serpentinization can help in the understanding of methane production pathways as well as carbon cycling within these sites and possibly in the deep subsurface where serpentinization occurs.

Although H_2 is very energy rich for microbes, not every microorganism can survive in high pH and reducing conditions in these extreme environments at sites of serpentinization. The microbial life that may exist in the extreme environment created by serpentinization could be supported by the availability of different carbon substrates in the organic and inorganic carbon pools. As a result, different sources of carbon available may support different autotrophic and heterotrophic metabolisms. Identifying which microbes can survive in these extreme environments and how they harness their energy for growth could give some insight into how microbes may also be contributing to cycling of methane, and potentially higher molecular weight hydrocarbons within sites of serpentinization.

Apart from abiogenic and microbial synthesis, hydrocarbons can form by the thermal decomposition of sedimentary organic matter (thermogenic hydrocarbons). Gaseous hydrocarbons produced through the thermal alteration of sedimentary organic matter underlying an ophiolite complex may migrate to the surface through the highly fractured weathered ultramafics.

Determining the source of hydrocarbon production at serpentinization sites can be challenging. Currently both isotope and compositional analysis of gases produced have been used to identify the carbon source and thus subsequent reaction pathways responsible for hydrocarbon synthesis (Kelley et al., 2005; Etiope et al., 2011b). However, in natural settings both biogenic and abiogenic processes may be contributing to hydrocarbon production (Sherwood Lollar et al., 2002; Proskurowski et al., 2008; Etiope et al., 2011a). The second Chapter of this thesis examines the geochemistry of the serpentinization springs found in the Tablelands and uses both isotopic and compositional analysis to determine the source of hydrocarbons within the fluids. The objectives of Chapter Two were to identify and characterize the ultra-basic springs at a site of serpentinization in the Tablelands Ophiolite to place in context with other sites of serpentinization; use composition and stable isotope analysis of the hydrocarbons (i.e., CH_4, ethane, propane, butane, pentane, and hexane) in the ultra-basic springs to determine the mechanisms responsible for their synthesis (microbial., thermogenic, or abiogenic); and assess the application of the Tablelands as an analogue site to determine how to source CH_4 detected in areas of serpentinization on Mars.

Although geochemical analysis can be useful to distinguish between different hydrocarbon production mechanisms (abiogenic, thermogenic, microbial), there is little

information on the microbial communities at these sites. If serpentinization reactions were more prevalent on early Earth, and could have or could potentially be occurring on Mars, understanding how the microbial community thrives in these present-day extreme environments could help in our interpretation of past or present life on Earth and other planets. Chapter 3 of this thesis focuses on identifying the microbial community and their possible metabolic pathways that allow the community to thrive in the highly reducing ultra-basic fluids. The objectives of Chapter Three were to identify the microbial community that is thriving in the ultra-basic fluids and community structure using life detection instrumentation and compositional analysis of the biomass and phospholipid fatty acids; and to identify the possible carbon source (s) and metabolic pathways used by the microbial community to gain a better understanding of how these microorganisms can survive in the extreme ultra-basic springs.

1.2 BACKGROUND

1.2.1 Sites of Serpentinization and The Tablelands, Gros Morne National Park

Sites of serpentinization were more prevalent on Achaean Earth during the evolution of chemolithotrophic bacteria, as a result of increased geothermal heat flow; abundance of ultramafic rocks, and high tectonic activity exposing ultramafic rocks to a highly reduced atmosphere (Sleep and Zahnle, 2001; Sleep et al., 2004). Today, ultramafic rocks undergoing serpentinization can be found in peridotite-hosted deep-sea hydrothermal vents (Charlou et al., 2002; Kelley et al., 2005), and in terrestrial sites where the oceanic crust has been tectonically emplaced on the continent as an ophiolite

(Barnes et al., 1967; Neal and Stanger, 1983; Abrajano et al., 1988; Fritz et al., 1992; Hosgormez, 2006).

Deep-sea hydrothermal vents where serpentinization may be occurring are difficult to study due to their location. Alternatively, continental ophiolites provide a more accessible opportunity to study *in-situ* active serpentinization and potentially abiogenic hydrocarbon production. In addition, these sites may provide rare ecosystems that support chemolithoautotrophic life in freshwater. The Tablelands at Gros Morne National Park in Newfoundland is one such site, which is undergoing active serpentinization in the subsurface, as evidenced by serpentinized ultra-mafic rocks and ultra-basic springs at the surface.

The rocks of the Tablelands are predominantly peridotites and are components of the ancient sea floor. Approximately 500 million years ago the ancient Iapetus Ocean began to close due to tectonic activity. During this process, rocks from the mantle (i.e., peridotites) were emplaced on the continental crust currently known as Western Newfoundland. Following the Wisconsinan glaciation (~25,000 to 10000 years ago), fresh unaltered rocks in the Tablelands were exposed to groundwater, which provided the starting materials for serpentinization (Jenness, 1960; Stevens, 1988).

Today, active sites of serpentinization in the Tablelands are evidenced by ultra-basic reducing groundwater discharging along the banks of the creeks. Groundwater passing through these rocks has formed springs, which are highly reducing (Eh up to -700 mV) and highly alkaline (pH 10-12). Travertine deposits, which are formed by the precipitation of carbonate minerals from solution at high pH conditions (pH>10) can be found in areas surrounding the ultra-basic reducing groundwater discharge locations.

Carbonate deposits have also been found in other continental locations where active serpentinization is occurring (Barnes and O'Neil, 1971; O'Neil and Barnes, 1971; Clark et al., 1992), and on Mars where serpentinization is thought to have occurred (Ehlmann et al., 2010)

1.2.2 Mechanisms of Organic Synthesis (Biogenic and Abiogenic)

The source of hydrocarbon gases in the geological environment can be classified into three subcategories: "microbial", "thermogenic", and "abiogenic" (Schoell, 1988). Microbial hydrocarbons are formed through biological activity as the result of metabolic and biosynthetic processes (e.g., methanogenesis, ethanogenesis, and propanogenesis). Thermogenic hydrocarbons are formed by thermally induced decomposition of once living organic matter (i.e., hydrothermal alteration of organic-rich sediments, ''cracking'' of kerogen; (Hunt, 1996). It is important to note that the production of both microbial and thermogenic hydrocarbons requires the presence of active or reworked biological material and thus the ultimate source of carbon is considered "biogenic" (Schoell, 1988). Alternatively, abiogenic hydrocarbons are formed independent of biological activity (e.g., Fisher- Tropsch-Type reaction).

The primary difficulty in studying abiogenic hydrocarbon synthesis in geological settings is that hydrocarbons in nature can be produced by more than one mechanism and are typically dominated by thermogenic and microbial products in near-surface environments (Whiticar, 1999). Furthermore, the geochemical signatures of abiogenic gaseous hydrocarbons are still being developed, and therefore it is difficult to distinguish them from microbial and thermogenic hydrocarbon sources (Proskurowski et al., 2008).

Therefore, both biogenic and abiogenic sources must be considered until multiple lines of evidence can distinguish an abiogenic source.

1.2.3 Distinguishing between Abiogenic and Biogenic Sources

Currently there is no single measurement or analysis that can independently identify an abiogenic or biogenic source. However, there are multiple lines of evidence, which when combined, can provide a strong argument for the abiogenic origin of hydrocarbons in the environment. One such line of evidence for determining the origin of methane involves the use of carbon ($^{13}C/^{12}C$) isotopes values of the gases being produced in combination with Bernard parameters ($CH_4/\sum C_{C2+}$) (Whiticar, 1999). Isotope data are reported in the standard δ-notation (e.g., $\delta^{13}C$, δD) and expressed in permil, ‰ units (Equation 1):

$$\delta = [(R_{sample} - R_{standard})/(R_{standard})] \times 1000\ (‰) \qquad \text{Eq. 1}$$

where R is the ratio of $^{13}C/^{12}C$ or D/H relative to the PDB and SMOW standards respectively. Different isotopic fractionation factors (α) are associated with different mechanisms of methane production. Isotopic fractionation factors can be determined using Equation 2:

$$\alpha_{X\text{-}Y} = (1000 + \delta_X)/(1000 + \delta_Y) \qquad \text{Eq. 2.}$$

Where x and y represent the product and reactant respectively. Fractionation factors can be used to determine isotopic enrichment factors (ε) using Equation 3:

$$\varepsilon = 1000(\alpha - 1) \qquad \text{Eq. 3}$$

Large isotopic fractionations between CO_2 and CH_4 ($\varepsilon_{CO2\text{-}CH4} > 20‰$) are typically observed for microbial autotrophic methane, where as smaller fractionations ($\varepsilon_{CO2\text{-}}$

$_{CH4}$<20‰) are observed for thermogenic methane (Whiticar, 1999). Likewise, Bernard parameters have been used to differentiate microbial ($CH_4/\sum C_{C2+}$ >1000) from thermogenic hydrocarbons ($CH_4/\sum C_{C2+}$ = 0 to 50) (Hunt, 1996). Distinguishing abiogenic from thermogenic methane is more difficult, as the abiogenic field has not yet been defined on a Bernard plot. Attempts to resolve this issue include using hydrogen isotopes in combination with stable carbon isotopes showing distinct isotopic patterns of low molecular weight hydrocarbons (Sherwood Lollar et al., 2002; Sherwood Lollar et al., 2006; Sherwood Lollar et al., 2008). In Chapter 2, isotopic analysis of methane and other hydrocarbon gases in combination with Bernard parameters were used to distinguish between microbial and non-microbial (i.e., thermogenic and/or abiogenic) methane.

1.2.4 Possible Microbial Carbon Cycling Pathways. at Sites of Serpentinization

Serpentinization produces H_2 gas that provides the reducing conditions favourable for chemolithotrophic life. Active sites of serpentinization can be found all over the world and in different locations on Earth;, however, the microbial communities that exist in these locations are poorly understood (Schrenk et al., 2004; Biddle et al., 2006; Brazelton et al., 2006). Furthermore, the highly reducing, ultra-basic fluids at sites of serpentinization provide both unique and extreme conditions for the thriving microbial community that exists.

Both phylogenic and metagenomic studies have been done at two sites of serpentinization, the Lost City Hydrothermal Vent Field (LCHF) situated at the Mid-Atlantic Ridge, and recently at the Tablelands Ophiolite in order to investigate the microbial diversity and the possible microbial metabolisms that exists in these serpentine-

hosted environments (Schrenk et al., 2004; Kelley et al., 2005; Brazelton and Baross, 2008; Brazelton et al., 2012). At LCHF, the production of methane and low-molecular weight hydrocarbons was determined to be abiogenic (Proskurowski et al., 2008). However it is not understood if these abiogenic organic compounds support microbial communities that exist at LCHF. Furthermore, at both LCHF and the Tablelands, metagenomic evidence yields the potential for both H_2 oxidizing and producing microbes(Brazelton et al., 2012). Although metagenomic and phylogenic evidence provides a great deal of information about the species, additional use of biochemical markers such as lipids has shown to provide complimentary quantitative information about the microbial community structure and its interaction with the environment without the need of culturing and isolation (White et al., 1996).

Phospholipid fatty acids (PLFA) are integral components of the cell membrane, which can be used to indicate the microbial community present. Additionally, PLFA can be analyzed for their natural abundance ^{13}C signatures directly related to the ^{13}C signature of the source of carbon used by bacteria in metabolic processes (Boschker et al., 1998). In Chapter 3, PLFA extracted from the serpentinization springs in the Tablelands Ophiolite were analyzed to determine changes in the community structure and to identify biomarkers to identify microbial groups that exist in the springs. Additionally, isotopic analysis of the biomass and individual lipids was used to identify possible metabolic pathways, in comparison to past microbial studies at the Tablelands.

1.3 CONTRIBUTIONS TO FIELD OF SCIENCE

Sites of present-day serpentinization, such as the Tablelands in Gros Morne are considered important analogs for early ecosystems both on Earths and other planets such as Mars. On Earth, and potentially other planets, the production and availability of H_2 is the fundamental starting point leading to the synthesis of organic compounds. Methane and higher molecular weight hydrocarbons can be produced when H_2 reacts with dissolved forms of oxidized carbon (i.e., CO_2 and CO; (McCollom and Seewald, 2006) and/or likewise be used as a source of energy by chemolithoautotrophic organisms to carry out metabolic functions.

Before the evolution of photosynthesis, organisms relied on chemical forms of metabolic energy (chemosynthesis). Thus, investigating modern earth environments such as active sites of serpentinization that may support chemolithothoautotrophs can help increase our understanding of life on early Earth.

Since the detection of methane in the Martian atmosphere and polar ice caps, there has been an increasing interest in understanding the mechanisms for methane production on Mars. Likewise, the crust and upper mantle of Mars are composed of ultramafic rocks similar to those of the ocean crust on Earth (Boston et al., 1992; Formisano et al., 2004; Ehlmann et al., 2008; Ehlmann et al., 2010) Thus, it is possible that geological processes produced methane on Mars now or many years ago.

The production of hydrocarbons via abiogenic and biogenic mechanisms have far reaching implications to fields of Earth and Planetary Sciences and the study of early life and life in extreme environments. An overall assessment of carbon cycling (abiogenic, thermogenic, and biogenic) at the Tablelands is required in order to distinguish methane

of abiogenic origin in addition to further understanding natural processes through which it is produced. Likewise, an assessment of the microbial community and its importance in carbon cycling within these sites can be useful to better understand the processes, which are responsible for past and present life on Earth, life in the deep subsurface and potentially life on other planetary bodies.

1.4 CO-AUTHORSHIP STATEMENT

Dr Penny Morrill described the initial concept of this project in a grant proposal prior to the start of this thesis. During the first semester, the first author (thesis author) completed a literature review and research proposal. During the progression of the thesis, modifications to the original proposal were based on collaborative discussions between Penny Morrill and the thesis author.

This thesis is a compilation of a submitted manuscript (Chapter 2) and a paper that will be prepared for submission to a research journal (Chapter 3). The first paper was submitted to the Journal ICARUS and thus follows the ICARUS manuscript submission guidelines:

Szponar, N., Brazelton, W. J., Schrenk, M. O., Bower, D. M., Steele, A. B., Morrill, P. L., 2012. Geochemistry of present-day serpentinization at the Tablelands, Gros Morne National Park: a Mars Anologue Site. Icarus. Article in Press.

Although the submitted manuscript is co-authored, the thesis author conducted all of the research surrounding the objective of this investigation, literature review, selection of samples, sample collection, sample analysis and manuscript writing. For Chapter 3 William. J. Brazelton and Mathew.O. Schrenk provided cell counts on fluid and carbonate

sediment samples, and Dina. M. Bower, and Andrew. B. Steele provided LAL assay measurements. All samples were collected in the field during the same sampling time.

Dr. Penny Morrill provided valuable guidance on the direction of the research, discussion of the results at various stages of research and editorial comments during the writing of the manuscript and thesis.

1.5 REFERENCES

Abrajano, T. A., N. C. Sturchio, J. K. Bohlke, G. L. Lyon, R. J. Poreda, and C. M. Stevens, 1988, Methane-hydrogen gas seeps, Zambales Ophiolite, Philippines: deep or shallow origin?: Chemical Geology, v. 71, p. 211-222.

Barnes, I., V. C. LaMarche, and H. G., 1967, Geochemical evidence of present-day serpentinization: Science, v. 156, p. 830-832.

Barnes, I., and J. R. O'Neil, 1971, Calcium-magnesium carbonate solid solutions from Holocene conglomerate cements and travertines in the Coast Range of California: Geochimica et Cosmochimica Acta, v. 35, p. 699-718.

Barnes, I., J. R. Oneil, and J. J. Trescases, 1978, Present Day Serpentinization in New-Caledonia, Oman and Yugoslavia: Geochimica Et Cosmochimica Acta, v. 42, p. 144-145.

Biddle, J. F., J. S. Lipp, M. A. Lever, K. G. Lloyd, K. B. Sorensen, R. Anderson, H. F. Fredricks, M. Elvert, T. J. Kelly, D. P. Schrag, M. L. Sogin, J. E. Brenchley, A. Teske, C. H. House, and K. U. Hinrichs, 2006, Heterotrophic Archaea dominate sedimentary subsurface ecosystems off Peru: Proceedings of the National Academy of Sciences of the United States of America, v. 103, p. 3846-3851.

Boschker, H. T. S., S. C. Nold, P. Wellsbury, D. Bos, W. de Graaf, R. Pel, R. J. Parkes, and T. E. Cappenberg, 1998, Direct linking of microbial population to specific biogeochemical processes by 13 C-labelling of biomarkers: Nature, v. 392, p. 801-805.

Boston, P. M., M. V. Ivanov, and C. P. McKay, 1992, On the possibility of chemosynthetic ecosystems in subsurface habitats on Mars: Icarus, v. 95, p. 300-308.

Brazelton, W. J., and J. A. Baross, 2008, Biological methane cycling at the lost city hydrothermal field Astrobiology Science Conference.

Brazelton, W. J., B. Nelson, and M. O. Schrenk, 2012, Metagenomic evidence for H2 oxidation and H2 production by serpentinite-hosted subsurface microbial communities: Frontiers in Extreme Microbiology: Deep Subsurface Microbiology Special Issue v. 2.

Brazelton, W. J., M. O. Schrenk, D. S. Kelley, and J. A. Baross, 2006, Methane- and sulfur metabolizing microbial communities dominate the Lost City hydrothermal field ecosystem: Applied and Environmental Microbiology, v. 72, p. 6257-6270.

Charlou, J. L., J. P. Donval., Y. Fouquet, P. Jean-Baptiste, and N. Holm, 2002, Geochemistry of high H2 and CH4 vent fluids issuing from ultramafic rocks at the Rainbow hydrothermal field (36j14VN, MAR): Chemical Geology, v. 191, p. 345– 359.

Clark, I. D., J. C. Fontes, and P. Fritz, 1992, Stable Isotope Disequilibria in Travertine from High Ph Waters - Laboratory Investigations and Field Observations from Oman: Geochimica Et Cosmochimica Acta, v. 56, p. 2041-2050.

Ehlmann, B. L., J. F. Mustard, and S. L. Murchie, 2010, Geologic setting of serpentine deposits on Mars Geophysical Research Letters, v. 37, p. L06201, doi:10.1029/2010GL042596.

Ehlmann, B. L., J. F. Mustard, S. L. Murchie, F. Poulet, J. L. Bishop, A. J. Brown, W. M. Calvin, R. N. Clark, D. J. Des Marais, R. E. Milliken, L. H. Roach, T. L. Roush, G. A. Swayze, and J. J. Wray, 2008, Orbital identification of carbonate-bearing rocks on Mars: Science, v. 322 p. 1828-1832.

Etiope, G., D. Z. Oehler, and C. C. Allen, 2011a, Methane emissions from Earth's degassing: Implications for Mars: Planetary and Space Science, v. 59, p. 182-195.

Etiope, G., M. Schoell, and H. Hosgörmezd, 2011b, Abiotic methane flux from the Chimaera seep and Tekirova ophiolites (Turkey): Understanding gas exhalation from low temperature serpentinization and implications for Mars: Earth and Planetary Science Letters, v. 310, p. 96-104.

Formisano, V., S. Atreya, T. Encrenaz, N. Ignatiev, and M. Giuranna, 2004, Detection of methane in the atmosphere of Mars: Science, v. 306, p. 1758 - 1761.

Foustoukos, D. I., and W. E. J. Seyfried, 2004, Hydrocarbons in hydrothermal vent fluids: the role of chrome-bearing catalysts: Science, v. 304, p. 1002-1005.

Fritz, P., I. D. Clark, J.-C. Fontes, M. J. Whiticar, and E. Faber, 1992, Deuterium and ^{13}C evidence for low temperature production of hydrogen and methane in a highly alkaline groundwater environment in Oman: Water-rock Interaction, p. 793-796.

Fu, Q., B. Sherwood Lollar, J. Horita, G. Lacrampe-Couloume, and J. Seyfried, W.E., 2007, Abiotic formation of hydrocarbons under hydrothermal conditions:

Constraints from chemical and isotope data: Geochimica et Cosmochimica Acta, v. 71, p. 1982-1998.

Horita, J., and M. E. Berndt, 1999, Abiogenic methane formation and isotopic fractionation under hydrothermal conditions: Science, v. 285, p. 1055-1057.

Hosgormez, H., 2006, Origin of the natural gas seep of Cirali (Chimera), Turkey: Site of the first Olympic fire: Journal of Asian Earth Sciences, v. 30, p. 131-141.

Hunt, J. M., 1996, Petroleum Geochemistry and Geology: New York, W.H. Freeman and Company, 743 p.

Janecky, D. R., and W. E. J. Seyfried, 1986, Hydrothermal serpentinization of periodotite within the oceanic crust: Experimental investigations of mineralogy and major element chemistry.: Geochimica et Cosmochimica Acta, v. 50, p. 1357-1378.

Jenness, S. E., 1960, LATE PLEISTOCENE GLACIATION OF EASTERN NEWFOUNDLAND: Geological Society of America Bulletin, v. 71, p. 161-180.

Kelley, D. S., and G. Frueh-Green, 1999, Abiogenic methane in deep-seated mid-ocean ridge environments: Insights from stable isotope analyses: Journal of Geophysical Research, v. 104, p. 10439-10460.

Kelley, D. S., J. A. Karson, G. L. Fruh-Green, D. R. Yoerger, T. M. Shank, D. A. Butterfield, J. M. Hayes, M. O. Schrenk, E. J. Olson, G. Proskurowski, M. Jakuba, A. Bradley, B. Larson, K. Ludwig, D. Glickson, K. Buckman, A. S. Bradley, W. J. Brazelton, K. Roe, M. J. Elend, A. Delacour, S. M. Bernasconi, M. D. Lilley, J. A. Baross, R. T. Summons, and S. P. Sylva, 2005, A serpentinite-hosted ecosystem: The lost city hydrothermal field: Science, v. 307, p. 1428-1434.

McCollom, T. M., B. S. Lollar, G. Lacrampe-Couloume, and J. S. Seewald, 2010, The influence of carbon source on abiotic organic synthesis and carbon isotope fractionation under hydrothermal conditions: Geochimica et Cosmochimica Acta, v. 74, p. 2717-2740.

McCollom, T. M., and J. S. Seewald, 2006, Carbon isotope composition of organic compounds produced by abiotic synthesis under hydrothermal conditions: Earth and Planetary Science Letters, v. 243, p. 74-84.

Neal., C., and G. Stanger, 1983, Hydrogen generation from mantle source rocks in Oman: Earth and Planetary Science Letters, v. 66, p. 315-321.

O'Neil, J. R., and I. Barnes, 1971, Cl3 and 018 compositions in some fresh-water carbonates associated with ultramafic rocks and serpentinites: western United States: Geochimica et Cosmochimica Acta, v. 35, p. 687-697.

Proskurowski, G., M. D. Lilley, J. S. Seewald, G. L. Früh-Green, E. J. Olson, L. J.E., S. P. Sylva, and D. S. Kelley, 2008, Abiogenic hydrocarbon production at Lost City Hydrothermal Field: Science, v. 319, p. 604-607.

Schoell, M., 1988, Multiple origins of methane in the earth: Chemical Geology, v. 71, p. 1-10.

Schrenk, M. O., D. S. Kelley, S. A. Bolton, and J. A. Baross, 2004, Low archaeal diversity linked to subseafloor geochemical processes at the Lost City Hydrothermal Field, Mid-Atlantic Ridge: Environmental Microbiology, v. 6, p. 1086-1095.

Schulte, M., D. Blake, T. Hoehler, and T. McMcCollom, 2006, Serpentinization and its implications for life on the early Earth and Mars: Astrobiology, v. 6, p. 364-376.

Sherwood Lollar, B., S. K. Frape, S. M. Weise, P. Fritz, S. A. Macko, and J. A. Welhan, 1993, Abiogenic methanogenesis in crystalline rocks: Geochimica et Cosmochimica Acta, v. 57, p. 5087-5097.

Sherwood Lollar, B., G. Lacrampe-Couloume, G. F. Slater, J. A. Ward, D. P. Moser, T. M. Gihring, L.-H. Lin, and T. C. Onstott, 2006, Unravelling abiogenic and biogenic sources of methane in the Earth's deep subsurface: Chemical Geology, v. 226, p. 328-339.

Sherwood Lollar, B., G. Lacrampe-Couloume, K. Voglesonger, T. C. Onstott, L. M. Pratt, and G. F. Slater, 2008, Isotopic signatures of CH4 and higher hydrocarbon gases from Precambrian Shield sites: A model for abiogenic polymerization of hydrocarbons: Geochimica et Cosmochimica Acta, v. 72, p. 4778-4795.

Sherwood Lollar, B., T. D. Westgate, J. A. Ward, G. F. Slater, and G. Lacrampe-Couloume, 2002, Abiogenic formation of gaseous alkanes in the Earth's crust as a minor source of global hydrocarbon reservoirs: Nature, v. 416, p. 522-524.

Sleep, N. H., A. Meibom, T. Fridriksson, R. G. Coleman, and D. K. Bird, 2004, H2-rich fluids from serpentinization: Geochemical and biotic implications: Proceedings of the National Academy of Sciences, v. 101, p. 12818 -12823.

Sleep, N. H., and K. Zahnle, 2001, Carbon dioxide cycling and implications for climate on ancient Earth: Journal of Geophysical Research-Planets, v. 106, p. 1373-1399.

Stevens, R. K., 1988, Ophiolite Oddities:preliminary notices if nephrite jade, Sr-aragonite, troilite, and hyperalkaline springs from Newfoundland, GAC MAC Joint Annual Meeting, St. John's, Newfoundland.

Taran, Y. A., G. A. Kliger, and V. S. Sevastianov, 2007, Carbon isotope effects in the open-system Fischer–Tropsch synthesis: Geochimica et Cosmochimica Acta, v. 71, p. 4474-4487.

White, D. C., J. O. Stair, and D. B. Ringelberg, 1996, Quantitative comparisons of in situ microbial biodiversity by signature biomarker analysis: Journal of Industrial Microbiology, v. 17, p. 185-196.

Whiticar, M. J., 1999, Carbon and hydrogen isotope systematics of bacterial formation and oxidation of methane: Chemical Geology, v. 161, p. 291-314.

Chapter 2: Geochemistry of a Continental Site of Serpentinization in the Tablelands Ophiolite, Gros Morne National Park: a Mars Analogue

2.1 ABSTRACT

The presence of aqueous altered olivine-rich rocks along with carbonate on Mars suggest that serpentinization may have occurred in the past and may be occurring presently, and possibly contributing methane (CH_4) to the Martian atmosphere. Serpentinization, the hydration of olivine in ultramafic rocks, yields ultra-basic fluids (pH ≥ 10) with unique chemistry (i.e., Ca^{2+}-OH^- waters) and hydrogen gas, which can support the abiogenic production of hydrocarbons (i.e., Fisher-Tropsch Type synthesis) and subsurface chemosynthetic metabolisms. Mars analogue sites of present-day serpentinization can be used to determine what geochemical measurements are required for determining the source of methane at sites of serpentinization on Earth and possibly on Mars. The Tablelands Ophiolite is a continental site of present-day serpentinization and a Mars analogue due to the presence of altered olivine-rich ultramafic rocks with both carbonate and serpentine signatures. This study describes the geochemical indicators of present-day serpentinization as evidenced by meteoric ultra-basic reducing groundwater discharging from ultramafic rocks, and travertine and calcium carbonate sediment, which form at the discharge points of the springs. Dissolved hydrogen concentrations (0.06 to 1.20mg/L) and methane (0.04 to 0.30mg/L) with $\delta^{13}C_{CH4}$ values (-28.5 to -15.6‰) were measured in the spring fluids. Molecular and isotopic analyses of CH_4, ethane, propane, butane, pentane and hexane suggest a non-microbial source of methane, and attribute the

origin of methane and higher hydrocarbon gases to either thermogenic or abiogenic pathways.

2.2 INTRODUCTION

The detection of methane (CH_4) and its short lifetime in the Martian atmosphere (Formisano et al., 2004; Krasnopolsky et al., 2004; Mumma et al., 2009), has led to much discussion regarding the source of methane on Mars. A possible source of methane has been attributed to serpentinization, a fluid-rock reaction common in ultramafic rocks that has been hypothesized to occur on Mars (Boston et al., 1992; Formisano et al., 2004; Atreya et al., 2007; Oze and Sharma, 2007). This reaction produces hydrogen (H_2) and the reducing conditions necessary for abiogenic hydrocarbon synthesis through the hydration of ultramafic rock, while also producing conditions for the production of methane through chemolithoautotrophic pathways. On Earth, serpentinization has been observed in ultramafic rocks on the sea floor at deep sea hydrothermal vents such as the Lost City hydrothermal field (Kelley et al., 2005), and on continents in ophiolites (Barnes et al., 1978; Abrajano et al., 1990; Blank et al., 2009; Etiope et al., 2011b). Ophiolites are sections of the ocean crust and upper mantle that have been obducted onto continental crust that can yield ground waters with unique chemistry that are ultra-basic (pH> 10), Mg^{2+}-OH, and/or Ca^{2+}-OH rich (Barnes et al., 1967). The Tablelands Ophiolite (also referred to in literature as the Bay of Islands Ophiolite) in Gros Morne National Park, Newfoundland, Canada is a continental site exhibiting present-day serpentinization. Olivine-rich ultramafic rocks, prerequisites for serpentinization, have been found on Mars (Hoefen et al., 2003; Hamilton and Christensen, 2005; Quesnel et al., 2009; Ehlmann et

al., 2010), and also occur at the Tablelands massif, thus making the Tablelands Ophiolite an important terrestrial analogue for Mars.

During serpentinization, ultramafic rocks composed of mostly olivine [$(Mg,Fe)_2SiO_4$] and pyroxene [orthopyroxene (Mg,Fe)-SiO_3 and clinopyroxenes $Ca(Mg,Fe)Si_2O_6$] undergo hydration producing serpentine. The reaction of ultramafic rocks with water is often presented as the following idealized reaction (Equation 1):

$$(Mg,Fe)_2SiO_4 + H_2O \rightarrow (Mg, Fe)_3Si_2O_5(OH)_4 + (Mg,Fe)OH_2 + Fe_3O_4 + H_{2(g)} \quad [1]$$

Olivine Serpentine Bructite Magnetite

where the Fe-endmember (fayalite) in olivine reacts with water to produce magnetite and hydrogen gas, and the Mg-endmember (forsterite) undergoes hydration producing serpentine and bructite. The hydration of olivine (i.e., production of bructite) and clinopyroxenes also releases OH^- and Ca^{2+} ions resulting in highly alkaline fluids, which can emerge from fractures in the ultramafic rocks (Coleman and Keith, 1971). Under basic conditions and in the presence of inorganic carbon, Ca^{2+} and Mg^{2+} form calcium and magnesium carbonate respectively (Equations 2, 3):

$$Ca^{2+} + CO_3^{2-} \rightarrow CaCO_{3\,(s)} \quad [2]$$

calcium carbonate

$$Mg^{2+} + 2\,HCO_3^- \rightarrow MgCO_{3\,(s)} + CO_2 + H_2O \quad [3]$$

magnesium carbonate

The production of hydrogen gas results in conditions capable of reducing dissolved inorganic carbon species and forming abiogenic hydrocarbons (Sleep et al., 2004). In the following generalized reaction for abiogenic hydrocarbon formation (i.e.,

the Fisher Tropsch Type synthesis; (Schulz, 1999), H_2 gas reduces inorganic carbon to form methane and other higher molecular weight hydrocarbon gases (Equation 4):

$$CO_2 + H_2 \rightarrow CH_4 + C_2H_6 + C_3H_8 + C_nH_n+2... + H_2O \quad [4]$$

In addition to abiogenic hydrocarbons, the ultra-basic reducing groundwaters associated with active serpentinization sites are suitable niches for microorganisms that can tolerate high pH environments with anaerobic microbial metabolisms including those of hydrogen-utilizing microbes, such as homoacetogens and methanogens (Kelley et al., 2005; Brazelton et al., 2006; Schulte et al., 2006). Therefore, sites of serpentinization may support the production of either abiogenic hydrocarbons or microbial methane or both. Apart from abiogenic and microbial synthesis, hydrocarbons can form by the thermal decomposition of sedimentary organic matter (thermogenic hydrocarbons). Gaseous hydrocarbons produced through the thermal alteration of sedimentary organic matter underlying an ophiolite complex may migrate to the surface through highly fractured weathered ultramafic rocks.

The Tablelands Ophiolite formed during the closure of the Iapetus Ocean and the collision of Laurentia and Gondwana continents approximately 485 million years ago (Elthon, 1991). Underlying ultramafic rocks of the Earth's mantle were obducted onto the continental margin of Laurentia, deforming and trapping clastic sedimentary rocks and limestones underneath the ophiolite complex through folding and faulting (Elthon, 1991). Thermal alteration of sedimentary organic matter could produce hydrocarbon gases. Therefore, thermogenic hydrocarbons may also be present at the Tablelands.

Ultra-basic reducing springs have been identified in the Tablelands Ophiolite (Stevens, 1988). One of the main objectives of this study is to determine if these springs

contain H_2, CH_4 and other hydrocarbons. Highly reducing conditions in ground waters discharging from the Tablelands may provide conditions amendable for either abiogenic and/ or biogenic production of CH_4 and subsequently other higher molecular weight hydrocarbons.

The process of serpentinization is of particular interest for the exploration of Mars and determining the origin of CH_4. Serpentinization leaves mineralogical evidence of a previous physicochemical environment that would provide conditions for the production of methane and potentially other hydrocarbon gases to the martian atmosphere (Schulte et al., 2006). Near-infrared data from the orbiting imaging spectrometer Mars Reconnaissance Orbiter- Compact Reconnaissance Imaging Spectrometer for Mars (MRO-CRISM) have shown the presence of Mg carbonate and serpentine signatures in several outcrops on Mars, indicating that serpentinization occurred in the past and was active at least >3-7 Gyr ago (i.e., Noachian) (Ehlmann et al., 2008; Ehlmann et al., 2010). Similarities in the martian crust to terrestrial ophiolites, and the lack of significant tectonic activity suggest that serpentinization would occur in localized areas where there is active fluid flow, potentially in the subsurface (Schulte et al., 2006). Orbital reconnaissance data has identified water ice extant in the subsurface, and the possible flows of liquid water (likely saline brines) in the upper martian regolith (Holt et al., 2008; McEwen, 2011). The presence of fluvial channels and water-forming minerals such as carbonates, phyllosilicates, and sulfates within the Martian crust support the potential for the process to be active in the past (Mustard et al., 2008; Boynton, 2009; Quesnel et al., 2009; Niles et al., 2010). However, if subsurface water on Mars is extant and in contact with ultramafic rocks, then serpentinization may still be occurring (Ehlmann et al., 2010).

Two possible source regions; Nili Fossae and North Eastern Syrtis, have been found where both reactants (olivine) and products (serpentine, carbonates) of serpentinization are present (Ehlmann et al., 2010). Methane measured at these source regions would require either recent serpentinization, where active fluid flows would be in contact with ultramafics, such as in the subsurface; or be the result of Noachian serpentinization, where methane would likely have been trapped for billons of years. The presence of methane clathrate reservoirs in the martian subsurface and/or polar ice caps would allow for the storage and slow release of methane to the atmosphere (Max and Clifford, 2000; Chastain, 2007). A solid understanding of the mineralogy and geochemistry associated with serpentinization is necessary for locating and sourcing methane on Mars. Terrestrial sites of serpentinization can be used to investigate the geochemical measurements required for determining the serpentinization process, and the reaction pathways that could be responsible for the methane detected in the Martian atmosphere.

The Gale Crater, the landing site for the Mars Science Laboratory (MSL) is interpreted as an ancient lake, which will likely provide context for Mars geological history, but not insight into the minerals associated with serpentinization that have been observed on the basis of the CRISM data. However, the Sample Analysis at Mars (SAM) investigation on the MSL will conduct in situ surveys of gases such as methane in the martian atmosphere to localize and understand the nature of their production (Mahaffy, 2008; Mahaffy, 2012).

The aim of this study is to present characteristic aqueous geochemistry, carbonate mineralogy, and hydrocarbon source signatures associated with present-day

serpentinization occurring at the Tablelands Ophiolite in Gros Morne National Park, Newfoundland, Canada, in attempt to provide geochemical parameters relevant for planning future Mars exploration missions.

2.3 MATERIAL AND METHODS

2.3.1 Site Description

Highly reducing, ultra-basic springs discharging from serpentinized peridotite (i.e., harzburgite with some lherzolites; (Suen et al., 1979) rocks were located in the Tablelands Ophiolite in Gros Morne National Park (N49°27' 58.9", W57°57' 29.0"; Figure 2.1). The spring fluids are Ca^{2+}-OH^{-1} type waters similar to those described by Barnes and O'Neil (1967). Inorganic carbon precipitates in these waters and is found as either carbonate sediment, travertine, or conglomerate cements that form where the springs discharge. Three sampling locations were identified on the north-eastern face of the Tablelands and within Winter House Creek: Wallace Brook (WB), Tablelands East (TLE), and Winter House Creek (WHC) are shown in Figure 2.2. TLE and WB were located on the slope of the Tablelands massif with travertine deposits and discharging Ca^{2+}-OH^{-1} type waters. Located in WHC is a pool of ultra-basic water (labelled WHC2) that is approximately 40cm deep and 126cm wide, and exposed to the atmosphere at the surface. A survey of the bottom of WHC2 pool using handheld pH and Eh meters showed that there were two distinct locations where the pH was the highest and the Eh was the lowest indicating that there are two ultra-basic, reducing spring discharge points at the bottom of WHC2 (labeled WHC2a and WHC2b). A third sampling location (WHC2c) was selected for this study. At this location freshwater from overland flow trickles into

the WHC2 pool. This site was of particular interest for studying the geochemical and biological interactions at a mixing site with large redox and nutrient gradients. The carbonate sediment at the bottom of the WHC2, and the travertine on the side of WHC2 spring were also sampled to determine the source of the inorganic carbon. A small and shallow oval shaped pool (approximately 2cm deep, 5cm wide) of ultra-basic spring water seeping from the travertine deposit was located approximately a meter from WHC2. It is identified as WHC1. WHC1 recharges at rate of 1mL/min, and its surface is continuously exposed to the atmosphere; however, this pool was continuously flushed with ultra-basic groundwater and no freshwater inputs to WHC1 were indentified. Winter House Brook (WHB) which flows along the bottom of Winter House Canyon was identified as the freshwater end member.

2.3.2 Aqueous geochemistry sampling and analysis

Daily field measurements of pH and redox potential (E_h) were obtained during sampling trips in July and September, 2009; June, August, and October, 2010; and June 2011. Redox and pH values of water samples were measured using an ORPTestr 10 meter (Eutech Instruments), pH paper and handheld pH meter (IQ Scientific Instruments GLP series IQ180G), respectively. Redox and pH values were measured during sampling to identify any changes in these parameters during or after water withdraw, and after rainfall events. Samples were collected at least 48 hrs following a rainfall event to minimize dilution effects.

Samples for total inorganic carbon (TIC) and dissolved organic carbon (DOC) were collected for both concentration and stable carbon isotope ($\delta^{13}C$) values in pre-combusted 40mL amber vials spiked with 200ul of mercuric chloride ($HgCl_2$) and 20% phosphoric acid (H_3PO_4) respectively. Samples for DOC were filtered through a 0.7µm pre-combusted glass microfiber filter. TIC and DOC concentrations and $\delta^{13}C$ values were determined using an OI Analytical Aurora 1030 TOC Analyzer equipped with a reduction furnace, water trap, and packed GC column; coupled to a ThermoElectron DeltaVPlus Isotope Ratio Mass Spectrometer (IRMS) system or a Finnigan MAT252 IRMS via a Conflo III interface. The Aurora uses a wet chemical oxidation process to extract carbon as CO_2 gas using phosphoric acid for total inorganic carbon (TIC) and Na-persulfate for total dissolved organic carbon (DOC). Accuracy and reproducibility for concentration was ± 1.5% RSD and ± 0.5‰ RSD for $\delta^{13}C$ (n=3). $\delta^{13}C$ values are reported in delta notation relative to the Vienna Pee Dee Belemnite (PDB) reference standard.

Water samples were collected for hydrogen and oxygen isotopes (δD_{H2O}, $\delta^{18}O_{H2O}$) in pre-combusted 4mL vials with no headspace. Oxygen and hydrogen isotope measurements were analyzed at Isotope Tracer Technologies in Waterloo, Ontario on a Picarro Cavity Ring Down Spectroscopy Analyzer (Model L1102-i). Precision on multiple $\delta^{18}O$ and δD measurements was ± 0.1‰ and ± 0.6‰ respectively. All results for oxygen and hydrogen are reported in delta notation relative to the Vienna Standard Mean Ocean water (SMOW) reference standard.

Water samples were collected for major-ions (i.e., Mg^{2+}, Ca^{2+}, Cl^-, Br^-) chemistry and measured on an inductively coupled plasma mass spectrometer (ICP-MS) at

Memorial University of Newfoundland using an ELAN DRCII ICP-MS. Samples for ICP-MS were filtered through a 0.45µm filter and collected in 125mL Trace-Clean bottles and immediately acidified with approximately 200ul 5N nitric acid. Certified reference materials were used for quality control. The detection limit on conservative ions Cl^- was <0.01mg/L, and <1.7mg/L for Br^-. The detection limit on Ca^{2+} and Mg^{2+} were <167µg/L and <0.35µg/L respectively. Total analytical error was ± 10% RSD.

2.3.3 Carbonate mineralogy and isotope analysis

Samples of travertine and carbonate sediment from spring locations were collected for trace element geochemistry and carbon ($\delta^{13}C$) and oxygen ($\delta^{18}O$) isotope analysis. Samples were frozen upon collection, freeze dried, and ground to a fine powder with a mortar and pestle. X-ray diffraction was employed on powdered carbonates to determine measurements of major minerals present.

$\delta^{13}C$ and $\delta^{18}O$ isotopes of carbonates were analyzed using a ThermoElectron Gas Bench II interfaced to an IRMS. Approximately 1mg of sample was measured into glass vials, placed in a heated block (50°C), and flushed with helium prior to injection with phosphoric acid. The resultant gases were passed through Nafion driers and a capillary column prior to entering the ion source. External calcium carbonate standards CBM, NBS-19, and SPEX were used throughout the sequence to determine the linearity and accuracy of the instrument. Reproducibility of $\delta^{18}O$ and $\delta^{13}C$ measurements were ± 0.1‰ and ± 0.05‰, (n=3), respectively, and values were reported in delta notation relative to SMOW and PDB standards respectively.

2.3.4 Dissolved gas sampling

Dissolved gases including H_2 and CH_4; and other hydrocarbons including ethane (C_2H_6, or C_2), propane (C_3H_8, or C_3), butane (C_4H_{10}, or C_4), pentane (C_5H_{12}, or C_5), and hexane (C_6H_{14}, or C_6) were sampled using a modified syringe gas phase equilibration technique by McAuliffe (1971) and Rudd et al.,(Rudd et al., 1974). Twenty millilitres of fluid was withdrawn with a 60mL sterile syringe and shaken vigorously for 5 min with an equal volume (20 mL) of helium (He), and repeated with a second syringe. This allowed for partitioning of the dissolved gas in the sample water into the gas phase. The entire gas phase from each syringe (20mL) was injected into a 30mL serum vial (i.e., total gas volume of 40mL), prefilled with degassed water and sealed with blue butyl stoppers. The dissolved gases in He displaced the water in the serum vial. Samples were collected in triplicates for most samples. The samples that were not sampled in duplicate of triplicate. Samples were fixed with 5μL-saturated solution of $HgCl_2$ to ensure there was no microbial growth in bottles.

Dissolved gases were sampled for $\delta^{13}C$ analysis by collecting 50mL of fluid using a 60mL sterile syringe and injecting directly into a pre-evacuated 125mL serum vial fixed with $HgCl_2$ and sealed with a blue butyl stopper. Samples were collected in triplicate.

2.3.5 Analysis of dissolved gases

Dissolved gases, including H_2 and CH_4 were analyzed for concentration using a portable SRI 8610 Gas Chromatograph (GC) with a Thermal Conductivity Detector (TCD) and a Flame Ionization Detector (FID) respectively. The gases were separated using a Carboxen 1000 column packed in stainless steel (15 ft × 1/8in, 2.1mm film thickness) with a temperature program: 35°C, hold 5min, ramp at 20°C/min to 225°C,

hold 15min with a He carrier gas. Hydrocarbons were also analyzed by a GC equipped with a FID on a Porabond-Q column (30m × 0.25mm, 0.25μm film thickness) with a temperature program of 35°C hold 8 min, 10°C/min to 150°C, hold 8min, ramp 5°C/min to 210°C, hold 10min. Peak areas were compared to hydrocarbon standard curves ($R^2 \geq 0.99$) to determine concentrations. Reproducibility on replicate samples was better than 5%.

Stable carbon isotope ratios of CH_4 were measured using an Agilent 6890 GC equipped with the Carboxen 1010 column coupled to a Finnigan MAT252 IRMS via combustion Conflo II Interface (GC-C-IRMS). Methane isotopes were determined using a 5:1 split ratio and a 100°C isothermal temperature program. Low molecular weight hydrocarbons (C_2, C_3, iC_4, nC_4, iC_5, nC_5, C_6) were determined on the Porabond Q column using a 5:1 split ratio and the same temperature program as used for concentration analysis.

Samples were withdrawn from serum bottles and injected directly into the GC-C-IRMS system. On each injection onto the Carboxen 1010 column, $\delta^{13}C$ of CH_4 was determined. On each injection onto the Porabond-Q column, $\delta^{13}C$ of low molecular weight hydrocarbons was determined. All results are reported in delta notation relative to the PDB standard reference material. Accuracy and reproducibility for $\delta^{13}C$ values were ± 0.5‰. This error incorporates both internal reproducibility on triplicate measurements and accuracy of instrumental measurement of a CH_4 standard with a known carbon isotope value. Methane standards were run through out the sequence to determine the linearity and accuracy of the instrument. All isotope ratios are reported in delta notation

(e.g., $\delta^{13}C$, $\delta^{18}O$, δD) relative to an international standard (e.g., V-PDB, SMOW) using (Equation 5):

$$\delta\ (‰) = (R_{sample}/R_{standard} - 1) \times 1000 \quad [5]$$

where R is the ratio of heavy to light isotopes.

2.4 RESULTS AND DISCUSSION

2.4.1 Origin of spring water

The δ^2D_{H2O} and $\delta^{18}O_{H2O}$ of the ultra-basic springs and freshwater including WHB, snowmelt, rainwater, and surface pond water collected from the top of the Tablelands massif plot close to the global meteoric water line (GMWL; Figure 2.3a), indicating that the ultra-basic spring fluids are meteoric in origin. This further suggests that the groundwater discharging from the peridotite rocks has been in recent contact with the atmosphere, excluding connate water or magmatic water sources.

The GMWL is representative of precipitation data collected from different locations globally as determined by (Craig, 1961) and therefore represents the global relationship between δ^2D_{H2O} and $\delta^{18}O_{H2O}$. The δ^2D_{H2O} and $\delta^{18}O_{H2O}$ data from the Tablelands do not plot directly on GMWL, which likely reflects the local conditions that control the δ^2D_{H2O} and $\delta^{18}O_{H2O}$ relationship. A linear regression of the freshwater sources was used in Figure 2.3a as a proxy of the local meteoric water line (LMWL) for the Tablelands. Spring fluid δ^2D_{H2O} and $\delta^{18}O_{H2O}$ values plot closely to the LMWL indicating a similar δ^2D_{H2O} and $\delta^{18}O_{H2O}$ relationship as the freshwater. Therefore, changes in local meteoric conditions (e.g., temperature) likely govern the δ^2D_{H2O} and $\delta^{18}O_{H2O}$ of

freshwater and ultra-basic springs. However, δ^2D_{H2O} and $\delta^{18}O_{H2O}$ of spring fluids may also reflect physical mixing of the δ^2D_{H2O} and $\delta^{18}O_{H2O}$ of freshwater with the ultra-basic water.

A positive relationship exists between temperature and δD_{H2O} and $\delta^{18}O_{H2O}$, with a greater fractionation associated with decreasing temperatures, resulting in a depletion of D_{H2O} and $^{18}O_{H2O}$. Samples were collected over winter-spring, summer-fall seasons and thus varied in different seasonal temperatures. Figure 2.4 plots $\delta^{18}O$ and δD of waters sampled from WHC2b and WHB during different seasons: July and September 2009 (summer-fall season), and June 2010 (winter-spring season). The most isotopically depleted D_{H2O} and $^{18}O_{H2O}$ values were observed in early June, and the most enriched D_{H2O} and $^{18}O_{H2O}$ values were observed in September (summer-fall season; Figure 2.4). The trend that was observed can be explained by changes seasonal temperatures, with an isotopic depletion during colder seasons (e.g., June) when there was snow cover on the Tablelands and colder surface temperatures and an enrichment during warmer seasons (e.g., September), when there was no snow cover and warmer surface temperatures.

2.4.2 Mixing of freshwater and ultra-basic fluids at springs

Average measurements of pH, redox, and dissolved gas composition of fluids from the Tablelands are reported in Table 2.1. Standard deviations reflect seasonal and annual variability in the geochemical parameters. The highest pH measurements were found at WHC1 (12.2), WHC2a (12.3), and WHC2b (12.3). Redox measurements remained consistently low at WHC2a and WHC2b (Eh -552 and -609mV) at the bottom

of the WHC pool where a distinct anoxic zone was observed. High redox values (+415mV) were measured for the more oxidizing WHB freshwater end member. The redox value of the groundwater spring discharging at WHC1 increased during sampling. This occurred because of the slow recharge rate of the seep and exposure to the atmosphere, which allowed for atmospheric O_2 to partition into spring water and increase the redox value while sampling. Redox measurements were higher at mixing spring locations with oxygen-containing freshwater inputs (i.e., WHC2c, TLE, and WB). Differences in redox measurements can be explained by different amounts of mixing of freshwater and ultra-basic water at different times of sampling.

To better understand changes in geochemical parameters in the springs, the contributions of freshwater and ultra-basic fluids were quantified at sites where mixing of the two end members was suspected. Figure 2.5 represents a conservative 2-component mixing model between the freshwater end member (represented by WHB) and the ultra-basic reducing end member (represented by WHC1). In this model bromine (Br^-) and chlorine (Cl^-) are assumed to be conservative tracers of these two end members The data from WHC2a, WHC2b, and WHC2c are well represented by the model and therefore suggest that the Cl^- or Br^- concentrations can be used to calculate the fraction of ultra-basic water (f_{UB}) contributing to the mixing sites (WHC2a, WHC2b, WHC2c). Sampling sites that fall off the WHB and WHC mixing line (i.e., TLE and WB), are not as well described by the mixing model. This could be due to differences in the geochemistry of the end members for the TLE and WB springs. Likewise, TLE and WB, which are located on a steep slope of the Tablelands massif, received water inputs in the form of surface

runoff, which could contribute to large differences observed in aqueous geochemistry seasonally, and account for larger standard deviations (Table 2.1).

2.4.3 Geochemical evidence of present-day serpentinization

Fluids found discharging from serpentinized peridotites at the Tablelands Ophiolite are geochemically distinct from freshwater as evidenced by high pH, negative redox potentials, and the presence of H_2.

Dissolved H_2 concentrations were the highest (1.04 and 1.18mg/L; Table 2.2) at the most reducing sites with the least amount of mixing with freshwater and minimum exposure to the atmosphere (WHC2a and WHC2b). Lesser amounts of dissolved hydrogen (0.57 to 0.36mg/L; Table 2.2) were measured at sites with greater mixing between the ultra-basic reducing groundwater and the surface freshwater (WHC2c, TLE) and at slow discharging sites where the ultra-basic groundwater was directly exposed to the atmosphere for at least 10 min before sampling could occur (WHC1). During this time frame, dissolved hydrogen gas may be released to the atmosphere. Dissolved hydrogen gas measurements were below detection at WB.

Likewise, major ions Mg^{2+} and Ca^{2+}, derived from the hydration of olivine and clinopyroxenes respectively, are often found in fluids discharging from serpentinized ultramafic rocks giving evidence for active serpentinization. High Ca^{2+}/Mg^{2+} are found in the ultra-basic springs at continental sites of serpentinziation such as Cazadero in California (Barnes et al., 1967). Through serpentinization, soluble Mg^{2+} concentrations become accommodated into serpentine and soluble Ca^{2+} gets released into the water.

Therefore, higher ratios of Ca^{2+} to Mg^{2+} are observed. Similarly, high Ca^{2+}/Mg^{2+} ratios were found in the ultra-basic springs at the Tablelands (see Table 2.1).

In Figure 2.6, Ca^{2+}/Mg^{2+} ratios from spring fluids at WHC2a, WHC2b, and WHC2c at certain sampling periods are well described by the 2-component conservative mixing model defined from the freshwater and ultra-basic end members. The highest Ca^{2+}/Mg^{2+} ratios are observed at most ultra-basic springs. However, Ca^{2+}/Mg^{2+} ratios observed at WHC2b (f_{UB}= 0.62) and WHC2c (f_{UB}= 0.32) are not well described by the 2-component model. A possible third end member rich in Mg^{2+}-HCO_3^- may be contributing to the spring fluids. As described by Barnes et al. (1967), Mg^{2+}-HCO_3^- rich fluids can be found in localities of incomplete or inactive serpentinization resulting in shallow, moderately basic groundwater that is related to the weathering of serpentine and other magnesium-bearing minerals. Likewise, serpentinization can be affecting Ca^{2+} and Mg^{2+} concentrations. High Mg^{2+} concentrations (Table 2.1) were observed at WHC2b (f_{UB}= 0.62) and WHC2c (f_{UB}= 0.32) suggesting possible mixing of Mg^{2+}-HCO_3^- fluids resulting in lower Ca^{2+}/Mg^{2+} ratios. Similar concentrations of Mg^{2+} and low Ca^{2+}/Mg^{2+} ratios were observed at TLE and WB (Table 2.1), suggesting possible incomplete or inactive serpentinization at these localities.

2.4.4 Carbonate mineralogy and deposition

Carbonates have been observed to precipitate at the discharge points of ultra-basic springs emanating from altered ophiolites (Barnes and O'Neil, 1971). Carbonates in the form of travertine and sediment were found at ultra-basic springs discharging from serpentinized peridotite in the Tablelands. X-Ray Diffraction (XRD) analyses of

travertine and carbonate sediments from the Tablelands suggest the carbonates found at all sites primarily consist of calcite (>90%) with a lesser amount of aragonite (<10%).

The isotopic composition of carbonates can be used to understand the geochemical conditions under which the carbonates were deposited and can be used to interpret the inorganic carbon origin (Clark and Fritz, 1997). Stable carbon and oxygen isotope compositions (as $\delta^{13}C$ and $\delta^{18}O$ values) in travertine and carbonate sediment were determined (Figure 2.7) and compared to the $\delta^{18}O$ value of water and $\delta^{13}C$ value of dissolved TIC (Table 2.3).

The large range in the $\delta^{13}C$ of the carbonates (-25 to -5‰) in this study (Figure 2.7) has also been observed in other freshwater carbonates at sites of present-day serpentinization (O'Neil and Barnes, 1971; Clark et al., 1992). Carbon isotope fractionation during chemical precipitation of freshwater carbonates is dependent on the rate of carbonate precipitation, temperature of precipitation, and the carbonate species present; therefore, a large range in the $\delta^{13}C_{CaCO3}$ can be observed (Romanek et al., 1992). During this process TIC provides carbon for carbonate precipitation. TIC is the sum of dissolved carbon species: $CO_{2\,(aq)}$, $H_2CO_{3(aq)}$, $HCO_3^-{}_{(aq)}$, and $CO_3^{2-}{}_{(aq)}$. In the ultra-basic springs at the Tablelands (pH>10), the carbonate ion, CO_3^{2-}, is the predominant inorganic carbon species and can be assumed to make up most of the TIC composition. The enrichment factor between CO_3^{2-} and $CaCO_3$ (i.e., calcite) is small (i.e., ~0.9‰ at 25°C; (Mook, 1974). Therefore, it is not unexpected that the $\delta^{13}C$ composition of carbonates reflects the $\delta^{13}C$ composition of the TIC within roughly 1‰.

Since the $\delta^{13}C_{CaCO3}$ is largely influenced by the isotopic composition of the TIC, it is necessary to understand the origin of inorganic carbon that is contributing to the isotopic composition of the TIC pool. Different sources of inorganic carbon (e.g., CO_2) for carbonates can contribute to $\delta^{13}C_{TIC}$ values, thus providing a wide range of isotope compositions. Relative contributions of $CO_{2\,(g)}$ can be contributed from the atmosphere ($\delta^{13}C$ ~-7‰; (Clark and Fritz, 1997); oxidized terrestrial organic matter ($\delta^{13}C \leq$ -24‰; (Deines, 1980); marine organic matter ($\delta^{13}C \geq$ -23‰); marine carbonate ($\delta^{13}C$ ~0‰; (Anderson, 1983) and CO_2 from microbial methane oxidation ($\delta^{13}C$ ~ -54 to-30‰, assuming a starting $\delta^{13}C$ methane of -60‰) (Whiticar, 1999). In addition to the isotopic composition of the initial carbon, the $\delta^{18}C$ value of carbonates is also influenced by the temperature-controlled fractionation between $CaCO_3$ and $CO_{2(g)}$. Without knowing the $\delta^{13}C$ value of CO_2 and the rate of precipitation only general conclusions can be made on $^{13}C_{CaCO3}$ values observed. A theoretical $\delta^{13}C$ value for $CO_{2\,(g)}$ contributing to the formation of carbonates was determined using the equilibrium calcite-$CO_{2(g)}$ isotope fractionation relationship ($1000\ln\alpha=1.435 \times 10^6/T^2 - 6.13$) reported by Bottinga (1969) and the measured temperatures of the sampled spring fluids (Table 2.3). The calculated starting $\delta^{13}C_{CO2(g)}$ value ranged from -36.2 to -27.1‰. which, is more depleted in ^{13}C compared to atmospheric $CO_{2(g)}$. Additionally, the $\delta^{18}C$ value of carbonates can be influenced by the temperature-controlled fractionation between $CaCO_3$ and CO_2. Using the measured temperatures of the sampled spring fluids, equilibrium calcite-$CO_{2(g)}$ isotope fractionations were calculated using the $\varepsilon_{Calcite\text{-}CO2\,(g)}$ relationship developed by (Bottinga, 1969); Table 2.3). Equilibrium fractionations ranged from 10.1 to 12.0‰. If

the precipitation of the carbonated were simply due to atmospheric $CO_{2(g)}$ dissolving into the water and precipitating, based on calculated equilibrium fractionations , the $\delta^{13}C$ of the carbonates would be expected to range from -19.0 to -17.4‰. Using the Bottinga (1969) relationship and calculated $\varepsilon_{Calcite\text{-}CO2\ (g)}$, the starting $\delta^{13}C$ values of $CO_{2\ (g)}$ were determined (Table 2.3). Starting $\delta^{13}C_{CO2\ (g)}$ values ranged from -36.2 to -27.1‰ suggesting, in addition to atmospheric CO_2 dissolution, there may be oxidation of terrestrial organic matter and/or methane contributing to the carbonates associated with the ultra-basic springs.

The $\delta^{18}O$ value of carbonates is influenced by the temperature-controlled fractionation between $CaCO_3$ and water, and the $\delta^{18}O$ value of the water. Additionally ^{18}O fractionation effects are largely influenced by the pH that defines the DIC speciation and consequently the overall $\delta^{18}O$ signature of the sum of the DIC species (Uchikawa and Zeebe, 2012). The observed $\delta^{18}O_{CaCO3}$ value for travertine and carbonate sediment ranged from 10.9 to 21.9 ‰ (Figure 2.7). Using the measured $\delta^{18}O$ values and temperatures of the sampled spring fluids, and calcite-water oxygen isotope fractionation relationship reported in Friedman and O'Neil ($1000\ln\alpha=2.78\ x10^6/T^2$ -2.89; (1977), theoretical calcite $\delta^{18}O_{CaCO3}$ VSMOW values were calculated (Table 2.3). This isotopic fractionation assumes that the carbonates were precipitated in isotopic equilibrium with the water. The calculated equilibrium $\delta^{18}O_{CaCO3}$ values ranged from 17.9 to 21.0 ‰. The $\delta^{18}O_{CaCO3}$ data collected from WHC2b and WB fall within range of the calculated equilibrium $\delta^{18}O$ values based on the $\delta^{18}O$ value of water and temperature at the time of sampling. Data from TLE, WHC2a, and WHC2c only partially fall within the range of calculated

equilibrium $\delta^{18}O$ values, where as data from WHC1 does not fall within the calculated equilibrium range at all. For the most part, measured $\delta^{18}O_{CaCO3}$ values that do not fall within the range of equilibrium $\delta^{18}O$ values are depleted in ^{18}O. A similar isotopic depletion in ^{18}O has been observed in travertine deposits and carbonate sediments at ultra-basic reducing springs at continental sites of serpentinization such as Cazadero, CA and the Oman ophiolite (O'Neil and Barnes, 1971; Clark et al., 1992). O'Neil and Barnes (1971) attributed this depletion in ^{18}O to the rapid precipitation of $CaCO_3$ in an alkaline solution where by two-thirds of the oxygen in the solid carbonate comes from the CO_2 and therefore isotopically depleted oxygen of $CaCO_3$ would have been expected.

2.4.5 Source of CH_4 and low molecular weight hydrocarbons in spring fluids

Dissolved hydrocarbon gases including methane, ethane, propane, n-butane, n-pentane, and n-hexane were measured in the ultra-basic reducing springs. Highest hydrocarbon concentrations were at the most reducing sites WHC2a and WHC2b (Table 2.2). Lesser amounts of dissolved hydrocarbon gases were measured at sites with greater mixing between the ultra-basic reducing groundwater and the surface freshwater (WHC2c) and at slow discharge rates (WHC1). In the latter case hydrocarbons may have been lost to the atmosphere before they could be sampled. To obtain a fresh spring water sample, all water was removed from WHC1 and the small depression in the travertine was allowed to fill again before the water was sampled. It was noted that the E_h became more positive while the pool was filling up, suggesting that the geochemistry of the water was changing in the presence of air. Therefore, hydrocarbons, inorganic carbon, and dissolved organic matter may have been partially or completely lost before sampling. At

sites with the greatest amount of mixing, dissolved hydrocarbon gases were below detection (TLE and WB).

As a first approach, a Bernard plot (Figure 2.8) was used to determine the primary source of CH_4 in the ultra-basic reducing springs. The, Bernard plot has been used previously to discriminate between microbial and thermogenic methane production (Bernard et al., 1977). Bernard et al., (1977) found that on a plot of $\delta^{13}C_{CH4}$ versus CH_4/C_{2+} (where C_{2+} is the sum of the concentrations of C_2, C_3, and C_4) that microbially produced methane has high CH_4/C_{2+} ratios (>400) and very negative $\delta^{13}C$ values (<-50 ‰) relative to thermogenic methane with lower CH_4/C_{2+} (<100) and more positive $\delta^{13}C$ values (>-50‰). Dissolved methane from the ultra-basic springs at the Tablelands plot in the thermogenic field suggesting that the primary source of methane is not microbial in these springs. This observation is consistent with initial microbiological studies of the Tablelands spring fluids, which found a lack of significant contribution from biological methanogenesis (Brazelton et al., 2012). All methanogens are members of the Archaea, and attempts to detect archaeal 16S ribosomal RNA genes in Tablelands fluids via the polymerase chain reaction have failed. In contrast, bacterial 16S ribosomal RNA genes are readily detected (Brazelton et al., 2012) Furthermore, metagenomic sequences predicted to represent methanogens comprise only 0.2% of the full metagenomic dataset from WHC2b (Brazelton et al., 2012); data are available at http://metagenomics.anl.gov under dataset"WHC2B sff"). These predictions are based on automated sequence similarity algorithms, and none of the predicted sequences actually encode proteins

directly involved in the methanogenesis pathway. In short, the available microbiological data indicate that if methanogens are present in WHC2b at all, they are extremely rare.

All of the measured methane samples were similar in $\delta^{13}C$ value (-28 to -25‰; Figure 2.8), except for one data point collected from WHC2c in August 2010 had an enriched value ($\delta^{13}C_{CH4}$= -15.9‰), where C_{2+} was below detection limit. This enriched CH_4 value may be evidence of methane oxidation occurring at WHC2c where O_2 is present. Assuming a carbon isotopic signature of oxidized methane similar to that reported in June 2010 (-25.6‰), and uptake of the isotopically light carbon for metabolism, the left over carbon pool will be enriched in ^{13}C as observed at WHC2c from August 2010. A decrease in CH_4 concentration and increase in TIC concentration was also observed in August 2010 (0.01ug/L, 14.8mg/L) as compared to June (0.03ug/L, 11.8mg/L) suggesting possible CH_4 oxidation and CO_2 consumption by microorganisms.

The methane measured may be thermogenic in origin. Thermogenic methane could be produced from the thermal alteration of the sedimentary organic matter underlying the Tablelands Ophiolite, that migrated to the surface through cracks and fissures in the altered peridotite. Sedimentary organic matter most likely exists in the siliclastic marine sandstones from the Blow-me-Down Brook formation, siliclastic marine mélange from the Crolly Cove formation, and carbonate limestone from McKenzie's formation (see geologic map, Figure 2.1). Therefore, a thermogenic origin of the methane must be considered; however, an abiogenic origin must also be considered.

Although an abiogenic field is not defined in the Bernard plot, experimental and field studies have shown the CH_4/C_{2+} for abiogenic hydrocarbons (0.01 to 200) can

overlap with the lower range of CH_4/C_{2+} ratios for thermogenic hydrocarbons, especially if mixing with thermogenic hydrocarbons (McCollom and Seewald, 2006; Taran et al., 2007; Yunyan et al., 2009; McCollom et al., 2010; Etiope et al., 2011b). CH_4/C_{2+} ratios from the Tablelands springs (0.68 to 3.78) fall within this range. Therefore, the Bernard plot cannot discriminate between thermogenic and abiogenic sources of CH_4 within this range.

To distinguish between thermogenic and abiogenic origins of methane and higher molecular weight hydrocarbons, patterns of $\delta^{13}C$ and $\delta^{2}H$ values of C_1-C_6 alkanes were considered. Thermogenic hydrocarbons display a ^{13}C enrichment with increasing carbon number. This isotopic trend is attributed to kinetic isotope effect where alkyl groups cleave from the source organic matter. The weaker ^{12}C-^{12}C bonds will break at a faster rate than the heavier ^{12}C-^{13}C bond (DesMarais et al., 1981; Sherwood Lollar et al., 2006). As a result, residual alkanes will be more enriched in the ^{13}C with increasing molecular mass. In contrast, it has been suggested that ethane can form abiogenically via a polymerization reaction that results in a depletion of ^{13}C and enrichment in ^{2}H with respect to methane (Sherwood Lollar et al., 2008). In this polymerization reaction, the lighter isotopes ^{12}C-^{12}C will bond at a faster rate than the heavier and lighter isotopes ^{12}C-^{13}C, resulting in a depletion of ^{13}C of ethane compared to that of methane. In this study, the $\delta^{13}C$ of alkanes from WHC2a and WHC2b follow a general isotopic depletion of C_2-C_6 relative to CH_4 with increasing carbon number and a clear ^{13}C depletion between methane and ethane similar to other putative abiogenic hydrocarbons (Figure 2.9). However, it must be noted that this ^{13}C depletion between methane and ethane is not

consistently observed for abiogenic hydrocarbons (Taran et al., 2007). Sherwood Lollar et al. (2008) proposed that a saw-tooth pattern, in this case a ^{13}C depletion between methane and ethane followed by a ^{13}C enrichment between ethane and propane, can be modeled assuming rapid abiogenic polymerized chain growth with negligible carbon isotope fractionation in the formation of C_2+ compounds (Figure 2.9). The Tablelands C_2+ data is not well described by such a model suggesting that the carbon isotopic patterns observed at the Tablelands may be due to fractionation effects associated with secondary alteration processes such as oxidation or diffusion, or mixing of hydrocarbons from thermogenic sources. Moreover, not all thermogenic and abiogenic hydrocarbons can be described by the isotopic trends and more research needs to be done to distinguish between the two mechanisms.

2.5 IMPLICATIONS AND CONCLUSIONS

Temporal variations in methane concentration have been observed in the Martian atmosphere suggesting the presence of localized source regions (Formisano et al., 2004; Mumma et al., 2009). This suggests that production and/or release of methane to the Martian atmosphere may be related to the geology of the planet's surface or subsurface. Possible source regions include Nili Fossae and NE Syrtis Major where aqueous altered olivine-rich rocks are exposed (Hamilton and Christensen, 2005; Mumma et al., 2009; Ehlmann et al., 2010). At Nili Fossae Mg- carbonates and Mg-rich serpentines have also be found (Ehlmann et al., 2010), and calcium pyroxenes have been detected at Syrtis Major (Rogers and Christensen, 2007). The presence of carbonate and serpentine signatures at localized methane source regions suggests that serpentinization may have

occurred in the past on Mars. Given the short residence time of methane, detected methane at source regions would suggest either recent serpentinization where liquid water would need to be present, possibly in the subsurface; or Noachian and trapped as methane clathrates in the subsurface and/or polar ice being released in the subsurface (Mumma et al., 2009).

The Tablelands Ophiolite is an active site of serpentinization and a Mars analogue for the presence of altered olivine-rich ultramafic rocks with both carbonate and serpentine signatures. Meteoric water reacting with ultramafic peridotites at the Tablelands forms geochemically distinct ultra-basic and reducing springs. These springs have characteristic Ca^{2+} and Mg^{2+} ion ratios. Calcium-rich carbonate sediment and travertine deposits have been found in and around the ultra-basic springs. Isotopic analyses of carbonates suggest that carbonate sediment and travertine derived carbon from CO_3^{2-} and are precipitated in non-equilibrium with the atmosphere and fluids. Dissolved gases including hydrogen, methane, and low molecular weight alkanes (C_2 to C_6) have been measured in ultra-basic springs. The primary source of methane sampled from the springs is not microbial., but either thermogenic or abiogenic in origin, or a mixture of both. Additional work is needed to distinguish between the two possible sources of hydrocarbons. One possible approach is to examine the stable isotope composition of hydrogen of the hydrocarbon gases to determine if they are abiogenic or thermogenic in origin (Sherwood Lollar et al., 2008). With the current Mars Science Laboratory rover, goals to survey gases such as methane in the martian atmosphere, stable isotope and abundance analyses of gases can be applied to help provide information on the source of methane on Mars. Likewise, serpentinization at the Tablelands Ophiolite

can be used as a mineralogical indicator to understand previous aqueous environment conditions and as a geochemical indicator to understand the conditions suitable for methane production on Earth and potentially on other ultramafic planetary bodies such as Mars.

Overall, key measurements on serpentinizing systems including aqueous geochemistry, carbonate mineralogy, and evidence of organic molecules can help in both interpreting data from MSL and planning future Mars exploration missions.

ACKNOWLEDGEMENTS

This study was supported in part by grants from the Canadian Space Agency (CSA) Canadian Analogue Research Network (CARN) and CSA's Field Investigations, Natural Sciences and Engineering Research Council (NSERC) Discovery Grant awarded to PI Morrill, NSERC Alexander Graham Bell Canada Graduate Scholarship, and MITACS Accelerate. We would like to acknowledge M. Wilson, M. Johnston, C. Earle, A. Rietze, H. Kavanagh with their help in the field, A. Pye and G. Van Biesen for their technical assistance in the lab, and N. Debond for the helpful comments on the manuscript. We would also like to thank the reviewers for their helpful comments on this manuscript.

2.6 FIGURES AND TABLES

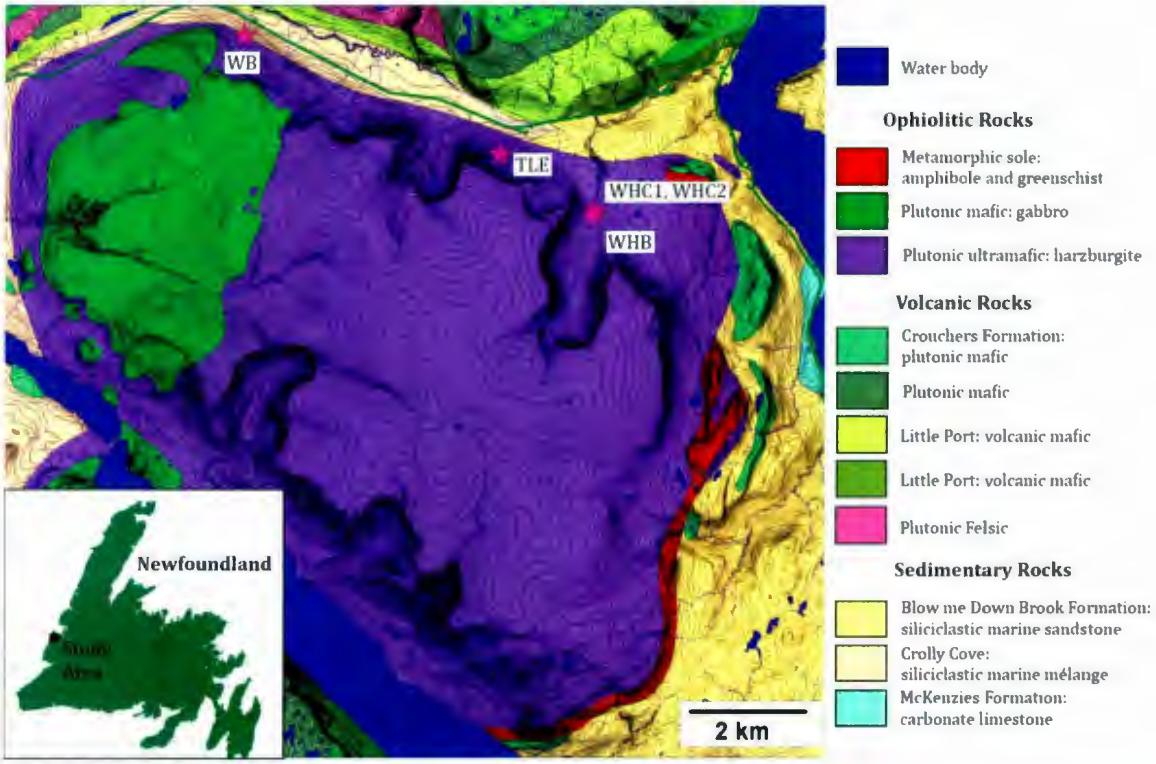

Figure 2.1 Geologic map, modified from (Berger et al., 1992), showing the Tablelands massif and approximate sampling locations (star symbols): Wallace Brook (WB), Tablelands East (TLE), Winterhouse Creek (WHC1, 2a, b, c); and Winterhouse Brook (WHB). The Tablelands is located in Gros Morne National Park in Newfoundland, Eastern Canada.

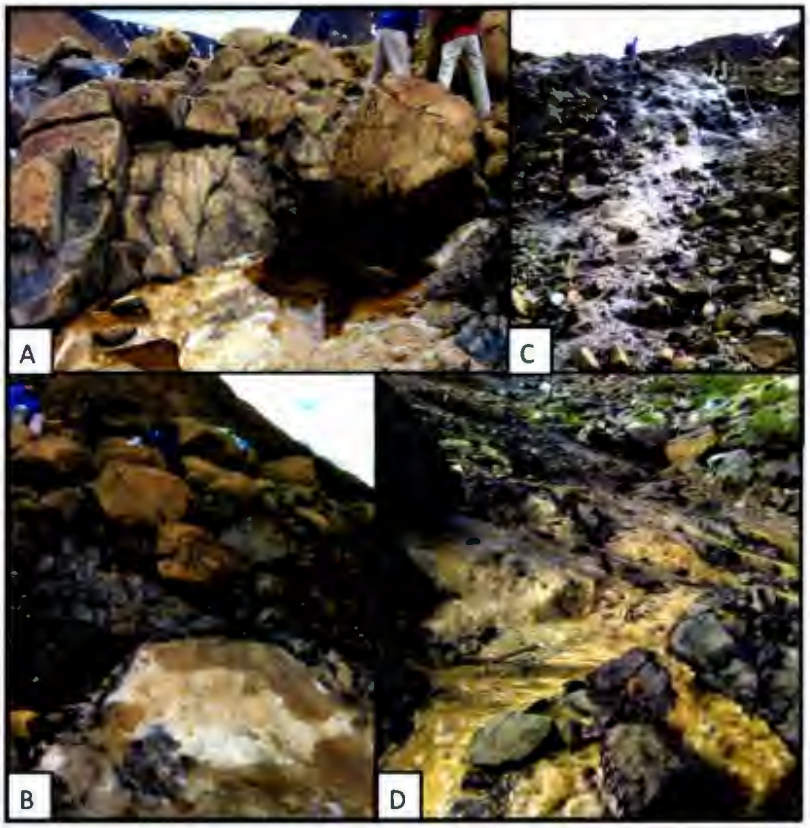

Figure 2.2 Images of springs and travertine deposits at sampling locations: Winterhouse Creek 1 (2.2a, human for scale ~1.70m); Winterhouse Creek 2 (2.2b, human for scale ~1.70m), Tablelands East (2.2c, human for scale ~1.70m); and Wallace Brook (2.2d, spatula for scale ~22cm).

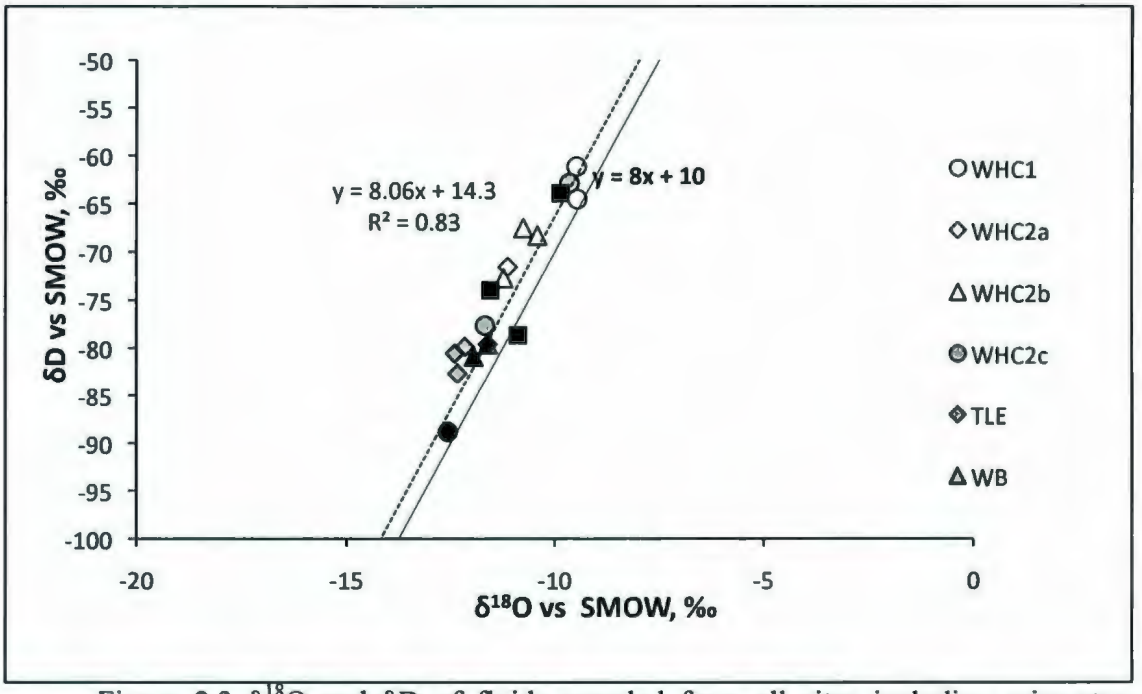

Figure 2.3 $\delta^{18}O$ and δD of fluids sampled from all sites including rainwater, snowmelt, and pond water collected from the top of the Tablelands. $\delta^{18}O$ and δD of fluids are plotted with the GMWL (solid line) and the linear regression for collected freshwater (i.e. WHB, pond water, rain, snowmelt) as a proxy for the LMWL (dashed line). Error on $\delta^{18}O$ and δD represent ±0.1 ‰ and ±0.6‰ respectively. Note that error bars are smaller than the plotted symbol.

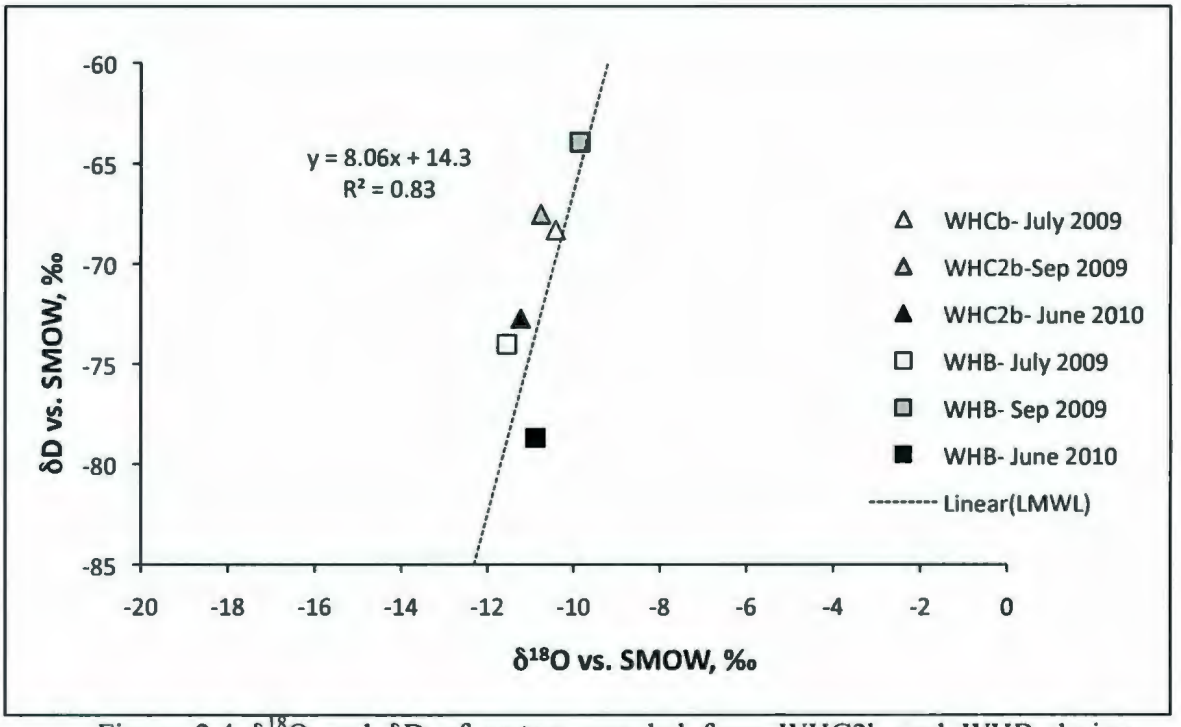

Figure 2.4 $\delta^{18}O$ and δD of waters sampled from WHC2b and WHB during different seasons: July and September 2009, and June 2010. Error on $\delta^{18}O$ and δD represent ±0.1 ‰ and ±0.6‰ respectively. Note that error bars are smaller than the plotted symbol.

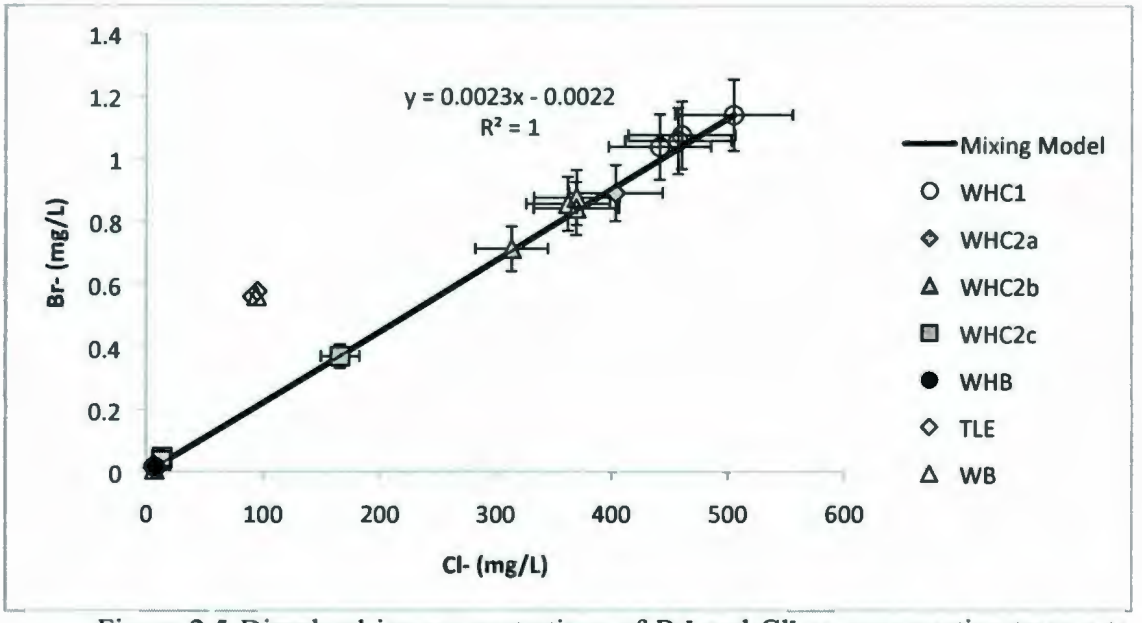

Figure 2.5 Dissolved ion concentrations of Br^- and Cl^- as conservative tracers to determine mixing of freshwater and ultra basic water. Samples plotted are from WHC1, WHC2a, WHC2b, WHC2c, TLE, WB, and WHB collected in September 2009 and June 2010. The solid line represents conservative mixing between the freshwater (WHB) and ultra basic (WHC01) end member. Note that TLE and WB do not plot on the conservative mixing line. Error bars are ±10% for Br^- and Cl^- and may appear smaller than the plotted symbol.

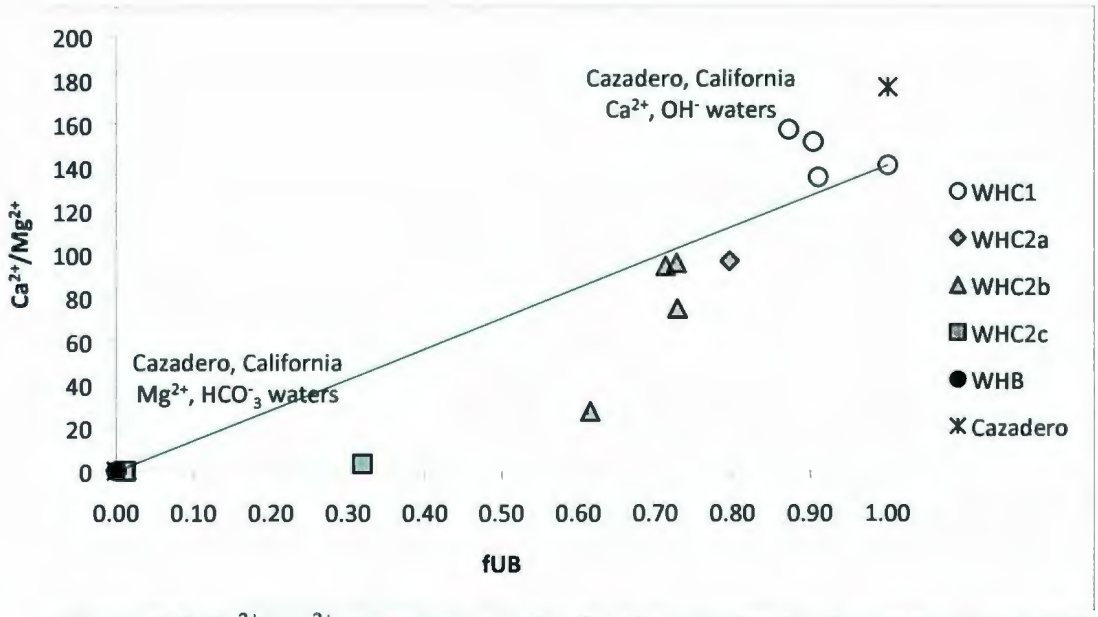

Figure 2.6 Ca^{2+}/Mg^{2+} plotted versus the fraction of ultra basic water mixing with the conservative mixing line. Ca^{2+}/Mg^{2+} ratios increase with greater fraction of ultra basic water. Ca^{2+}/Mg^{2+} of waters from the Tablelands are plotted against Ca^{2+}/Mg^{2+} ratios of spring (Ca^{2+}/Mg^{2+}= 177) and meteoric water (Ca^{2+}/Mg^{2+}= 0.14) from another continental site of present-day serpentinization in Cazadero, California (Barnes et al., 1967). Error bars of $Ca^{2+}/Mg^{2+}$are ±10% and may appear smaller than the plotted symbol.

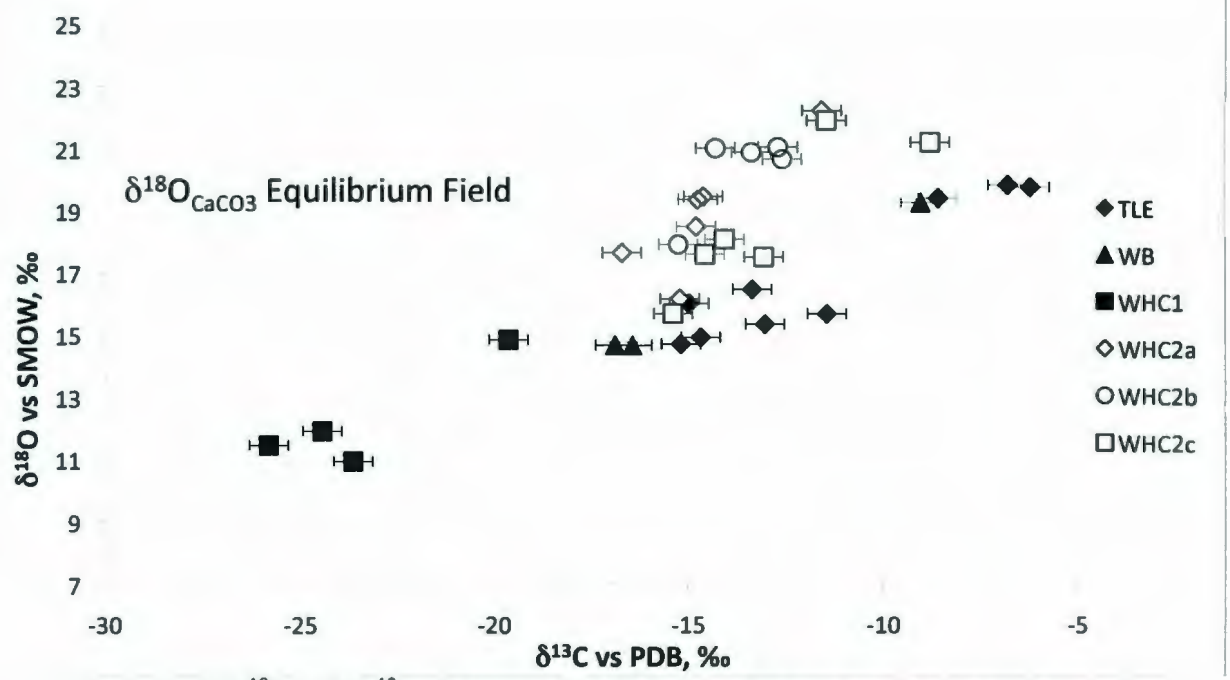

Figure 2.7 $\delta^{18}O$ and $\delta^{13}C$ of travertine (filled symbols) and carbonate sediment (open symbols) from serpentinization sites plotted with the equilibrium field for $^{18}O_{CaCO3}$ (17.9 to 21.0‰) determined by (O'Neil, 1969) corrected in (Friedman and O'Neil, 1977) assuming chemical precipitation of calcium carbonate in equilibrium with Tableland source waters. Error bars represent ±0.1 ‰ and ±0.5‰ for ^{18}O and ^{13}C respectively. Note that $\delta^{18}O$ bars are smaller than the plotted symbol.

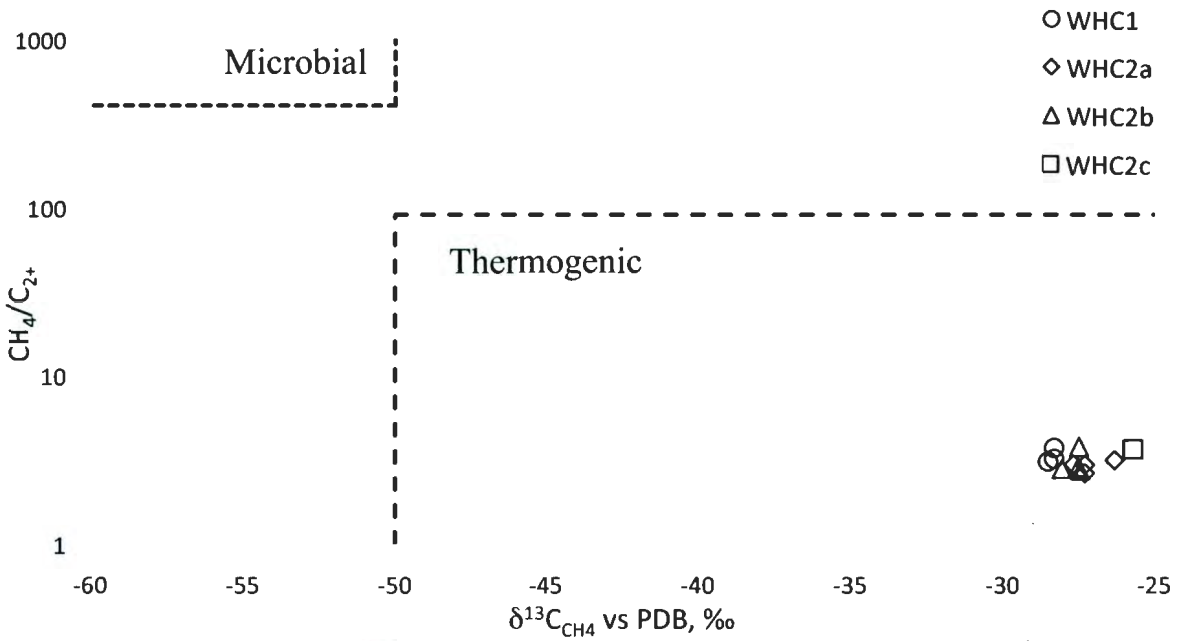

Figure 2.8 Modified Bernard plot of $CH_4/[C_{2+}= C_2+C_3+nC_4]$ versus $\delta^{13}C$ of methane from serpentinization springs. Two distinct fields for microbially and thermogenically produced methane are plotted. Data points for methane gas collected at the Tablelands fall within the thermogenic field.

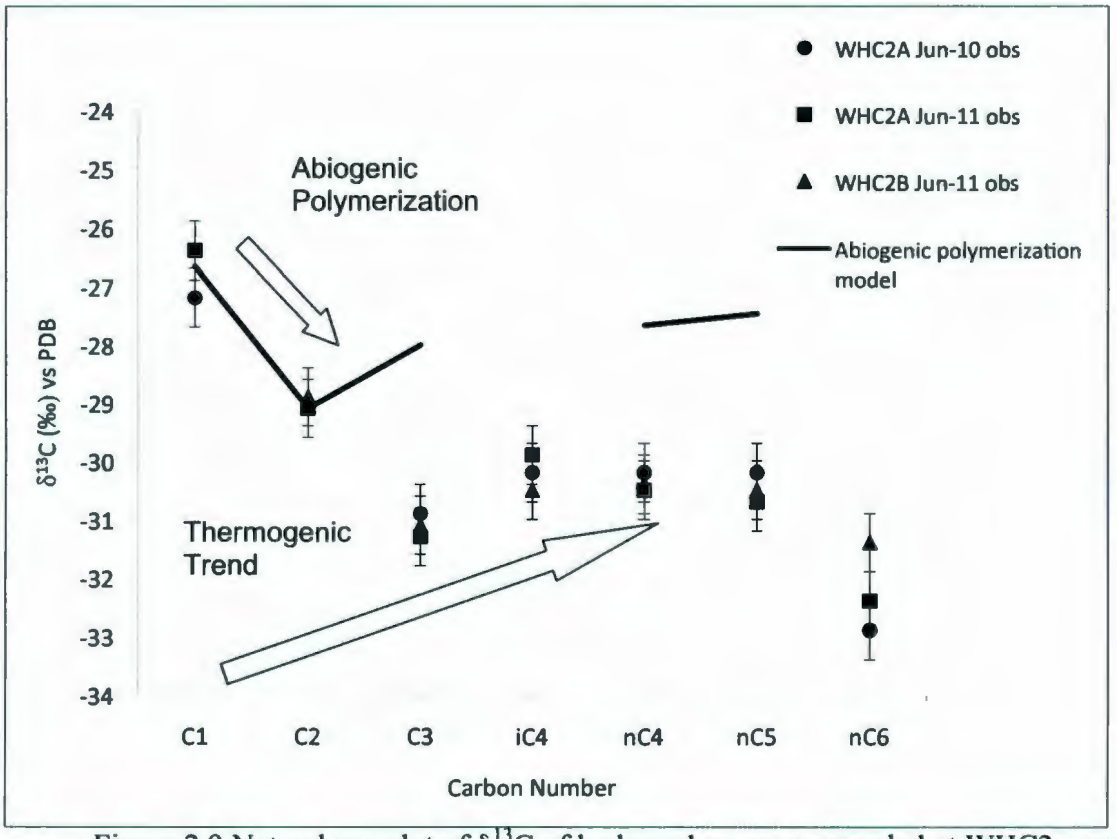

Figure 2.9 Natural gas plot of $\delta^{13}C$ of hydrocarbon gases sampled at WHC2a, and WHC2b in June 2010, June 201. Error bars represent ±0.5‰ for $\delta^{13}C$. The block arrows represent general abiogenic and thermogenic isotopic trends. The solid line shows the predicted $\delta^{13}C$ values using an abiogenic polymerization model developed by Sherwood Lollar et al. (2008) using the following equations: $\delta^{13}C_{C2} = 1000\ln\alpha + \delta^{13}C_{CH4}$ (eq. 7), $\delta^{13}C_{C3} = 0.33\ \delta^{13}C_{CH4} + 0.66\ \delta^{13}C_{C2}$ (eq. 8), $\delta^{13}C_{nC4} = 0.25\ \delta^{13}C_{CH4} + 0.75\ \delta^{13}C_{C3}$ (eq. 9), and $\delta^{13}C_{nC54} = 0.2\ \delta^{13}C_{CH4} + 0.8\ \delta^{13}C_{C4}$ (eq. 10), where $\alpha = (1000 + \delta^{13}C_{C2})/(1000 + \delta^{13}C_{CH4})$ (eq. 11). The initial input data ($\delta^{13}C_{CH4}$ and $\delta^{13}C_{C2}$) for the abiogenic polymerization model were the average carbon isotope values of methane and ethane measured at the Tablelands.

Table 2.1 A comparison of average (± std, 1σ) aqueous geochemical parameters of spring waters.

	Freshwater Endmember	Mixing Springs with Freshwater Inputs					Ultra-Basic Endmember
	WHB	TLE	WB	WHC2c	WHC2b	WHC2a	WHC1
pH	7.6(± 0.7)	10.6 (± 0.5)	10.7(± 0.2)	11.8 (± 0.8)	12.3(± 0.3)	12.3(± 0.3)	12.2(± 0.2)
Eh (mv)	415 (± 26)	186 (± 55)	318(± 64)	-437 (± 229)	-552 (± 103)	-609 (± 118)	121 (± 12)
Cl- (mg/L)	3.7(± 0.23)	49 (± 61)	50 (± 61)	166 (± 17)	340(± 38)	403(± 40)	479(± 37)
Br- (mg/L)	0.009 (± 0.002)	0.29 (± 0.39)	0.29 (± 0.39)	0.37 (± 0.04)	0.79 (± 0.1)	0.89 (±0.09)	1.1 (± 0.06)
Mg^{2+} (mg/L)	13.3(± 1.3)	1.12(± 0.4)	1.47(± 0.05)	7.57(± 0.4)	1.12(± 0.7)	0.61(± 0.1)	0.06(± 0.01)
Ca^{2+}/Mg^{2+}	0.08 (± 0.01)	29 (± 18)	23 (± 20)	3 (± 0.3)	57 (± 42)	97 (± 9.0)	144 (± 5.0)
TIC (mg/L)	8.06 (± 1.7)	0.83 (± 0.5)	0.8 (± 1.0)	14.9 (± 2.5)	4.45 (± 6.3)	1.1 (± 0.5)	27.25 (± 15)
TIC $\delta^{13}C$ ‰	-1.7 (± 0.8)	-11.4 (± 2.4)	-18.6 (± 3.0)	-12.5 (± 0.8)	-16.2 (± 3.0)	-15.2 (± 2.9)	-29.4 (± 1.7)
DOC (mg/L)	0.46 (± 0.2)	0.16 (± 0.1)	0.19 (± 0.1)	1.24(± 0.4)	0.96 (± 0.6)	1.62 (± 1.0)	2.04 (± 0.6)
DOC $\delta^{13}C$ ‰	-27.1 (± 0.6)	-23.3 (± 0.5)	<d.l.	-23.7(± 1.5)	-22.1 (± 6.0)	-17.7 (± 1.8)	-18.2 (± 1.1)

<d.l.= less than detection limit

Table 2.2 Gaseous composition of spring waters

	TLE	WHC2c	WHC2b	WHC2a	WHC1
H_2 (mg/L)	0.13 to 0.36	0.07 to 0.57	0.47 to 1.04	0.47 to 1.18	0.06
CH_4 (mg/L)	<d.l.	0.03 to 0.05	0.04 to 0.32	0.16 to 0.38	0.03 to 0.06
C_2H_6 (mg/L)	<d.l.	0.004 to 0.03	0.01 to 0.03	0.02 to 0.04	0.004 to 0.01
C_3H_8 (mg/L)	<d.l.	0.01 to 0.03	0.01 to 0.04	0.03 to 0.05	0.004 to 0.01
nC_4H_{10} (mg/L)	<d.l.	0.01	0.01 to 0.02	0.01 to 0.02	0.004
nC_5H_{12} (mg/L)	<d.l.	0.01	0.01	0.01 to 0.02	0.004
nC_6H_{14} (mg/L)	<d.l.	0.005 to 0.01	0.01 to 0.02	0.02 to 0.04	0.004 to 0.01
C_1/C_{2+}	NA	0.68 to 3.65	2.78 to 3.78	2.62 to 3.14	3.08 to 3.72
$\delta^{13}C_{CH4}$	<d.l.	-15.9 to -26.3	-26.4 to -28.0	-26.4 to -27.7	-27.2 to -28.5

<d.l.= less than detection limit, NA= not analyzed

Table 2.3 Isotopic composition of total inorganic carbon, water, and carbonates

Site	Measured $\delta^{13}C_{TIC}$, ‰	Measured $\delta^{13}C_{CaCO3}$, ‰	Measured $\delta^{18}O_{CaCO3}$, ‰	Measured Avg. $\delta^{18}O_{H2O}$	T_M (°C)	Calculated $\varepsilon_{Calcite\text{-}CO2\,(g)}$ [a]	Calculated $\delta^{13}C_{CO2\,(g)}$ ‰ [b]	Calculated $\delta^{18}O_{CaCO3}$, ‰ [c]
WHC1	-30.6 to -28.2	-25.8 to -19.6	10.9 to 14.8	-9.5 (± 0.1)	21.3 to 24.3	10.1 to 10.4	-36.2 to -35.9	19.0 to 19.7
WHC2a	-19.8 to -13.0	-16.7 to -11.6	16.1 to 22.2	-11.0 (± 0.2)	10.5 to 15.5	11.1 to 11.7	-28.4 to -27.8	19.5 to 20.7
WHC2b	-19.2 to -12.5	-15.2 to -12.6	17.9 to 21.0	-10.8 (± 0.3)	10.4 to 16.2	11.0 to 11.7	-26.9 to -26.2	19.5 to 20.9
WHC2c	-13.3 to -16.5	-15.4 to -8.8	15.7 to 21.9	-10.5 (± 0.5)	11.3 to 17.2	10.9 to 11.6	-27.0 to -26.3	19.6 to 21.0
WB	-20.7 to -16.5	-16.7 to -9.9	14.6 to 19.2	-11.6 (± 0.1)	10.0 to 19.9	10.6 to 11.8	-28.5 to -27.3	17.9 to 20.2
TLE	-15.5 to -9.9	-15.2 to -6.2	14.7 to 19.8	-12.3 (± 0.1)	8.3 to 9.1	11.9 to 12.0	-27.2 to -27.1	19.7 to 19.9

T_M =Temperature measured, $\delta^{13}C$ reported vs. PDB and $\delta^{18}O$ reported vs. SMOW.

[a] Calculated equilibrium carbon enrichment between calcite and $CO_{2\,(g)}$ using fractionation equation: $1000\ln\alpha=1.435 \times 10^6/T^2 - 6.13$ (Bottinga, 1969)

[b] Calculated equilibrium $\delta^{13}C_{CO2\,(g)}$ using εcalcite-$CO_{2\,(g)}$ and measured $\delta^{13}C_{CaCO3}$

[c] Calculated equilibrium carbonate oxygen isotope composition using fractionation equation: $1000\ln\alpha=2.78 \times 10^6/T^2 - 2.89$ (O'Neil, 1969); corrected in (Friedman and O'Neil, 1977)

2.7 REFERENCES

Abrajano, T. A., N. Sturchio, B. M. Kennedy, G. L. Lyon, K. Muehlenbachs, and J. K. Bohlke, 1990, Geochemistry of reduced gas related to serpentinization of the Zambales ophiolite, Philippines: Applied Geochemistry, v. 5, p. 625-630.

Anderson, T. F., Arthur, M.A., 1983, Stable isotopes of oxygen and carbon and their application to sedimentologic and paleoenvironmental problems Stable Isotopes in Sedimentary Geology, v. 10, p. 11-1151.

Atreya, S. K., P. R. Mahaffy, and A. S. Wong, 2007, Methane and related trace species on Mars: Origin, loss, implications for life, and habitability: Planetary and Space Science, v. 55, p. 358-369.

Barnes, I., V. C. LaMarche, and H. G., 1967, Geochemical evidence of present-day serpentinization: Science, v. 156, p. 830-832.

Barnes, I., and J. R. O'Neil, 1971, Calcium-magnesium carbonate solid solutions from Holocene conglomerate cements and travertines in the Coast Range of California: Geochimica et Cosmochimica Acta, v. 35, p. 699-718.

Barnes, I., J. R. Oneil, and J. J. Trescases, 1978, Present Day Serpentinization in New-Caledonia, Oman and Yugoslavia: Geochimica Et Cosmochimica Acta, v. 42, p. 144-145.

Bernard, B., J. M. Brooks, and W. M. Sackett, 1977, A geochemical model for characterization of hydrocarbon gas sources in marine sediments: Offshore Technology Conference, Ninth, p. 435-438.

Blank, J. G., S. Green, D. Blake, J. W. Valley, N. T. Kita, A. Treiman, and P. F. Dobson, 2009, An alkaline spring system within the Del Puerto Ophiolite (California, USA): A Mars analog site: Planetary and Space Science, v. 57, p. 533-540.

Boston, P. M., M. V. Ivanov, and C. P. McKay, 1992, On the possibility of chemosynthetic ecosystems in subsurface habitats on Mars: Icarus, v. 95, p. 300-308.

Bottinga, Y., 1969, Calculated fractionation factors for carbon and hydrogen isotope exchange in the system calcite-carbon dioxide- graphite-methane-hydrogen-water vapor: Geochimica et Cosmochimica Acta, v. 33, p. 49-64.

Boynton, W. V., Ming, D.W., Kounaves, S.P., Young, S.M.M., Arvidson, R.E., Hecht, M.H., Hoffman, J., Niles, P.B., Hamara, D.K., Quinn, R. C., Smith, P.H., Sutter, B., Catling, D.C., and Morris, R.V., 2009, Evidence for Calcium Carbonate at the Mars Phoenix Landing Site: Science, v. 325, p. 61-64.

Brazelton, W. J., B. Nelson, and M. O. Schrenk, 2012, Metagenomic evidence for H2 oxidation and H2 production by serpentinite-hosted subsurface microbial communities: Frontiers in Extreme Microbiology: Deep Subsurface Microbiology Special Issue v. 2.

Brazelton, W. J., M. O. Schrenk, D. S. Kelley, and J. A. Baross, 2006, Methane- and sulfur metabolizing microbial communities dominate the Lost City hydrothermal field ecosystem: Applied and Environmental Microbiology, v. 72, p. 6257-6270.

Chastain, B., 2007, Methane clathrate hydrates as a potential source for martian atmospheric methane: Planetary and Space Science, v. 55, p. 1246-1256.

Clark, I., and P. Fritz, 1997, Environmental Isotopes in Hydrogeology: New York, Lewis Pubishers, 328 p.

Clark, I. D., J. C. Fontes, and P. Fritz, 1992, Stable Isotope Disequilibria in Travertine from High Ph Waters - Laboratory Investigations and Field Observations from Oman: Geochimica Et Cosmochimica Acta, v. 56, p. 2041-2050.

Coleman, R. G., and T. E. Keith, 1971, A chemical study of serpentinization-burro mountain, California: Journal of Petrology, v. 12, p. 311-328.

Craig, H., 1961, Isotopic variations in meteoric waters: Science, v. 133, p. 1702-1703.

Deines, P., 1980, The isotopic composition of reduced organic carbon, *in* P. Fritz, and J.-C. Fontes, eds., Handbook of Environmental Isotope Geochemistry, Elsevier, p. 329-406.

DesMarais, D. J., J. H. Donchin, N. L. Nehring, and A. H. Truesdell, 1981, Molecular carbon isotopic evidence for the origin of geothermal hydrocarbons: Nature, v. 292, p. 826-828.

Ehlmann, B. L., J. F. Mustard, and S. L. Murchie, 2010, Geologic setting of serpentine deposits on Mars Geophysical Research Letters, v. 37, p. L06201, doi:10.1029/2010GL042596.

Ehlmann, B. L., J. F. Mustard, S. L. Murchie, F. Poulet, J. L. Bishop, A. J. Brown, W. M. Calvin, R. N. Clark, D. J. Des Marais, R. E. Milliken, L. H. Roach, T. L. Roush, G. A. Swayze, and J. J. Wray, 2008, Orbital identification of carbonate-bearing rocks on Mars: Science, v. 322 p. 1828-1832.

Elthon, D., 1991, Geochemical evidence for formation of the Bay of Islands ophiolite above a subduction zone: Nature, v. 354, p. 140-143.

Etiope, G., M. Schoell, and H. Hosgörmezd, 2011, Abiotic methane flux from the Chimaera seep and Tekirova ophiolites (Turkey): Understanding gas exhalation from low temperature serpentinization and implications for Mars: Earth and Planetary Science Letters, v. 310, p. 96-104.

Formisano, V., S. Atreya, T. Encrenaz, N. Ignatiev, and M. Giuranna, 2004, Detection of methane in the atmosphere of Mars: Science, v. 306, p. 1758 - 1761.

Friedman, I., and J. R. O'Neil, 1977, Compilation of stable isotope fractionation factors of geochemical interest: M. Fleischer (Ed.) Data of Geochemistry, U.S. Geological Survey Professional Paper 440-KK, 6th ed., U.S.G.S., Reston VA.

Hamilton, V. E., and P. R. Christensen, 2005, Evidence for extensive, olivine-rich bedrock on Mars: Geology, v. 33, p. 433-436.

Hoefen, T. M., R. N. Clark, J. L. Bandfield, M. D. Smith, J. C. Pearl, and P. R. Christensen, 2003, Discovery of olivine in the Nili Fossae region of Mars: Science, v. 302, p. 627-630.

Holt, J. W., A. Safaeinili, J. J. Plaut, J. W. Head, R. J. Phillips, R. Seu, S. D. Kempf, P. Choudhary, D. A. Young, N. E. Putzig, D. Biccari, and Y. Gim, 2008, Radar Sounding Evidence for Buried Glaciers in the Southern Mid-Latitudes of Mars: Science, v. 322, p. 1235-1238.

Kelley, D. S., J. A. Karson, G. L. Fruh-Green, D. R. Yoerger, T. M. Shank, D. A. Butterfield, J. M. Hayes, M. O. Schrenk, E. J. Olson, G. Proskurowski, M. Jakuba, A. Bradley, B. Larson, K. Ludwig, D. Glickson, K. Buckman, A. S. Bradley, W. J. Brazelton, K. Roe, M. J. Elend, A. Delacour, S. M. Bernasconi, M. D. Lilley, J. A.

Baross, R. T. Summons, and S. P. Sylva, 2005, A serpentinite-hosted ecosystem: The lost city hydrothermal field: Science, v. 307, p. 1428-1434.

Mahaffy, P., 2008, Exploration of the Habitability of Mars: Development of Analytical Protocols for Measurement of Organic Carbon on the 2009 Mars Science Laboratory: Space science reviews, v. 135 (1-4), p. 255-268.

Mahaffy, P., 2012, The Sample Analysis at Mars Investigation and Instrument Suite: Space science reviews, p. 1-78.

Max, M. D., and S. M. Clifford, 2000, The state, potential distribution and biological implications of methane in the Martian crust: J. Geophys. Res., v. 105, p. 4165-4171.

McAuliffe, C., 1971, GC determination of solutes by multiple phase equilibration: Chemical Technology, v. 1, p. 46-51.

McEwen, A., 2011, Seasonal Flows on Warm Martian Slopes: Science (New York, N.Y.), v. 333, p. 740-743.

Mook, W. G., 1974, Carbon isotope fractionation between dissolved bicarbonate and gaseous carbon dioxide: Earth and Planetary Science Letters, v. 22, p. 169-176.

Mumma, M. J., G. L. Villanueva, R. E. Novak, T. Hewagama, B. P. Bonev, M. A. DiSanti, A. M. Mandell, and M. D. Smith, 2009, Strong Release of Methane on Mars in Northern Summer 2003: Science, v. 323, p. 1041-1045.

Mustard, J. F., S. L. Murchie, S. M. Pelkey, B. L. Ehlmann, R. E. Milliken, J. A. Grant, J. P. Bibring, F. Poulet, J. Bishop, E. N. Dobrea, L. Roach, F. Seelos, R. E. Arvidson, S. Wiseman, R. Green, C. Hash, D. Humm, E. Malaret, J. A. McGovern, K. Seelos, T. Clancy, R. Clark, D. Des Marais, N. Izenberg, A.

Knudson, Y. Langevin, T. Martin, P. McGuire, R. Morris, M. Robinson, T. Roush, M. Smith, G. Swayze, H. Taylor, T. Titus, and M. Wolff, 2008, Hydrated silicate minerals on mars observed by the Mars reconnaissance orbiter CRISM instrument: Nature, v. 454, p. 305-309.

Niles, P. B., W. V. Boynton, J. H. Hoffman, D. W. Ming, and D. Hamara, 2010, Stable isotope measurements of martian atmospheric CO2 at the Phoenix landing site: Science, v. 329, p. 1334-1337.

O'Neil, J. R., and I. Barnes, 1971, Cl3 and 018 compositions in some fresh-water carbonates associated with ultramafic rocks and serpentinites: western United States: Geochimica et Cosmochimica Acta, v. 35, p. 687-697.

Oze, C., and M. Sharma, 2007, Serpentinization and the inorganic synthesis of H2 in planetary surfaces: Icarus, v. 186, p. 557-561.

Quesnel, Y., C. Sotin, B. Langlais, S. Costin, M. Mandea, M. Gottschalk, and J. Dyment, 2009, Serpentinization of the martian crust during Noachian: Earth and Planetary Science Letters, v. 277, p. 184-193.

Rogers, A. D., and P. R. Christensen, 2007, Surface mineralogy of Martian low-albedo regions from MGS-TES data: Implications for upper crustal evolution and surface alteration: Journal of Geophysical Research E: Planets v. 112.

Romanek, C. S., E. L. Grossman, and J. W. Morse, 1992, Carbon isotopic fractionation in synthetic aragonite and calcite; effects of temperature and precipitation rate: Geochimica et Cosmochimica Acta, v. 56, p. 419-430.

Rudd, J. W. M., R. D. Hamilton, and N. E. R. Campbell, 1974, Measurement of microbial oxidation of methane in lake water: Limnology and Oceanography, v. 19, p. 519-524.

Schulte, M., D. Blake, T. Hoehler, and T. McMcCollom, 2006, Serpentinization and its implications for life on the early Earth and Mars: Astrobiology, v. 6, p. 364-376.

Schulz, H., 1999, Short history and present trends of Fischer-Tropsch synthesis: Applied Catalysis A: General., v. 186, p. 3-12.

Sherwood Lollar, B., G. Lacrampe-Couloume, G. F. Slater, J. A. Ward, D. P. Moser, T. M. Gihring, L.-H. Lin, and T. C. Onstott, 2006, Unravelling abiogenic and biogenic sources of methane in the Earth's deep subsurface: Chemical Geology, v. 226, p. 328-339.

Sherwood Lollar, B., G. Lacrampe-Couloume, K. Voglesonger, T. C. Onstott, L. M. Pratt, and G. F. Slater, 2008, Isotopic signatures of CH4 and higher hydrocarbon gases from Precambrian Shield sites: A model for abiogenic polymerization of hydrocarbons: Geochimica et Cosmochimica Acta, v. 72, p. 4778-4795.

Sleep, N. H., A. Meibom, T. Fridriksson, R. G. Coleman, and D. K. Bird, 2004, H2-rich fluids from serpentinization: Geochemical and biotic implications: Proceedings of the National Academy of Sciences, v. 101, p. 12818 -12823.

Stevens, R. K., 1988, Ophiolite Oddities:preliminary notices if nephrite jade, Sr-aragonite, troilite, and hyperalkaline springs from Newfoundland, GAC MAC Joint Annual Meeting, St. John's, Newfoundland.

Suen, C. J., F. A. Frey, and J. Malpas, 1979, Bay of Islands ophiolite suite, Newfoundland: Petrologic and geochemical characteristics with emphasis on rare

earth element geochemistry: Earth and Planetary Science Letters, v. 45, p. 337-348.

Uchikawa, J., and R. E. Zeebe, 2012, The effect of carbonic anhydrase on the kinetics and equilibrium of the oxygen isotope exchange in the CO2,ÄìH2O system: Implications for Œ¥18O vital effects in biogenic carbonates: Geochimica Et Cosmochimica Acta, v. 95, p. 15-34.

Whiticar, M. J., 1999, Carbon and hydrogen isotope systematics of bacterial formation and oxidation of methane: Chemical Geology, v. 161, p. 291-314

Chapter 3: Microbial Community Composition and Cycling of Carbon in the Ultra-basic and Reducing Springs at a Site of Serpentinization in the Tablelands- Gros Morne National Park

3.1 ABSTRACT

Highly reducing and ultrabasic springs at a site of active serpentinization in the Tablelands Ophiolite in Gros Morne National Park, Newfoundland hosts an extreme environment for a thriving microbial community. However, little is known about the microbial community that exists at sites of serpentinization.

A variety of different possible substrates are available to the microbial community including large amounts of H_2 gas and variable amounts of dissolved inorganic and organic carbon compounds. Likewise, non-microbial methane and low molecular weight hydrocarbons have been previously detected in the springs, and may provide a carbon substrate for the microbial community. This study uses lipid profiling to identify the microbial community that thrives in the reducing and ultra basic springs at the surface and possibly in the subsurface. Lipid biomarkers identified a microbial community dominated by gram-negative bacteria with lesser amounts of microeukaryotes, gram-positive bacteria, fungi, and lipid biomarkers belonging to non-specific bacteria. Additionally, an integrated lipid profiling and isotope approach was used in identifying both autotrophic and heterotrophic metabolisms.

3.2 INTRODUCTION

Serpentinization,- the hydration of olivine in ultramafic rocks,- produces an abundance of hydrogen (H_2) gas and associated fluids that are highly reducing and ultra-basic. This reaction produces conditions favourable for both abiogenic synthesis of methane and other hydrocarbons while also producing conditions amenable for chemosynthetic microbial metabolisms such as methanogenesis. Locations where serpentinization is occurring have been reported worldwide including: the Lost City Hydrothermal Vent Field (LCHF) which is a marine location (Kelley et al., 2001), deep subsurface mines (Sherwood Lollar et al., 2002); and other continental locations (i.e., ophiolites) including Oman (Barnes et al., 1978; Neal and Stanger, 1983), Turkey (Hosgormez, 2006; Etiope et al., 2011b), Zambales, Philippines (Abrajano et al., 1990), and in Cazadero, California (Barnes et al., 1967; Morrill et al., submitted). At these sites, both abiogenic methane and biogenic methane production have been reported (Barnes et al., 1967; Abrajano et al., 1988; Sherwood Lollar et al., 2002; Kelley, 2005; Morrill et al., 2008; Etiope et al., 2011b). Additionally, hydrocarbons can be synthesized through the thermal degradation of sedimentary organic matter (i.e., thermogenesis) which commonly underlie an ophiolite complex. Evidence for thermogenic synthesis has been reported at a site of serpentinization in Terikova, Turkey (Etiope et al., 2011b). There has been a great deal of emphasis on the geochemistry at locations of serpentinization, however little is known about the microbial community that may exist at these sites.

The Tablelands Ophiolite in Gros Morne National Park, Newfoundland is experiencing active serpentinization in its subsurface as evidenced by springs found near serpentinized peridotites that are ultra-basic (pH ≥ 10), calcium rich, highly reducing and

linked with the production of hydrogen gas (Chapter 2). Associated work has shown that the methane produced at the Tablelands springs is non-microbial and attributed to thermogenic or possible abiogenic origin (Szponar et al., In Press).

The land cover at the Tablelands is primarily peridotite rocks. Perdotites lack the usual nutrients to sustain plant life. Peridotites limit plant growth by having high magnesium content, and toxic amounts of heavy metals (e.g., Ni; (Berger et al., 1992). Therefore, the Tablelands is mostly barren with limited plant growth (Berger et al., 1992). Additionally, the ultra-basic and reducing springs at the Tablelands provide an extreme environment for microbial communities. Similar to other sites of serpentinization, the microbial community that potentially exists at the Tablelands is poorly understood. Studying the microbial community that exists in the ultra-basic springs in the Tablelands can help provide information about life in these extreme environments and likewise provide a window to possible communities that may exist in the deep subsurface.

Previous genomic data have shown the presence of hydrogen oxidizers and hydrogen producers in the ultra-basic springs at the Tablelands (Brazelton et al., 2012). However, little is known about the microbial cycling of carbon in the springs. Phospholipid fatty acids (PLFA) are integral components of bacterial cell membranes which can be used to profile the structure of microbial communities, detect shifts in microbial ecology, and compare carbon turnover in different ecosystems *in situ* (Steinberger et al., 1999; Boschker et al., 2002; Kramer and Gleixner, 2006). Likewise, different PLFA indicator compounds can be used to identify specific groups of microorganisms such as bacteria, fungi, algae, or protozoa (Steinberger et al., 1999).

Phospholipid fatty acids have natural abundance $\delta^{13}C$ signatures directly related to the $\delta^{13}C$ value of the carbon pool used by bacteria for metabolic processes (Boschker and Middelburg, 2002). Phospholipids turnover quite rapidly during metabolism and therefore are indicative of a viable biomass (White, 1979). Therefore, the isotopic composition of PLFA is indicative of the carbon source of the active microbial community (Vestal and White, 1989). Isotopic analysis of both dissolved organic carbon (DOC) and total inorganic carbon (TIC) pools can be compared to the isotopic composition of PLFA to identify heterotrophic and autotrophic metabolisms, respectively. Large carbon isotope fractionations between TIC and PLFA are associated with autotrophic metabolism relative to minimal isotopic fractionation between DOC and PLFA in heterotrophic metabolism. Therefore, carbon-isotope fractionations can provide useful information about possible substrates used by the microbial community and possible biosynthetic pathways.

The overall objective of the study was to identify microbial community composition in the ultra-basic springs and identify possible microbial metabolisms. The first aim of the study was to identify a viable biomass in the ultra-basic and reducing springs and determine the relative microbial abundance. A handheld field instrument, (i.e., Limulus Amoebocyte Lysate (LAL) assay) was used for a qualitative observation of living biomass in the springs, specifically detecting gram-negative bacteria. Cell counts on fluids and rocks were used to obtain relative biomass abundance in the springs. The second aim of the study was to identify the microbial community composition and possible autotrophic and heterotrophic metabolisms. Phospholipid biomarkers were used

to identify groups of microorganism that are living in the springs. Autotrophic and heterotrophic metabolisms were determined by comparing the carbon isotope composition ($\delta^{13}C$) of reduced and oxidized carbon reservoirs to the $\delta^{13}C$ value of PLFA and the total biomass, and their fractionations respectively.

3.3 SAMPLING AND ANALYTICAL METHODS

3.3.1 Site Description

The Tablelands Ophiolite is situated in Gros Morne National Park, Newfoundland, Canada. Active serpentinization is occurring in the subsurface of the Tablelands as evidenced by highly reducing, ultra-basic springs discharging from serpentinized peridotites, surrounded by calcium carbonate travertine deposits. The spring fluids are Ca^{2+}-OH^- type waters contributing to inorganic carbon precipitates as carbonate sediment in the spring fluids and travertines near spring discharge outlets (see Chapter 2). A site of serpentinization at Winter House Canyon (WHC) was selected for this study. WHC contains two sampling pools (i.e., WHC1 and WHC2) that are continually recharged with ultra-basic reducing water. WHC1 is a shallow pool (approximately 2 cm deep, 5 cm wide) of ultra-basic spring water seeping from the travertine deposit and located approximately a meter from WHC2. This pool recharges at rate of 1mL/min, and no freshwater inputs to WHC1 were indentified. The ultra-basic water at WHC1 is exposed to the atmosphere and thus redox values measured reflect more positive values (~Eh of 137mV; pH of 12.7). In this study WHC1 was sampled for microbial abundance in fluids using Limulus Amoebocyte Lysate measurements only. Not enough carbonate sediment could be collected at WHC1 for lipid analysis.

WHC2 was selected to study the geo-biological interactions due to large redox and nutrient gradients within the pool. WHC2 is larger (approximately 0.5 meter deep, 1 meter wide). In particular, two highly reducing ultra-basic (~Eh of -600 to -700mvV; pH of 12.3 to 12.6) spring discharge points are located at the bottom of the WHC2 pool (labelled WHC2a and WHC2b). A third sampling location that receives trickling freshwater input from overland flow was selected for this study (labelled WHC2c), The WHC2c site was selected because it is a mixing site with large redox (~Eh of -100mV to – 470mV) and nutrient gradients. Additionally, Winter House Brook (WHB) which flows along the bottom of Winter House Canyon was chosen as the freshwater end member and used to compare Limulus Amoebocyte Lysate (LAL) measurements from the ultra-basic springs.

3.3.2 LAL Assay

The Limulus Amoebocyte Lysate (LAL) Assay was employed at the Tablelands to find traces for life in the ultra-basic springs. The LAL assay used was part of the Endosafe®- PTS (Portable Test System) which contains a sample test cartridge and a hand-held spectrophotometer. The LAL assay uses the LAL enzyme found uniquely in horseshoe crabs to detect gram-negative cell walls of bacteria by reacting with the endotoxins in the cells (Watson et al., 1977). Endotoxins from the gram-negative bacteria degrade rapidly between 15 to 30 min and therefore the LAL assay can detect live cells. In particular, the LAL assay detects single celled microorganisms (i.e., gram negative bacteria), in terms of endotoxin units per ml of fluid.

The instrument was calibrated using cartridges with a tolerance range of 0.01, 0.05, and 0.1-10 EU/mL (R^2=0.99). The quantification limit for this study was determined to be 200EU/ml based on a 1:20 dilution of the sample. Sampling locations WHC2b and WHC2c, and WHB were swabbed in triplicate for life detection using the LAL assay. A dilution of 1:400 was applied for sample WHC1 and dilutions of 1:20 were applied for samples WHC2b and WHC2c to obtain a reading on the instrument within the calibration curve. Nuclease free water was used as a control to test the LAL assay to ensure corrections were made for non-vital reactivity and luminescence. Error associated with the LAL endocrine concentrations is ± standard deviation (1σ) associated with single injections of a triplicate sample.

3.3.3 Microscopic Cell Abundance

Fluids and carbonate sediment were collected for cell counts in June 2010. Fluid samples were collected in 50ml sterile falcon tubes and fixed with 10 ml of 37% formalin. After one to six hours, the fixed samples were filtered using vacuum filtration through 0.22µm black polycarbonate membrane filters (Millipore). The collected cells were stained for 20 min using a 2.0 µg/ml solution of 4',6' diamidino-2phenylindole (DAPI) (Porter and Feig, 1980). A 10ml volume of sample was filtered in triplicate. The filters were then placed onto microscope slides, using type A immersion oil and stored at -20°C in the dark.

Cells were extracted from carbonate sediment using a modified extraction method by Chevaldonné and Godfroy (1997). Carbonate sediment samples were collected in 60ml falcon tubes and submersed in 2% paraformaldehyde/phosphate buffered saline solution

(PFA:PBS). The mixture was sonicated for 30 min, and centrifuged. The supernatant was transferred to eppendorf tubes, and vortexed for 30-60 sec. Extracts were filtered at 0.1ml and 0.5ml following the procedure as per fluid samples. The carbonate sediment sample was air dried and weighed. Average cell counts were determined per ml and converted to weight specific counts by multiplying volume based counts by the total volume extracted and dividing by the dry weight of the carbonate sediment sample. Based on extraction efficiencies determined for extracting cells from solid samples by Chevaldonné and Godfroy (1997) a similar extraction efficiency of 46% is assumed for this study.

Cell counts were determined on both fluid and carbonate sediments at East Carolina University on an Olympus BX61 Spinning Disk epiflourescence confocal microscope (100x magnification) using blue light excitation. Cell abundance values are reported as average cells counted per gram of mineral (dry weight) for carbonate sediment and average cells counted per mL for fluid samples. The minimum detection limit on bacterial cell counts was 10^3cells/mL Upper and lower 95% confidence intervals for average cell counts are listed in Table 3.1.

3.3.4 Dissolved organic matter and total inorganic carbon

Fluid samples were collected for dissolved organic carbon (DOC) and total inorganic carbon (TIC) concentration, and stable carbon isotope ($\delta^{13}C$) analysis. Samples for DOC were filtered through a 0.7µm pre-combusted glass microfiber filter using a 60ml syringe and filter holder. A 30mL filtered sample was collected in pre-combusted 40mL amber vials spiked with 20% phosphoric acid (H_3PO_4) Samples for TIC were collected without headspace in pre-combusted 40mL amber vials spiked with mercuric

chloride ($HgCl_2$). DOC and TIC concentrations and $\delta^{13}C$ values were determined using an OI Analytical Aurora 1030 TOC Analyzer equipped with a reduction furnace, water trap, and packed GC column; coupled to a ThermoElectron DeltaVPlus Isotope Ratio Mass Spectrometer (IRMS) system via a Conflo III interface, or a Finnigan MAT252 IRMS via a Conflo II interface. The Aurora uses a wet chemical oxidation process to extract carbon as CO_2 gas using phosphoric acid for TIC and Na-persulfate for total DOC. Error associated with DOC and TIC concentration were less than ±0.5‰ for $\delta^{13}C$. The error determination is based on the ± mean standard deviation (1σ) on triplicate samples, which incorporates both instrumental error and error from samples run in triplicate. Isotopic standards with a concentration range of 0.50mg/L to 20mg/L were used for calibration for of both TIC and DOC. TIC samples ≤ 0.10 mg/L and DOC samples ≤ 0.50 mg/L were below detection for carbon isotope analysis. Therefore the $\delta^{13}C$ values of TIC and DOC are only reported for samples with measured concentrations greater than 0.10mg/L and 0.50 mg/L respectively. $\delta^{13}C$ values are reported in delta notation using the following relationship (Equation 1):

$$\delta^{13}C\ (‰) = [(^{13}C/^{12}C_{sample})/ (^{13}C/^{12}C_{standard})-1] \times 1{,}000 \quad [1]$$

where, $^{13}C/^{12}C_{standard}$ is the carbon isotope ratio of the international Vienna Pee Dee Belemnite (PDB) reference standard. All carbon isotope data is reported relative to PDB.

3.3.5 C/N ratios and $\delta^{13}C$ of bulk organic matter

Carbonate sediment was collected at the bottom of the Winter House Canyon (WHC2) spring for bulk organic matter (OM) analysis. The bulk organic matter is a

combination of both living and non living material (i.e., detritus). Source information on the OM can be obtained by analyzing the elemental and isotope composition of the OM. Bulk OM was analyzed for percent carbon and nitrogen to determine C:N ratios, and carbon isotope composition. Carbonate sediments were treated three times with 5M HCl to remove any inorganic carbon and oven-dried at 40°C overnight. Samples were grounded using a mortar and pestle and stored in 4ml pre-combusted glass vials prior to analysis. The percent carbon and nitrogen of the OM was measured using a Carlo Erba NA1500 Series II Elemental Analyzer (EA) calibrated using an internal sulfanilamide standard with a known carbon and nitrogen ratio. Replicate analysis (n=5) of the sulphanilamide standard gave a precision of less than ± 0.3% (1σ) for both carbon and nitrogen.

Stable carbon isotope values of organic matter ($\delta^{13}C_{OM}$) were measured on the EA coupled to a ThermoElectron DeltaVPlus Isotope Ratio Mass Spectrometer (IRMS), calibrated with the sulfanilamide standard, and using isotopically characterized MUN-CO_2 Suprapur $CaCO_3$ and IAEA- CH-6 Sucrose as check standards. Check standards were isotopically characterized at Memorial University of Newfoundland. Replicate analyses of checks standards (n=5) and duplicate analysis of samples (n=2) gave a precision of less than ±0.3‰ (1σ). The $\delta^{13}C_{OM}$ value of bulk organic carbon is reported in standard notation (Equation 1) relative to PeeDee Belemnite (PDB). Error associated with $\delta^{13}C_{OM}$ is ± 0.3‰, which incorporates both instrumental error and error from samples prepared and ran in duplicate.

3.3.6 Phospholipid Fatty Acid identification and quantification

Phospholipid fatty acid (PLFA) analyses were performed on lyophilized carbonate sediment samples collected from the three sampling sites (WHC2a, WHC2b, and WHC2c) within the WHC pool. Only one sample, WHC2c from June 2010 was used to determine PLFA recovery. This sample was split into two subsamples. Only one WHC2c June 2010 subsample was spiked with a PLFA standard (1,2-diheptadecanoyl-sn-glycerol-3phosphocholine from Avanti Polar Lipids) to determine PLFA recovery, and the other was used for comparison. Both WHC2c 2010 subsamples were extracted separately, to determine reproducibility on the extraction method. PLFAs were extracted from the lyophilized carbonate sediment samples using a modified Bligh and Dyer method (Bligh and Dyer, 1959). Neutral and glycolipids were further isolated using solid phase silica gel chromatography. Phospholipids were converted to fatty acid methyl esters (FAMEs) by mild alkaline methanolysis (Guckert et al., 1985). FAMEs were separated using an Agilent 6890 Gas Chromatography (GC) (30m x 0.25mm BPX-70 column, 30m x 0.32mm, 0.25μm film thickness) interfaced with an Agilent 5973 mass spectrometer and quantified using an Agilent 6890 equipped with a flame ionization detector. The temperature program used was 70°C, ramp at 10°C/min to 160°C, hold for 5 min, ramp at 4°C/min to 280°C, hold for 20min. FAMES were identified using a bacterial reference standard (Bacterial Acid Methyl Esters (BAME) CP Mix, Matreya Inc, mass-fragment patterns, and retention times. FAMEs were quantified using external FAME standards of different carbon chain length: C_{14}, C_{15},C_{16}, C_{17}, C_{18}, C_{19}, C_{20}. Ethyl ester $C_{20:0}$ FAMEs generated from PLFA are designated according to $C_{n:m}$, where *n* is the number of carbon atoms in the chain and *m* is the number of double bonds. Recovery of PLFA on the

WHC2c June 2010 sample was better than 65%. PLFA are reported as mol% relative to the total PLFA. Reproducibility on WHC2c June 2010 subsamples was < 10% relative standard deviation. Therefore, an assumed error of ± 10% is applied to mol% of all PLFA samples quantified.

3.3.7 Phospholipid fatty acid stable isotope analysis

Compound-specific stable carbon isotope analyses of fatty acid methyl esters (FAMEs) were performed on an Aglilent 6890 GC interfaced with a Finnigan MAT 252 stable isotope mass spectrometer via a Conflo II interface. Precision and accuracy of $\delta^{13}C_{PLFA}$ analyses were determined by multiple injections and compared to a commercially available bacteria methyl ester $\delta^{13}C$ standard mixture supplied by Indiana University. Reproducibility for isotopically characterized Indiana standards was better than ±0.6‰ (1σ, n=8).

FAMEs were injected into a split/splitless injector set to splitless at 300°C prior to separation on a gas chromatography capillary column (BPX-70, 50m, 0.32 mm internal diameter, 0.3um film thickness). The temperature program used was the same as for lipid quantification. A small aliquot of methanol used during methylation was analyzed for its $\delta^{13}C$ value on an OI Analytical Aurora 1030 TOC Analyzer coupled to a Finnigan MAT252 IRMS. FAME $\delta^{13}C$ values were corrected for the added methyl carbon via the relationship (Equation 2):

$$\delta^{13}C_{FAME} = [(N+1)*\delta^{13}C_{measured} - \delta^{13}C_{MEOH}]/N \quad [2]$$

where N is the number of carbon atoms. All the $\delta^{13}C$ values are reported in standard delta notation (Equation 1) relative to PeeDee Belemnite (PDB) reference material.

3.3.8 Data Analysis

Data were statistically analysed using Excel (Microsoft Excel; release 12.2.3, 2008) and StatPlus (Mac OS; version 2009) software (Appendix B). Normal distribution of data was determined in StatPlus using the Kolmogorov-Smirnov/Lilliefor Test based on the maximum difference between the sample cumulative distribution and the hypothesized cumulative distribution; the Shapiro-Wilk W using power properties to compute normality; and the D'Agostino test based on the skewness coefficient, the kurtosis coefficient, and combination of both coefficients. In cases where data were not normally distributed, non-parametric analysis was employed in addition to parametric analysis. An equal-variance t-test or "General Linear Model" analysis of variance ANOVA was used. The Mann-Whitney U test or Wilcoxon Rank-Sum Test: a non-parametric substitute for the equal-variance t-test was used when the assumption of normality was not valid. The non-parametric test for difference of medians (Kruskall-Wallis Test) was used to test differences between sampling times and between sampling locations for stable carbon isotope values and C:N ratios of organic matter; stable carbon isotope values and concentrations of total inorganic carbon (TIC) and dissolved organic carbon (DOC).

Upper and lower 95% confidence intervals were computed for cell counts (Table 3.1). A Model II regression (Reduced Major Axis Regression) was also employed using

Excel on data where a relationship was being determined between two variables having error as both dependant and independent variables (Riggs et al., 1978). In particular, the Model II regression was employed to determine the relationship between the fractionation in fatty acids and TIC, and the fractionation between fatty acids and DOC.

3.4 RESULTS

3.4.1 Life detection in ultra-basic springs

As a first line of evidence for life detection in the ultra-basic springs, the Limulus Amoebocyte Lysate (LAL) Assay was deployed in the field due to its advantage of detecting viable biomass in *situ*. In particular, the LAL assay detects endotoxins which are a major constituent of the outer cell wall of gram-negative bacteria (Table 3.1). Endotoxins from the gram-negative bacteria degrade rapidly, within 15 to 30 min, following cell lyses, and therefore, the LAL assay gives the advantage of detecting live viable cells *in situ*. However, LAL results are to be seen as qualitative measurements of the relative abundance of gram-negative bacteria in the different sampling locations. The LAL assay detected the least amount of endotoxins units (EU) in the freshwater endmember WHB (5 ± 0.3 EU/mL, pH 8.5, Eh +439mV); followed by ultrabasic spring WHC1 (45 ±11EU/mL, pH 12.3, Eh +137mV); WHC2b (62±10 EU/ml, pH 12.6, Eh -642); and above detection limits at WHC 2c (>200 EU/mL, pH 11.5, Eh -468mV). The error associated with endotoxin concentrations represents the reproducibility on a triplicate sample (1σ, n=3).

The LAL assay is limited to detecting only gram-negative bacteria, and thus is not a quantitative measurement of the entire microbial community that exists in the springs. Therefore quantitative measurements of microbial abundance using traditional laboratory cell counts were employed (Table 3.1). Cell counts were measured on fluids and carbonate sediments. Average cell concentrations in the carbonate sediment from WHC2a and WHC2b were $4.88x10^8$ and $1.25x10^9$ cell/g (wet weight), respectively. Cell counts from the ultra basic fluids at WHC2a were $1.67x10^5$ cells/ml, $7.14x10^4$ cells/ml at WHC2b and $2.12x10^4$ cells/ml at WHC2c.

3.4.2 Organic matter analysis and carbon isotope composition

Organic matter (OM) in carbonate sediment was studied to determine its source in the ultrabasic springs. Composed of either living or once living organisms, OM can also be the product of decomposition and/or capable of decomposition. Therefore, OM can be used as biomass (energy source) for the microbial community that exists in the springs. Elemental (i.e., C:N) and stable carbon isotopic composition ($\delta^{13}C_{OM}$) of bulk organic matter (OM) can provide information about the source of OM. Table 3.2 lists C:N ratios and $\delta^{13}C_{OM}$ values for bulk organic matter from carbonate sediments collected from WHC2a, WHC2b, and WHC2c in June and August 2012, and June 2011. Comparison between spring locations and between sampling years are made in attempt to identify significant differences and changes in microbial biomass.

No significant difference (Kruskall-Wallis ANOVA) in $\delta^{13}C_{OM}$ was observed between spring locations WHC2a, WHC2b, and WHC2c sampled in June and August 2010 and June 2011. A significant annual difference (Mann Whitney U) on average

$\delta^{13}C_{OM}$ from all sampling locations was observed between June 2010 and June 2011 ($p<0.05$). Average $\delta^{13}C_{OM}$ on OM samples from June 2010 was -26.8±0.3‰ (n=3, 1σ); and -25.7 ± 0.2 ‰ (n=3, 1σ) for June 2011. In general., the average $\delta^{13}C_{OM}$ value measured in 2011 was higher by ~1‰ than the average $\delta^{13}C_{OM}$ value measured in 2010.

No significant difference (Kruskall-Wallis ANOVA) between C:N ratios on OM was observed between spring locations WHC2a, WHC2b, and WHC2c sampled in June and August 2010 and June 2011. However a significant annual difference (Mann Whitney U) on average C:N ratios of OM from all spring locations was observed between June 2010 and June 2011 ($p<0.05$). The average C:N ratio on OM in June 2010 was 14.6±1.4 (n=3, 1σ), and higher than the average C:N ratio 12.1 ± 0.2 (n=3,1σ) for June 2011.

3.4.3 DOC and TIC analysis

The concentrations and $\delta^{13}C$ values of dissolved organic carbon (DOC) and total inorganic carbon (TIC) were measured to characterize the bulk oxidized and reduced pools of dissolved carbon in the ultra-basic springs and to determine the changes in these pools over the summer season and between two years. DOC and TIC concentrations and carbon isotope values are listed in Table 3.2.

No significant difference (Kruskall-Wallis ANOVA) in average DOC concentrations and $\delta^{13}C_{DOC}$ values was observed between spring locations (i.e., WHC2a, 2b, 2c). Likewise no significant annual difference (Mann Whitney U) in average DOC concentrations and $\delta^{13}C_{DOC}$ values was observed between June 2010 and June 2011 for all spring locations.

A significant difference (Kruskall-Wallis ANOVA) in average TIC concentration was observed between spring locations (i.e., WHC2a, 2b, 2c), with the lowest TIC concentrations in WHC2a, followed by WHC2b, and highest TIC concentrations in WHC2c (Table 3.2).

No significant difference (Kruskall-Wallis ANOVA) in average $\delta^{13}C_{TIC}$ was observed between spring locations (i.e., WHC2a, 2b, 2c) sampled in 2010 and June 2011. Likewise no significant annual difference (Mann Whitney U) in average $\delta^{13}C_{TIC}$ was observed between June 2010 and June 2011 for all spring locations.

3.4.4 Phospholipid fatty acids analysis

Changes in microbial community structure between sampling sites, over the 2010 summer season (June and August 2010), and over a one year period (between 2010 and June 2011) were determined by analyzing the distribution of different types of PLFA (i.e., monounsaturated, polyunsaturated, saturated, branched, and cyclic fatty acids) at each sampling location (Figures 3.1, 3.2, 3.3). The PLFA composition of the biomass calculated as mol% of the total PLFA from carbonate sediment collected in the ultra-basic springs is listed in Table 3.3. PLFA can be grouped based on their carbon structure.

Figure 3.4 plots the relative abundance of fatty acids by mol% of PLFA group. In general, monounsaturated fatty acids comprised the majority of the total PLFA at all sampling sites during June and August 2010, and June 2011 with the exception of WHC2a from June 2010 where the majority of PLFA were comprised of shorter saturated straight chain fatty acids (<20 carbon atoms: comprising of C_{14} to C_{18}); followed by polyunsaturated fatty acids, saturated fatty acids (>20C: comprising of C_{19} to C_{24}),

branched fatty acids, and cyclic fatty acids. The total mol% of monounsaturated fatty acids ranged from 31.8 to 56.5%; from 14.8 to 36.3 mol% of the shorter (<20 carbons atoms) saturated fatty acids; from 13.1 to 26.8 mol% of the polyunsaturated fatty acids; from 2.2 to 14.7 mol% of the longer (>20 carbon atom) saturated fatty acids; 2.4 to 10.2% of the branched fatty acids; and 0 to 1.4 mol% of the cyclic fatty acids. No significant difference (Mann Whitney U) in the mol% of PLFA values was observed between June and August 2010 at spring locations WHC2b and WHC2c and between June 2010 and June 2011 at spring locations WHC 2a and WHC2c for all groups.

3.4.5 Isotopic composition of PLFA

Differences in carbon substrate and metabolic pathways between sampling sites, over the 2010 summer season, and over a one year period (between June 2010 and June 2011) were determined by analyzing the $\delta^{13}C$ value of each PLFA at each sampling location. Likewise, the difference in the $\delta^{13}C$ value of PLFA between monounsaturated, branched, polyunsaturated, and short carbon chained saturated fatty acids were also determined. The $\delta^{13}C$ value of PLFA from carbonate sediments collected from ultra-basic springs in June, August 2010 and June 2011 are presented in Table 3.3, and are shown in Figures 3.1, 3.2, and 3.3.

A significant difference (Mann Whitney U) in the PLFA $\delta^{13}C$ values of all fatty acids (i.e., monounsaturated, branched, polyunsaturated, and saturated (<20C) fatty acids) was observed between from June 2010 and June 2011 at spring locations WHC2a and WHC2c. No significant difference (Mann Whitney U) in the PLFA $\delta^{13}C$ values of all fatty acids [i.e., monounsaturated, branched, polyunsaturated, and saturated (<20C) fatty

acids] was observed between from June and August 2010 at spring locations WHC 2b and WHC2c. In general., PLFA $\delta^{13}C$ values of fatty acids from samples collected in June 2011 are more enriched in ^{13}C than $\delta^{13}C_{PLFA}$ values collected in 2010.

3.5 DISCUSSION

3.5.1 Evidence for life in the ultra-basic reducing springs

A geochemical study of the ultra-basic springs at the Tablelands determined that the methane in the fluids is non-microbial in origin (Chapter 2). However, extant life was detected in the extreme pH environment of the ultra-basic reducing springs using the Limulus Amoebocyte Lysate (LAL). In particular, the LAL detected gram-negative bacteria at all ultra-basic springs measured.

Cell counts from fluids and carbonate sediments sediment in the ultra-basic reducing springs provide quantitative measurements of the viable biomass that can exist in the extreme pH environment. High cell counts were determined in carbonate sediments (10^8-10^9 cells/g) and in spring fluids (10^4-10^6cells/ ml). Similarly, high cell densities (10^6-10^9 cells/g carbonate mineral) were determined on biofilms that cover carbonate chimneys at a site of serpentinization in the Lost City Hydrothermal Vent Field (Schrenk et al., 2004). Although, high cell densities were determined at both the Tablelands and in previous studies of LCHF by Schrenk et al., (2004), phylogenic studies of both sites have shown low diversity in the carbonates and fluids; thus, understanding the microbial structure that exists in the ultra-basic springs seeps is of particular interest (Schrenk et al., 2004; Brazelton et al., 2006; Brazelton et al., 2012).

The LAL assay was useful in quickly determining the presence of a viable community (i.e., in particular gram-negative bacteria), and cell counting was useful in identifying general abundance levels of biomass at the serpentinization springs. However, cell counts in this study do not discriminate between live and dead cells (Nannipieri et al., 2003). Furthermore, the LAL assay, and cell counts do not provide information on microbial composition or associated metabolisms. Additional phospholipid fatty acid (PLFA) analysis of carbonate sediments provide a tool to profile the living microbial community in the ultra-basic reducing springs *in situ.* In addition $\delta^{13}C$ analysis of PLFA can be used to indentify the major sources and fate of organic matter in the environment.

3.5.2 Microbial community composition

Phospholipid fatty acids (PLFA) can be used as biomarkers to indicate specific groups of organisms (White et al., 1996). Interpretations of the PLFA biomarkers in this study are based on literature reviews (Table 3.4). In particular, monounsaturated and cyclopropyl unsaturated fatty acids are indicative of gram-negative bacteria (Wilkinson, 1988). In this study, the combination of monounsaturated and cyclopropyl unsaturated PLFA (16:1w7, 18:1w9t, 18:1w9c, 18:3w3), are assigned to gram-negative bacteria. Gram negative lipid biomarkers made up the largest group of the total PLFA (range of 32 % to 56.5%) at all springs with the exception of WHC2a in June 2010 where the dominant lipid group belonged to non-specific bacteria commonly found in all bacteria (36%) (Boschker, 2002).

The second largest lipid group detected were the straight-chained (< 20 carbon) saturated fatty acids (14:0, 15:0, 16:0, 17:0, 18:0), indicative of non-specific bacteria (range of 14.8% to 29.2%).

Polyunsaturated fatty acids (16:2w6, 18:2w5, 20:3w6, 20:4w6, 22:6w6) and the straight-chained (greater than 20 carbon) saturated fatty acids (20:0, 22:0) are indicative of microeukaryotes; made up the third largest lipid group (11.7% to 16.7%) with the exception of WHC2b in August 2010 where microeukaryotes made up the fourth largest lipid group. The microeukaryotes also include green algae and some diatom biomarkers (18:3w3, 18:4w3, 20:5w3, 22:5w6) (Volkman et al., 1989; Boschker, 2002).

Fungal biomarkers (18:2w6, 18:3w6, and 24:0) were also observed (Froostegard and Tunlid, 1993, 1996). Fungi made up the third largest lipid group at WHC2b in August 2010 and fourth largest lipid group at all other sites and sampling times (ranging from 4.1% to 10.3%). The smallest mol% of total PLFA in this study were the methyl branched fatty acids (i15:0, a15:0. i16:0, i17:0) indicative of gram-positive bacteria (O'Leary and Wilkinson, 1988).

3.5.3 Source of bulk organic matter

The elemental composition of organic matter (OM) can provide information on the nutrient status of a microbial community (Bianchi and Canuel, 2012). Organic matter which is composed of both living and non-living organic material can be derived from both terrestrial sources and can be derived from lipids, carbohydrates, proteins and other organic matter components produced by living or once living organisms. Therefore, source information on the OM is retained in the C:N ratio and the $\delta^{13}C_{OM}$ value. Newly

reworked OM will have higher C:N ratios due to the preferential microbial uptake and breakdown nitrogen over carbon. Alternatively, older OM will contain lower C:N ratios due to lower nitrogen concentrations and uptake of organic carbon.

The C/N ratios of OM were similar between spring locations (WHC2a, 2b, 2c) and between summer 2010 (June and August) and June 2011 (Table 3.2). The OM collected from the springs has high C/N ratios (ranging from 11.9 to16.2) suggesting that the OM is freshly reworked, either consistently decomposed at the bottom of the springs, or decomposed OM is washing downstream into the springs.

The $\delta^{13}C_{OM}$ values can be used to distinguish between terrestrial plant sources. Terrestrial C_3 plants have $\delta^{13}C$ values that range from -29 to-25‰ , while C_4 plants range from -22 to -16‰ (Oleary, 1988). However, no C_4 plants have been identified in the Tablelands (Berger et al., 1992). The average $\delta^{13}C_{OM}$ value for samples collected in June and August 2010 (-27.1 ±0.4‰, n=5, 1σ) and June 2011(-25.7 ± 0.2‰, n=3, 1σ) fall within isotopic range for C_3 plant derived OM.

3.5.4 Isotopic analysis of microbial community

Phospholipid fatty acids (PLFA) have $\delta^{13}C$ values directly related to the $\delta^{13}C$ value of the carbon pool used by bacteria for metabolic processes (Boschker and Middelburg, 2002). Additionally, phospholipids turnover quite rapidly during metabolism and thus provide a snapshot into the viable biomass present in the environment (White, 1979). To determine possible metabolisms in the springs, average PLFAs were analyzed for their $\delta^{13}C$ values and compared to the isotopic composition of carbon substrates (Table 3.5). Carbon sources including DOM and TIC substrate pools were identified, as

well as OM which can be utilized by microbial community in the springs in either heterotrophic or autotrophic metabolisms respectively.

Average $\delta^{13}C$ of PLFA were calculated from Table 3.3 for PLFA groups identified in Table 3.4. Average $\delta^{13}C$ of PLFA from summer 2010 (June and August) determined for non-specific bacteria (-31.2 ± 0.6‰, n=5, 1σ); gram-negative bacteria (-29.2 ± 0.9‰, n=5, 1σ); gram-positive bacteria (-27.1± 0.4‰, n=2, 1σ); fungi (-31.6 ± 0.9‰, n=2, 1σ) and algae (-38.8± 1.2‰, n=2, 1σ). Average $\delta^{13}C$ of PLFA from June 2011 were determined for non-specific bacteria (-25.1 ± 0.7‰, n=2, 1σ); gram-negative bacteria (-24.8 ± 1.3‰, n=2, 1σ); gram-positive bacteria (-23.4± 1.7‰, n=2, 1σ); fungi (-29.4 ± 3.1‰, n=2, 1σ). and algae (-29.0 ± 1.7‰, n=2, 1σ).

Average $\delta^{13}C$ of PLFA from June 2011 for all PLFA groups were more enriched in ^{13}C relative to average $\delta^{13}C$ of PLFA from June 2010. This observation is consistent with the observed enrichment in ^{13}C in the bulk organic carbon from the carbonate sediment biomass in 2011 (-25.7 ±0.2‰) relative to June 2010 (-26.8 ±0.3‰). An enrichment in ^{13}C of the biomass from 2010 to 2011, may be the result of changes in the available substrates in combination with changes in the predominant metabolic pathways.

Both autotrophic (i.e., algae) and heterotrophic (i.e., fungi) metabolisms were identified (Table 3.4). Freshwater algae utilize dissolved CO_2 which is commonly in isotopic equilibrium with atmospheric CO_2 (~-7‰) (Meyers, 1994) In the ultrabasic springs at the Tablelands, the dissolved carbon species are predominately bicarbonate due to the high pH nature of the fluids. If the total inorganic carbon pool (i.e., $\delta^{13}C_{TIC}$ ranging from -19.2 to -11.5‰) is being utilized by the algae, the $\delta^{13}C$ of algal PLFA would reflect

the isotopic signature for TIC. The average $\delta^{13}C$ for algae lipid biomarker (20:5w3) ranged from –39.1 to -27.8‰. The depleted $\delta^{13}C$ of algal LFA may be the result of a more depleted source of inorganic carbon that is metabolized by the algae, such as CO_2 produced via microbial methane oxidation, or the result isotope fractionation associated with different modes of carbon fixation (House et al., 2003).

Fungi utilize organic carbon for metabolism. If the dissolved organic carbon (i.e., $\delta^{13}C_{DOC}$ ranging from -23.7 to -16.3‰ is being utilized by the fungi, the $\delta^{13}C$ of fungi PLFA would reflect the isotopic signature for DOC. The fungal biomarkers (18:2w6, 18:3w6) had average $\delta^{13}C$ values that ranged from -32.9 to -27.2‰, also reflecting a more depleted organic carbon source. However, isotope fractionation is associated with the isotope value of the source of carbon being metabolized and the different biosynthetic pathways (Hayes, 2001). Therefore, differences in the isotopic value of source carbon and heterotrophic metabolisms can help explain the observed range in the $\delta^{13}C$ value for fungal PLFA.

The average $\delta^{13}C$ value of bacterial lipids ranged from -30.4 to -25.7‰ for gram-negative bacteria, from -27.4 to -22.2‰ for gram-positive bacteria, and -31.9 to -24.5‰ for non-specific bacteria. The isotopic values of bacterial lipids can reflect either or a combination of heterotrophic and autotrophic metabolisms.

3.5.5 Possible autotrophic and heterotrophic metabolism

Isotopic fractionations between fatty acids and the bulk oxidized and reduced pools of dissolved carbon in the ultra-basic springs can be used to determine possible metabolic pathways and in particular to distinguish between heterotrophic and autotrophic

metabolisms (Hayes, 2001). The isotopic fractionation between the organism and its carbon source is related to the size of the carbon bearing molecule being utilized. Reduction of smaller inorganic carbon molecule through autotrophy will result in large isotopic fractionation, where as assimilation of larger carbon molecules (i.e., organic matter) in heterotrophy will result in lower fractionations.

Carbon isotopic enrichment factors were calculated to determine the isotopic fractionations between fatty acids and total inorganic carbon ($\varepsilon_{FA\text{-}TIC}$; Table 3.5), and dissolved organic carbon ($\varepsilon_{FA\text{-}DOC}$; Table 3.5). Fractionations were calculated using $\delta^{13}C_{TIC}$, and $\delta^{13}C_{DOC}$ values presented in Table 3.2, and average $\delta^{13}C_{PLFA}$ that were grouped based on biomarker fatty acids indicative of different groups of microorganisms (Table 3.4). Three major groups of organisms were identified including fungi which are predominately heterotrophic, algae which are predominately photosynthesizers and thus autotrophic, and bacteria (i.e., gram-positive, gram-negative, and non–specific) which can include both autotrophic and heterotrophic metabolisms.

The isotopic fractionation between fatty acids and TIC ($\varepsilon_{FA\text{-}TIC}$) relative to the fractionation between fatty acids and DOC ($\varepsilon_{FA\text{-}DOC}$) is plotted in Figure 3.5. In Figure 3.5 a weak relationship between isotopic fractionations are observed between each individual taxonomic group: gram-negative (R^2=0.27), gram-positive bacteria (R^2=0.27), and fungi (R^2=0.16), and non-specific bacteria (R^2=0.34), with a slightly stronger relationship in algae (R^2=0.68). A weak relationship is observed between $\varepsilon_{FA\text{-}TIC}$ and $\varepsilon_{FA\text{-}DOC}$ in all PLFA groups (R^2=0.51), In general gram-negative, gram-positive, and fungi have smaller $\varepsilon_{FA\text{-}}$

$_{TIC}$ and $\varepsilon_{FA\text{-}DOC}$ than algae. Smaller fractionation between fatty acids and TIC and DOC respectively suggest heterotrophic activity.

Variable enrichments between PLFA and TIC; and PLFA and DOC may also be a reflection of variability in the isotopic composition of the substrate used and the fractionation associated with either the fixation or assimilation of carbon.

Relative sources of inorganic carbon can include carbon dioxide (CO_2) derived from marine limestones ($\delta^{13}C$= 0‰; (Anderson, 1983); a crustal source of CO_2 (-7 ‰; (Anderson, 1983); atmospheric CO_2 ($\delta^{13}C$ = -7‰); dissolved carbonate species (i.e., CO_3^{2-} at pH>10, $\delta^{13}C_{CO32-}$ = -15.5‰, at 25°C; (Clark and Fritz, 1997); and CO_2 from microbial oxidation ($\delta^{13}C$ ~ -23 to +4‰, assuming a starting $\delta^{13}C$ methane of -27‰; Chapter 2). Changes observed in the autotrophic PLFA that cannot be explained by changes in $\delta^{13}C$ of the inorganic carbon (i.e., same $\delta^{13}C_{TIC}$ values measured) may be due to either temperature changes (i.e., spring and summer) or different photosynthetic pathways.

The $\delta^{13}C$ value of heterotrophic substrate is much more difficult to determine because heterotrophs use a variety of organic compounds found in DOC. Variability in the $\delta^{13}C_{DOC}$ was observed between sampling sites and sampling times ($\delta^{13}C_{DOC}$ ranging from -23.7 to -16.3‰). The $\delta^{13}C$ of DOC can be difficult to resolve due to the contribution from primary production, food web release, marine organic matter (-23 to -18‰) and terrestrial sources (-29 to -25‰) to DOM with varying isotopic signatures (Oleary, 1988).

An isotopic fractionation is also associated with the total biomass and PLFA. Lipids in general are depleted in ^{13}C relative to the total biomass by 3-6‰, however other studies have shown more variable enrichment factors between +4‰ to -9‰ (Boschker et al., 1998; Zhang et al., 2004). Enrichments between fatty acids and biomass are metabolism-specific. In this study the ε_{FAOM} varied between -13‰ to 5‰ (Table 3.5). In particular, fatty acids belonging to algae, fungi, and bacteria, including gram-negative and non gram-specific bacteria were depleted in ^{13}C relative to the biomass (by -2 to -13‰), where as other fatty acids including all gram-positive, gram-negative, and non-specific bacteria were enriched in ^{13}C relative to biomass (1-4‰).

Other available substrates for the microbial community including H_2, nitrates, phosphates, sulphates and organic acids such as acetate have also been identified (Brazelton et al., 2012; Kavanagh et al., 2012). No lipid biomarkers diagnostic of methanotrophic bacteria (PLFA 16:1w8 and 18:1w8) were detected in the springs. This agrees with recent geochemical data from Chapter 2 and microbial studies by Brazelton et al. (2012) which suggest that the methane detected in the springs is non microbial. However, the presence of CH_4 produced at sites of serpentinization could also provide a substrate for methane oxidation which has not yet been identified.

3.5.6 Linking phospholipid fatty acid analysis to previous microbial studies

Brazelton et al. (2012) provided a metagenomic and phylogenetic survey (16SrRNA) of bacteria present in the ultra-basic spring WHC2b at the Tablelands to determine the potential of H_2 primary production. Both metagenomic and phylogenetic studies are useful in profiling the microbial diversity, taxonomic classification of

organisms, and determining possible metabolisms of particular kinds of microbes such as bacteria and fungi (Brock, 1975). However, the additional use of lipid-based analysis is a complimentary technique to study the microbiology of the springs because it can provide both quantitative concentration and carbon isotope signatures to help understand relative biomass and the carbon source metabolized by the microbial community *in situ*. The samples collected by Brazelton et al. (2012) were collected during the same sampling period as the current study and thus samples from the PLFA analysis can be directly compared to the metagenomic and phylogenetic survey.

Brazelton et al., (2012) found the dominance of β-proteobacteria (species *Hydrogenophaga*, within the order *Burkholderiales*) followed by the presence of firmicutes (within *Bacillales* and *Clostridales* orders) in lesser amounts in the fluids collected at WHC2b in August 2010. Proteobacteria are faculative autotrophs and gram-negative bacteria (Schwartz et al., 2009). The dominance of proteobacteria in the ultra-basic springs agrees with the presence of gram-negative bacteria determined with the LAL assay, and dominance of gram-negative lipid biomarkers. The *Bacillales* (facultative aerobes) and *Clostridales* (obligate anaerobe) orders are commonly gram-positive bacteria (Schwartz et al., 2009). Gram-positive lipid biomarkers were also detected in lesser amounts in the ultra-basic springs.

This PLFA study demonstrated that the organisms in the ultra-basic springs were ubiquitous among the ultra-basic springs, with PLFA belonging to bacteria, and fungi, and eukaryote groups. Different metabolic pathways (both heterotrophic and autotrophic) are likely occurring in the Tableland springs as evidenced by the different fractionations

associated with individual PLFA and presence of different organisms as determined by different biomarker compounds. It is difficult to determine exact metabolic pathways and resolve carbon sources solely using $\delta^{13}C_{TIC}$ and $\delta^{13}C_{DOC}$ due to overlapping signatures in the carbon pool. Further labelling studies in combination to isotopic analysis of PLFA on pure cultures isolated from the serpentinization springs may help in resolving the substrates and metabolic pathways used with the microorganisms present in the springs.

3.6 CONCLUSION

Serpentinization provides both the reducing conditions and organic carbon (i.e., methane, other low molecular weight compounds) to support microbial life that may inhabit the ultramafic subsurface (McCollom and Shock, 1997; Proskurowski et al., 2008). However, the microbial community existing at sites of serpentinization are poorly understood. The highly reducing and high pH conditions should inhibit the growth of most organisms, therefore life that can survive in the springs associated with serpentinization is considered to be extreme.

This is the first phospholipid fatty acid study conducted at a continental site of serpentinization. As a first line of evidence using life detection instrumentation including the LAL assay and cell counts, there is evidence for life in the ultra-basic springs at the Tablelands. PLFA biomarkers were used to determine groups of microorganisms that live in the springs and they were analyzed for their isotopic composition to help determine possible carbon substrate and metabolic pathways.

The largest mol% of total PLFA in the ultra-basic springs were monounsatured and cyclopropane unsaturated PLFA which are indicative of gram-negative bacteria. The

presence of lipid compounds related to gram-negative bacteria agrees with observations of gram-negative bacteria determined using the LAL assay. The dominance of gram-negative bacteria PLFA is also consistent with initial microbiological studies of the Tablelands spring fluids, which have found the presence of gram-negative proteobacteria (Brazelton et al., 2012). Likewise, the presence of gram-positive PLFA signatures supports the presence of Firmicutes as determined through microbiological studies of the spring fluids (Brazelton et al., 2012).

The $\delta^{13}C$ value of PLFA from June 2011 were more enriched in ^{13}C relative to June and August 2010, which is consistent with the observed enrichment in $^{13}C_{OM}$ of the total biomass in 2011 relative to 2010. Isotopic variability in both PLFA and biomass may be the result of changes in the available substrates in combination to changes in the metabolic pathways as reflected in variability in enrichment factors (ε) between FA and biomass, FA and TIC, and FA and DOC. PLFA biomarkers identified both heterotrophic and autotrophic microorganisms in the ultra-basic springs.

The lack of a methanogenic indicator PLFA further suggests that the methane detected is not produced from microbial methanogenesis via the carbonate reduction pathway. This observation is consistent with past studies where methane from ultra-basic springs was determined non-microbial (Chapter 2) in addition to microbiological studies (Brazelton et al., 2012).

Although it is difficult to resolve exact metabolic pathways without labelled studies on pure cultures from the Tableland springs, PLFA provided useful information

on the changing community structure, while isotope fractionations were useful in identifying possible metabolisms and shifts within the community.

3.7 FIGURES AND TABLES

Table 3.1Cell abundance and endotoxins detected from the Tablelands ultra-basic fluids as evidence for life

Sample	pH	Redox (mV)	Carbonate sediment			Fluids			Avg LAL (EU/mL)[a]
			Avg (cells/g)	95% LCI	95% UCI	Avg (cells/ml fluid)	95% LCI	95% UCI	
WHC1	12.3	137	n.d.			3.39E+06	3.2E+06	3.6E+06	45 (±11)[c]
WHC2A	12.5	-647	4.88E+08	4.7E+08	5.1E+08	1.67E+05	1.5E+05	1.8E+05	n.d.
WHC2B	12.6	-642	1.25E+09	1.1E+09	1.3E+09	7.14E+04	6.3E+04	7.9E+04	62 (±10)[d]
WHC2C	11.5	-468	n.d.			2.12E+04	1.9E+04	2.4E+04	>QL[b,d]
WHB	8.5	439	n.d.			n.d.			5 (±0.3)

[a]EU = endocrine units ; [b]>QL = greater than quantification limit (>200EU/mL); n.d.= not determined;
[c] Corrected for a 1:400 dilution [d] Corrected for a 1:20
LAL averages are based on a triplicate sample (n=3, 1σ).
LALmeasurements were obtained from samples in July 2009. Redox and pH measurements were obtained in June 2010 (Szponar et al., In Press). Cell abundance data was obtained from samples collected in June 2010.

Table 3.2 Geochemical analyses of possible carbon substrates in ultra-basic springs for microbial metabolism including bulk organic matter (OM), dissolved organic carbon (DOC), and total inorganic carbon (TIC)

Sample site and time		pH	Eh	$\delta^{13}C_{OM}$‰[a]	C: N[b]	DOC [mg/L]	$\delta^{13}C_{DOM}$, ‰	TIC [mg/L]	$\delta^{13}C_{TIC}$, ‰
WHB	Jun-10	8.5	439	n.d.	n.d.	0.44 (±0.02)	<d.l.	7.47 (±0.20)	-1.1 (±0.02)
	Aug-10	7.9	413	n.d.	n.d.	0.35 (±0.01)	<d.l.	10.36 (±0.15)	-3.0 (±0.1)
	Jun-11	7.8	382	n.d.	n.d.	0.30 (±0.01)	<d.l.	7.1 (±0.4)	-2.1 (±0.1)
WHC2a	Jun-10	12.5	-647	-26.7	16.2	1.93 (±0.16)	-16.3 (±0.9)	0.39 (±0.05)	-12.5 (±0.1)
	Aug-10	12.4	-642	-27.4	15.5	2.67 (±0.11)	-17.2 (±0.6)	1.17 (±0.03)	-19.2 (±0.1)
	Jun-11	12.4	-690	-25.9	12.3	0.35 (±0.20)	<d.l.	1.13 (±0.4)	-14.7 (±0.9)
WHC2b	Jun-10	12.6	-642	-27.1	13.9	0.44 (±0.08)	<d.l.	1.73 (±0.2)	-13.0 (±0.3)
	Aug-10	12.3	-596	-27.6	15.4	1.09 (±0.03)	-26.5 (±0.7)	2.16 (±0.4)	-17.3 (±1.5)
	Jun-11	12.3	-618	-25.8	12.2	0.29 (±0.03)	<d.l.	1.20 (±0.4)	-17.6 (±0.4)
WHC2c	Jun-10	11.5	-468	-26.7	13.8	1.93 (±0.04)	-22.3 (±0.4)	11.7 (±0.2)	-11.5 (±0.1)
	Aug-10	12.0	-106	n.d.	n.d.	1.37 (±0.01)	-23.0 (±0.1)	14.7 (±0.4)	-12.6 (±0.2)
	Jun-11	12.2	-458	-25.6	11.9	0.84 (±0.01)	-23.7 (±0.02)	13.5 (±0.6)	-11.8 (±0.03)

[a] Error associated with $\delta^{13}C_{org.}$ is ±0.3‰ (1σ) which includes both analytical and instrumental error on a sample ran in duplicate.

[b] Error associated with C:N ratio is ±0.3 (1σ) which includes both analytical and instrumental error on a sample ran in duplicate.

Error associated with DOC and TIC concentration and stable carbon isotope measurements is ± standard deviation (n=3, 1σ) and less than ±0.5‰ for $\delta^{13}C$ on triplicate samples.

n.d. = not determined, <d.l.= below linearity for $\delta^{13}C$ detection (≤ 0.50 mg/L)

Table 3.3 Distribution of mol% and $\delta^{13}C$ of PLFA as detected in June, August 2010, and June 2011

	WHC 2a				WHC 2b				WHC 2c					
	Jun-10		Jun-11		Jun-10		Aug-10		Jun-10		Aug-10		Jun-11	
PLFA I.D.	Mol %	$\delta^{13}C_{PLFA}$,‰	Mol %	$\delta^{13}C_{PLFA}$,‰	Mol %	$\delta^{13}C_{PLFA}$,‰	Mol %	$\delta^{13}C_{PLFA}$,‰	Mol %	$\delta^{13}C_{PLFA}$,‰	Mol %	$\delta^{13}C_{PLFA}$,‰	Mol %	$\delta^{13}C_{PLFA}$,‰
a-15:0	0.0		2.5	-21.3 (± 3.6)	4.1		0.0		2.1	-26.8 (± 1.0)	3.3		2.2	-24.0 (± 0.5)
i-15:0	4.1		2.7	-23.1 (± 2.0)	3.8		2.4	-27.4 (±0.6)[b]	2.1	-26.7 (± 1.4)	4.7		2.1	-25.3 (± 0.3)
i-16:0	0.0		1.3		0.0		0.0		1.1		1.3		0.9	
i-17:0	0.0		1.0		0.0		0.0		0.9		1.0		0.6	
Δ 17:0	0.0		1.4		0.0		0.0		1.0		1.1		0.8	
16:1w7	12.4	-31.3 (± 0.6)	15.2	-22.0 (± 0.4)	17.7	-28.7 (± 0.3)	7.3	-29.8 (± 1.7)	14.7	-30.5 (± 1.2)	13.0		17.1	-23.4 (±0.5)
$18:1w4^{trans}$	0.0		0.9		0.0		0.0		1.5		0.0		0.8	
$18:1w9^{cis}$	10.8	-27.8 (± 3.1)	14.1	-24.9 (± 0.4)	13.5	-27.2 (±0.9)	36.7	-28.3 (± 0.6)	20.1	-29.5 (± 0.4)	23.6	-28.3 (± 0.8)	17.0	-25.9 (± 0.2)
$18:1w9^{trans}$	8.6	-30.1 (± 1.5)	4.4	-24.6 (± 0.4)	6.3	-29.1 (± 2.3)	12.4	-28.7 (±1.5)	5.5	-31.2 (± 0.9)	6.2	-28.8 (± 0.9)	4.1	-27.8 (± 0.2)
16:2w6	0.0		1.9		0.0		0.0		1.3		0.0		1.8	
18:2w5	0.0		0.9		0.0		0.0		1.7		3.7		1.2	
18:2w6	4.0		3.5	-26.6 (± 1.7)	3.8		3.5		4.5	-33.9 (± 0.4)	4.3		3.9	-30.7 (± 1.1)
18:3w3	0.0		3.2	-30.0 (± 0.6)[b]	0.0		0.0		2.3	-37.8(± 0.6)[b]	1.2		3.3	-32.5 (± 0.4)
18:3w6	5.4		3.3	-27.8 (± 0.6)	4.4	-31.1 (±0.4)	10.1	-31.1 (± 0.4)	3.2	-32.0 (± 0.5)	4.5	-31.3 (± 0.8)	1.8	-32.4 (± 1.8)
18:4w3	0.0		2.1		0.0		0.0		1.0		0.0		1.4	
20:4w6	0.0		1.5		2.4		2.0		1.7		1.3		1.0	
20:5w3	0.0		8.3	-25.5 (± 0.6)	3.6		5.7	-37.4(±0.6)[b]	4.9	-39.1 (± 0.8)	2.4		9.0	-27.9 (± 0.1)
22:5w6	3.7		0.9		0.0		0.0		0.8		0.8		0.7	
22:6w6	0.0		1.1		0.0		0.0		0.7		0.0		1.0	
14:0	5.7		3.8	-22.4 (± 2.1)	4.7		2.3		3.0	-32.2 (± 0.4)	2.9		3.5	-23.5 (±0.9)
15:0	0.0		0.9		0.0		0.0		0.9		0.0		0.7	
16:0	19.9	-33.1 (± 0.6)	15.8	-23.1 (± 0.3)	17.0	-30.3 (± 1.1)	7.1	-31.4 (± 0.3)	14.3	-32.4 (± 0.8)	16.2	-32.0 (± 0.7)	18.2	-25.1 (± 0.5)
17:0	0.0		0.0		0.0		0.0		0.7		1.0		0.6	
18:0	10.8	-30.6 (± 0.6)	3.5	-28.1 (± 0.4)	7.6	-30.3 (± 0.3)	5.4	-30.8 (± 0.9)	3.9	-31.0 (±0.6)	4.5	-30.4 (± 0.3)	2.6	-28.2 (± 1.0)
20:0	5.9		1.5		4.1		3.2		1.3		1.3		0.8	
22:0	4.7		1.2		3.4		1.8		1.0		1.0		0.6	
24:0	4.1		1.1		3.6		0.0		0.9		0.8		0.7	
16:1w? [b]	0.0		1.8		0.0		0.0		2.8		0.0		1.7	
TOTAL	100		100		100		100		100		100		100	

Error on PLFA mol % is ± 10% relative standard deviation (see methods) Error associated with $\delta^{13}C$ represents standard deviations on multiple samples

[a] isotope value of a single measurement, error represents the standard deviation on FAME Indiana standard (n=6). [b] The position of the double bond for PLFA 16:1w? is unknown.

Table 3.4 PLFA detected in this study and their interpretation for the Tablelands ultra-basic springs

PLFA	Type	Group	Reference
i15:0, a15:0. i16:0, i17:0	Methyl Branched	Bacteria, Gram positive	(Wilkinson, 1988), (White et al., 1996), (O'Leary and Wilkinson, 1988)
16:1w7, Δ 17:0, 18:1w9t, 18:1w9c, 18:1w4t, 18:3w3	Monounsaturated and cylcopropane unsaturated	Bacteria, Gram negative	(Wilkinson, 1988), (White et al., 1996);
18:2w6, 18:3w6, 24:0	Monounsaturated and polyunsaturated	Fungi	(Frostegard et al., 1993), (Frostegard and Baath, 1996), (Wells et al., 1996)
18:3w3, 18:4w3, 20:5w3, 22:5w6	Polyunsaturated	Green Algea and some diatoms	(Volkman et al., 1989), (Boschker, 2002)
16:2w6, 18:2w5, 20:3w6, 20:4w6, 22:6w6	Polyunsaturated	Microeukaryotes	(Volkman et al., 1989), (Lechevalier, 1977), (Zelles, 1999)
14:0, 15:0, 16:0, 17:0, 18:0	Saturated straight chained (<20C)	Bacteria (non-specific)	(Lechevalier, 1977), (Boschker, 2002)
20:0, 22:0	Saturated straight chained (>20C)	Microeukaryotes, higher plants, mosses	(Zelles, 1999)

*16:1w7 and 18:1w9c can occur in Gm +ve bacteria and eukaryotes in lesser amounts (Leckie, 2005), however for this study, these PLFA are grouped with Gm –ve Bacteria.

Table 3.5 Enrichment factors of microbial., fungal., and algal groups as determined in this study

	Jun-10			Aug-10		Jun-11	
Bacteria (n.s)	WHC2a	WHC2b	WHC2c	WHC2b	WHC2c	WHC2a	WHC2c
Avg $\delta^{13}C_{FA}$	-31.7 (± 2.0)	-30.3 (± 0.1)	-31.9 (± 0.7)	-31.1 (± 0.5)	-31.2 (± 1.2)	-24.5 (± 3.1)	-25.6 (± 2.4)
$\varepsilon_{FA\text{-}OM}$ (‰) [a]	-5.2 (± 0.01)	-3.3 (± 0.01)	-5.4 (± 0.01)	-3.6 (± 0.01)		1.4 (± 0.01)	0.0 (± 0.01)
$\varepsilon_{FA\text{-}TIC}$ (‰) [a]	-19.5 (± 0.04)	-17.6 (± 0.01)	-20.6 (± 0.01)	-14.1 (± 0.05)	-18.8 (± 0.01)	-10.0 (± 0.10)	-13.9 (± 0.06)
$\varepsilon_{FA\text{-}DOC}$ (‰) [a]	-15.7 (± 0.05)		-9.8 (± 0.01)	-11.0 (± 0.01)	-8.5 (± 0.01)		-2.0 (± 0.01)
Fungi							
Avg $\delta^{13}C_{FA}$		-31.1 (± 0.6)[b]	-32.9 (± 0.01)	-31.1 (± 0.6)[b]	-31.3 (± 0.6)[b]	-27.2 (± 0.8)	-31.6 (± 0.5)
$\varepsilon_{FA\text{-}OM}$(‰) [a]		-4.1 (± 0.01)	-6.4 (± 0.01)	-3.6 (± 0.01)		-1.4 (± 0.01)	-6.2 (± 0.01)
$\varepsilon_{FA\text{-}TIC}$ (‰) [a]		-18.4 (± 0.01)	-21.6 (± 0.01)	-14.1 (± 0.06)	-18.9 (± 0.01)	-12.7 (± 0.03)	-20.0 (± 0.01)
$\varepsilon_{FA\text{-}DOC}$ (‰) [a]			-10.9 (± 0.01)	-11.0 (± 0.01)	-8.5 (± 0.01)		-8.1 (± 0.01)
Gm -ve							
Avg $\delta^{13}C_{FA}$	-29.7 (± 1.8)	-28.3 (± 1.0)	-30.4 (± 0.9)	-28.9 (± 0.8)	-28.5 (± 0.3)	-23.8 (± 1.6)	-25.7 (± 2.2)
$\varepsilon_{FA\text{-}oOM}$ (‰) [a]	-3.1 (± 0.01)	-1.2 (± 0.01)	-3.8 (± 0.01)	-1.4 (± 0.01)		2.1 (± 0.01)	-0.2 (± 0.01)
$\varepsilon_{FA\text{-}TIC}$ (‰) [a]	-17.5 (± 0.03)	-15.6 (± 0.01)	-19.1 (± 0.01)	-11.9 (± 0.05)	-16.1 (± 0.01)	-9.3 (± 0.04)	-14.1 (± 0.05)
$\varepsilon_{FA\text{-}DOC}$ (‰) [a]	-13.7 (± 0.05)		-8.3 (± 0.01)	-8.8 (± 0.01)	-5.7 (± 0.01)		-2.1 (± 0.01)
Gm +ve							
Avg $\delta^{13}C_{FA}$			-26.8 (± 0.3)	-27.4 (± 0.6)[b]		-22.2 (± 1.1)	-24.7 (± 0.2)
$\varepsilon_{FA\text{-}OM}$ (‰) [a]			-0.1 (± 0.01)	0.2 (± 0.01)		3.8 (± 0.01)	0.9 (± 0.01)
$\varepsilon_{FA\text{-}TIC}$ (‰) [a]			-15.4 (± 0.01)	-10.3 (± 0.04)		-7.6 (± 0.03)	-13.0 (± 0.01)
$\varepsilon_{FA\text{-}DOC}$ (‰) [a]			-4.6 (± 0.01)	-7.2 (± 0.01)			-1.0 (± 0.01)
ME, algal							
Avg $\delta^{13}C_{FA}$			-39.1 (± 0.9)	-37.4 (± 0.6)[b]		-27.8 (± 3.2)	-30.2 (± 3.3)
$\varepsilon_{FA\text{-}OM}$ (‰) [a]			-12.8 (± 0.01)	-10.1 (± 0.01)		-1.9 (± 0.01)	-4.8 (± 0.03)
$\varepsilon_{FA\text{-}TIC}$ (‰) [a]			-27.9 (± 0.01)	-20.5 (± 0.08)		-13.3 (± 0.1)	-18.6 (± 0.1)
$\varepsilon_{FA\text{-}DOC}$ (‰) [a]			-17.2 (± 0.01)	-17.4 (± 0.01)			-6.7 ± (0.04)

[a] Enrichment factor between two substances. $\varepsilon_{A\text{-}B} = ((\delta^{13}C_A+1000)/(\delta^{13}C_B+1000)-1) \times 1000$. FA= average total fatty acids; OM= bulk organic matter; TIC= total inorganic carbon; DOC= dissolved organic carbon. Errors were calculated using error of propagation by division. $\delta^{13}C$ values for bulk organic carbon, TIC, and DOC are listed in Table 2.[b] Standard deviation on average values is ±0.6‰ which is standard deviation on FAME Indiana standard (n=6).

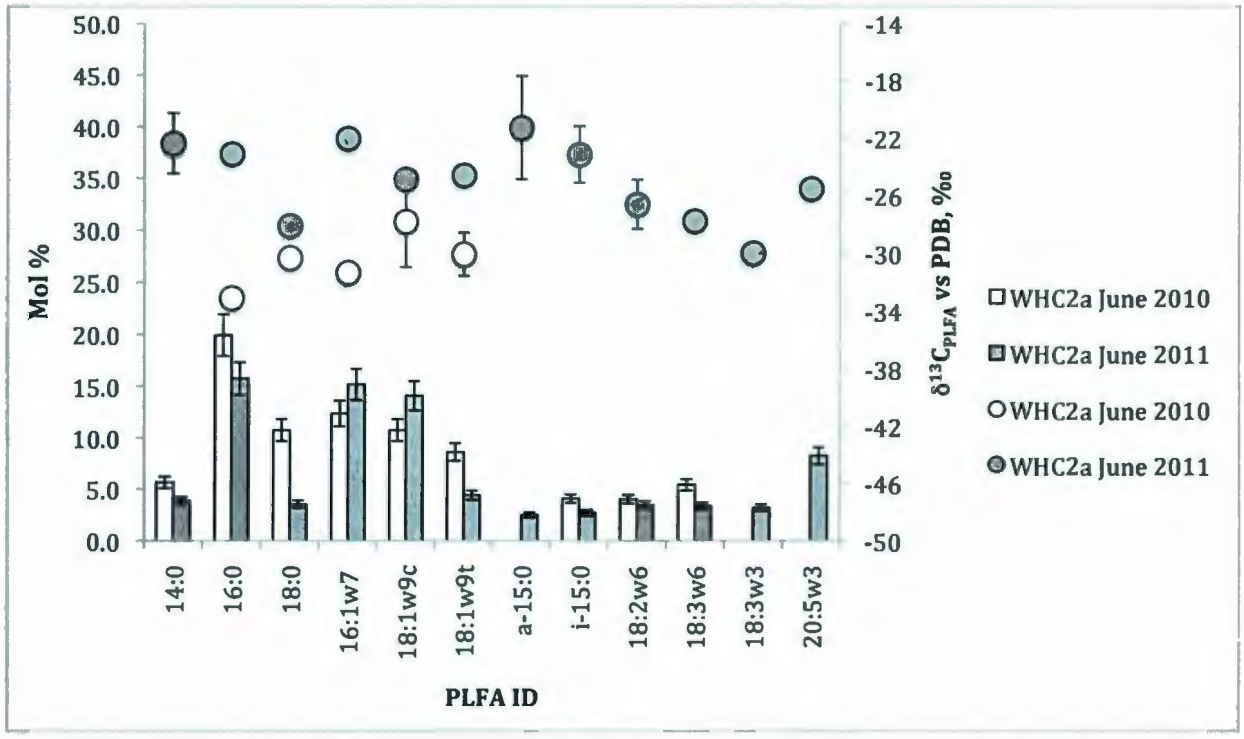

Figure 3.1 Spatial and temporal changes in microbial mol% (bars) and $\delta^{13}C$ (circles) of PLFA in ultra-basic spring **WHC2a**. Error bars associated with PLFA mol % are ± 10% RSD, and error bars associated with $\delta^{13}C$ represents standard deviations on replicate samples. Error bars may be smaller than the plotted point. Please note that not all PLFA have $\delta^{13}C$ values because they were either not detected or below detection limits. Please note the different scales for the y-axis.

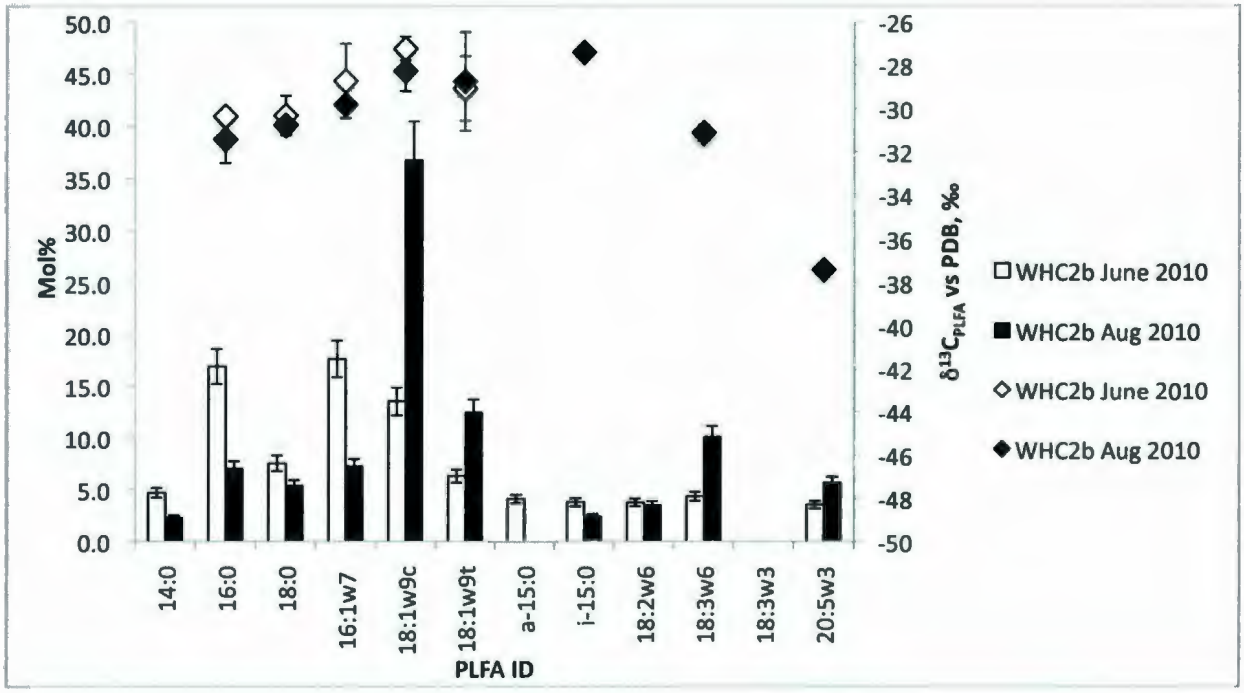

Figure 3.2 Spatial and temporal changes in microbial mol% (bars) and $\delta^{13}C$ (diamonds) of PLFA in ultra-basic spring **WHC2b** Error bars associated with PLFA mol % are ± 10% RSD, and error bars associated with $\delta^{13}C$ represents standard deviations on replicate samples. Error bars may be smaller than the plotted point. Please note that not all PLFA have $\delta^{13}C$ values because they were either not detected or below detection limits. Please note the different scales for the y-axis.

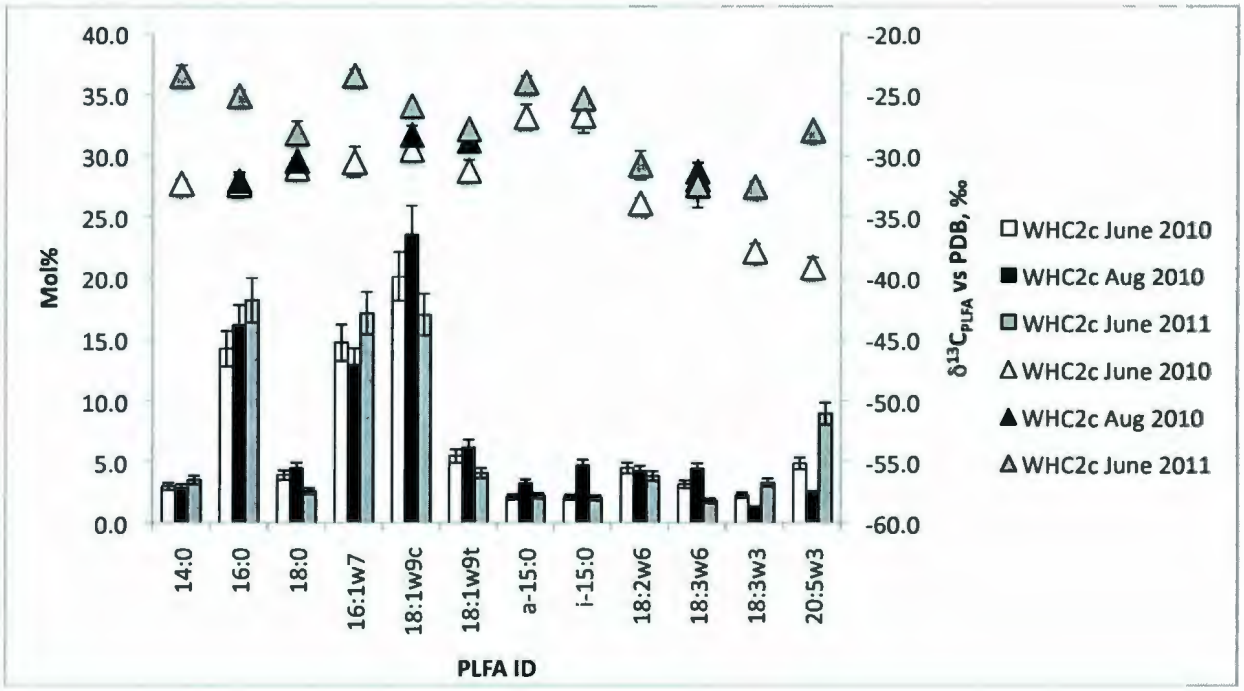

Figure 3.3 Spatial and temporal changes in microbial mol% (bars) and $\delta^{13}C$ (triangles) of PLFA in ultra-basic spring **WHC2c** Error bars associated with PLFA mol % are ± 10% RSD, and error bars associated with $\delta^{13}C$ represents standard deviations on replicate samples. Error bars may be smaller than the plotted point. Please note that not all PLFA have $\delta^{13}C$ values because they were either not detected or below detection limits. Please note the different scales for the y-axis.

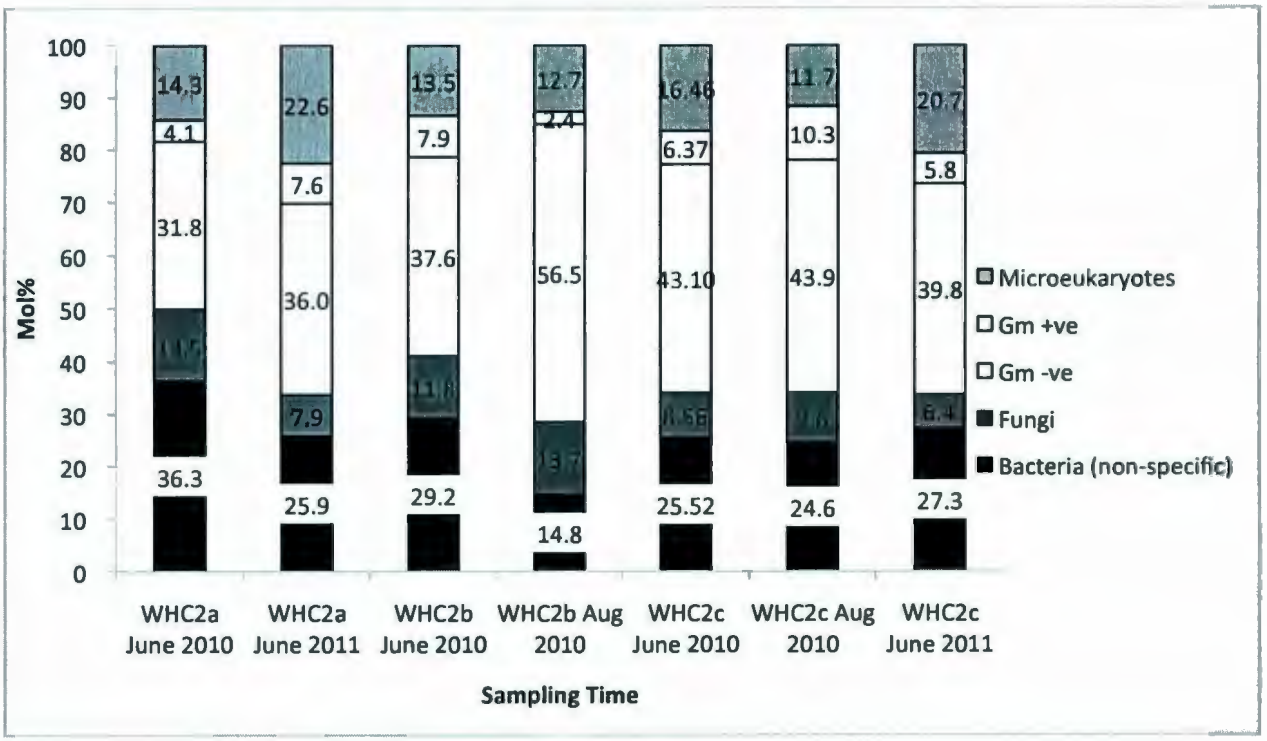

Figure 3.4 Comparing the mol% of PLFA from the Tablelands ultra-basic springs by group type. Microeukaryotes include polyunsaturated fatty acids and fatty acids with carbon # greater than 20 and can include algae and some diatoms. Gram-positive bacteria include branched fatty acids. Gram-negative bacteria include monounsaturated fatty acids and cyclic fatty acids. Bacteria (non-specific) are saturated single chained fatty acids with carbon # less than 20. See Table 3.4 for list of PLFA signatures and their corresponding group. Note WHC2c from June 2010 represents average mol% for a duplicate sample.

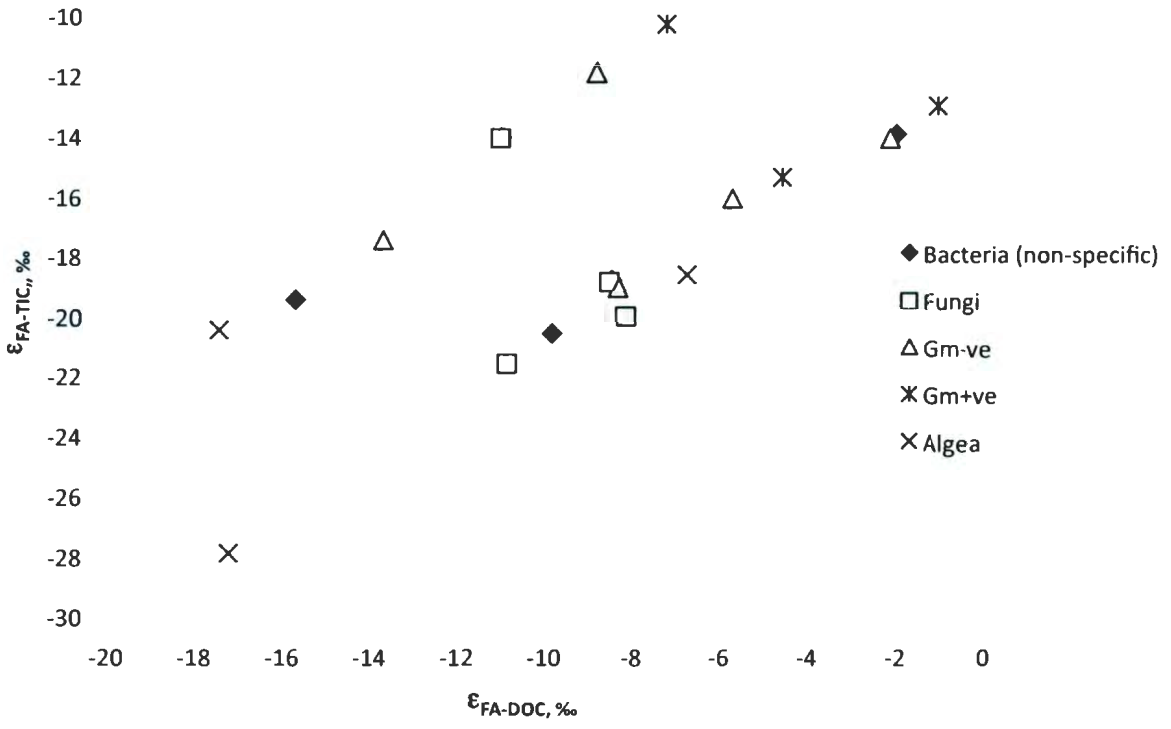

Figure 3.5 Plot of fractionation between fatty acids and total inorganic carbon ($\varepsilon_{FA\text{-}TIC}$) versus the fractionation between fatty acids and dissolved organic matter ($\varepsilon_{FA\text{-}DOC}$). Errors on enrichment factors are smaller than the plotted point.

3.8 REFERENCES

Abrajano, T. A., N. Sturchio, B. M. Kennedy, G. L. Lyon, K. Muehlenbachs, and J. K. Bohlke, 1990, Geochemistry of reduced gas related to serpentinization of the Zambales ophiolite, Philippines: Applied Geochemistry, v. 5, p. 625-630.

Abrajano, T. A., N. C. Sturchio, J. K. Bohlke, G. L. Lyon, R. J. Poreda, and C. M. Stevens, 1988, Methane-hydrogen gas seeps, Zambales Ophiolite, Philippines: deep or shallow origin?: Chemical Geology, v. 71, p. 211-222.

Anderson, T. F., Arthur, M.A., 1983, Stable isotopes of oxygen and carbon and their application to sedimentologic and paleoenvironmental problems Stable Isotopes in Sedimentary Geology, v. 10, p. 11-1151.

Barnes, I., V. C. LaMarche, and H. G., 1967, Geochemical evidence of present-day serpentinization: Science, v. 156, p. 830-832.

Barnes, I., J. R. Oneil, and J. J. Trescases, 1978, Present Day Serpentinization in New-Caledonia, Oman and Yugoslavia: Geochimica Et Cosmochimica Acta, v. 42, p. 144-145.

Berger, A. R., A. Bouchard, I. A. Brookes, D. R. Grant, S. G. Hay, and R. K. Stevens, 1992, Geology, Topography, and vegetation, Gros Morne National Park, Newfoundland; Geological Survey of Canada (1:1500000).

Bianchi, T. S., and E. A. Canuel, 2012, Chemical biomarkers in aquatic ecosystems: Princeton, Princeton University Press, xvii, 396 p. p.

Bligh, E. G., and W. J. Dyer, 1959, A Rapid Method of Total Lipid Extraction and Purification: Canadian Journal of Biochemistry and Physiology, v. 37, p. 911-917.

Boschker, H. T. S., 2002, Stable isotopes and biomarkers in microbial ecology: FEMS microbiology ecology, v. 40, p. 85-95.

Boschker, H. T. S., S. C. Nold, P. Wellsbury, D. Bos, W. de Graaf, R. Pel, R. J. Parkes, and T. E. Cappenberg, 1998, Direct linking of microbial population to specific biogeochemical processes by 13 C-labelling of biomarkers: Nature, v. 392, p. 801-805.

Brazelton, W. J., B. Nelson, and M. O. Schrenk, 2012, Metagenomic evidence for H2 oxidation and H2 production by serpentinite-hosted subsurface microbial communities: Frontiers in Extreme Microbiology: Deep Subsurface Microbiology Special Issue v. 2.

Brazelton, W. J., M. O. Schrenk, D. S. Kelley, and J. A. Baross, 2006, Methane- and sulfur metabolizing microbial communities dominate the Lost City hydrothermal field ecosystem: Applied and Environmental Microbiology, v. 72, p. 6257-6270.

Chevaldonné, P., and A. Godfroy, 1997, Enumeration of microorganisms from deep-sea hydrothermal chimney samples: FEMS microbiology letters, v. 146, p. 211-216.

Clark, I., and P. Fritz, 1997, Environmental Isotopes in Hydrogeology: New York, Lewis Pubishers, 328 p.

Etiope, G., M. Schoell, and H. Hosgörmezd, 2011, Abiotic methane flux from the Chimaera seep and Tekirova ophiolites (Turkey): Understanding gas exhalation from low temperature serpentinization and implications for Mars: Earth and Planetary Science Letters, v. 310, p. 96-104.

Guckert, J. B., C. P. Antworth, P. D. Nichols, and D. C. White, 1985, Phospholipid, Ester-Linked Fatty-Acid Profiles as Reproducible Assays for Changes in

Prokaryotic Community Structure of Estuarine Sediments: FEMS microbiology ecology, v. 31, p. 147-158.

Hayes, J. M., 2001, Fractionation of carbon and hydrogen isotopes in biosynthetic processes: Stable Isotope Geochemistry, v. 43, p. 225-277.

Hosgormez, H., 2006, Origin of the natural gas seep of Cirali (Chimera), Turkey: Site of the first Olympic fire: Journal of Asian Earth Sciences, v. 30, p. 131-141.

House, C. H., J. W. Schopf, and K. O. Stetter, 2003, Carbon isotopic fractionation by Archaeans and other thermophilic prokaryotes: Organic Geochemistry, v. 34, p. 345-356.

Kavanagh, H., N. Szponar, W. J. Brazelton, and P. L. Morrill, 2012, Aqueous geochemistry and substrate utilization by microorganisms at active sites of serpentinization, Tablelands Ophiolite, Newfoundland, Geological Association of Canada- Minerological Association of Canada Joint Assembly, St John's, Newfoundland.

Kelley, D. S., 2005, A serpentinite-hosted ecosystem: The Lost City hydrothermal field: Science, v. 307, p. 1428-1434.

Kelley, D. S., J. A. Karson, D. K. Blackman, G. L. Fruh-Green, D. A. Butterfield, M. D. Lilley, E. J. Olson, M. O. Schrenk, K. K. Roe, G. T. Lebon, and P. Rivizzigno, 2001, An off-axis hydrothermal vent field near the Mid-Atlantic Ridge at 30° N: Nature, v. 412, p. 145-149.

McCollom, T. M., and E. L. Shock, 1997, Geochemical constraints on chemolithoautotrophic metabolism by microorganisms in seafloor hydrothermal systems: Geochimica et Cosmochimica Acta, v. 61, p. 4375-4391.

Meyers, P. A., 1994, Preservation of elemental and isotopic source identification of sedimentary organic matter Chemical Geology, v. 114, p. 289-302.

Morrill, P. L., O. J. Johnson, J. Cotton, J. L. Eigenbrode, K. H. Nealson, B. Sherwood Lollar, and M. L. Fogel, 2008, Isotopic evidence of microbial methane in ultrabasic reducing waters at a continental site of active serpentinization in N. California: Geochimica et Cosmochimica Acta v. 72 p. A652-A652

Morrill, P. L., O. J. Johnson, J. Cotton, J. L. Eigenbrode, K. H. Nealson, B. Sherwood Lollar, and M. L. Fogel, Submitted, Microbial hydrocarbon gases in ultrabasic reducing waters at a continental site of active serpentinization in N. California: Geochimica et Cosmochimica Acta.

Nannipieri, P., J. Ascher, M. T. Ceccherini, L. Landi, G. Pietramellara, and G. Renella, 2003, Microbial diversity and soil functions: European Journal of Soil Science, v. 54, p. 655-670.

Neal, C., and G. Stanger, 1983, Hydrogen generation from mantle source rocks in Oman: Earth and Planetary Science Letters, v. 66, p. 315-321.

O'Leary, W. M., and S. G. Wilkinson, 1988, Gram-positive bacteria: Microbial Lipids: London, Academic Press.

Oleary, M. H., 1988, Carbon Isotopes in Photosynthesis: Bioscience, v. 38, p. 328-336.

Porter, K. G., and Y. S. Feig, 1980, The Use of Dapi for Identifying and Counting Aquatic Microflora: Limnology and Oceanography, v. 25, p. 943-948.

Proskurowski, G., M. D. Lilley, J. S. Seewald, G. L. Früh-Green, E. J. Olson, L. J.E., S. P. Sylva, and D. S. Kelley, 2008, Abiogenic hydrocarbon production at Lost City Hydrothermal Field: Science, v. 319, p. 604-607.

Riggs, D. S., J. A. Guarnieri, and S. Addelman, 1978, Fitting straight lines when both variables are subject to error: Life Sciences, v. 22, p. 1305-1360.

Schrenk, M. O., D. S. Kelley, S. A. Bolton, and J. A. Baross, 2004, Low archaeal diversity linked to subseafloor geochemical processes at the Lost City Hydrothermal Field, Mid-Atlantic Ridge: Environmental Microbiology, v. 6, p. 1086-1095.

Schwartz, E., B. Voigt, D. Zuhlke, A. Pohlmann, O. Lenz, D. Albrecht, A. Schwarze, Y. Kohlmann, C. Krause, M. Hecker, and B. Friedrich, 2009, A proteomic view of the facultatively chemolithoautotrophic lifestyle of Ralstonia eutropha H16: Proteomics, v. 9, p. 5132-5142.

Sherwood Lollar, B., T. D. Westgate, J. A. Ward, G. F. Slater, and G. Lacrampe-Couloume, 2002, Abiogenic formation of gaseous alkanes in the Earth's crust as a minor source of global hydrocarbon reservoirs: Nature, v. 416, p. 522-524.

Szponar, N., W. J. Brazelton, M. O. Schrenk, D. M. Bower, A. B. Steele, and P. L. Morrill, In Press, Geochemistry of present-day serpentinization at the Tablelands, Gros Morne National Park: a Mars Anologue Site: Icarus.

Volkman, J. K., S. W. Jeffrey, P. D. Nichols, G. I. Rogers, and C. D. Garland, 1989, Fatty-Acid and Lipid-Composition of 10 Species of Microalgae Used in Mariculture: Journal of Experimental Marine Biology and Ecology, v. 128, p. 219-240.

Watson, S. W., T. J. Novitsky, H. L. Quinby, and F. W. Valois, 1977, Determination of Bacterial Number and Biomass in Marine-Environment: Applied and Environmental Microbiology, v. 33, p. 940-946.

White, D., 1979, Determination of the sedimentary microbial biomass by extractible lipid phosphate: Oecologia, v. 40, p. 51-62.

White, D. C., J. O. Stair, and D. B. Ringelberg, 1996, Quantitative comparisons of in situ microbial biodiversity by signature biomarker analysis: Journal of Industrial Microbiology, v. 17, p. 185-196.

Wilkinson, S. G., 1988, Gram-negative bacteria: Microbial Lipids: London, Academic Press.

Zhang, C. L., B. W. Fouke, G. T. Bonheyo, A. Peacock, D. C. White, Y. Huang, and C. S. Romanek, 2004, Lipid Biomarkers and carbon-isotopes of modern travertine deposits (Yellowstone National Park, USA); Implications for biogeochemical dyamics in hot-spring systems: Geochemica et Cosmochimica Acta, v. 68, p. 3157-3169.

Chapter 4: Summary

4.1 SUMMARY AND FUTURE WORK

Serpentinization is an exothermic reaction where ultramafic rocks undergo hydration and produce an abundance of hydrogen gas (H_2), resulting in conditions favourable for the synthesis of hydrocarbon gases such as methane. Current studies on sites of serpentinization today include the Lost City Hydrothermal Vent Field (LCHF), which is a marine location (Kelley et al., 2001), deep subsurface mines in the Precambrian Shield (Sherwood Lollar et al., 2006); and other continental locations including the ophiolite at Oman (Neal and Stanger, 1983), Turkey (Hosgormez, 2006), Philippines (Abrajano et al., 1990), and Cazadero, California (Barnes et al., 1967; Morrill et al., submitted). At these sites, characteristic ultra-basic and reducing fluids rich in hydrogen gas and variable amounts of hydrocarbons have been identified. A common focus in these studies has been to identify the source of hydrocarbon gases, particularly methane, and attribute its synthesis to either abiogenic or biogenic synthesis. Understanding and identifying the source(s) of methane is of particular interest as sites of serpentinization are considered important analogues for organic synthesis both on early Earth and potentially on other planets such as Mars (Oze, 2005; Schulte et al., 2006). The potential for microbial production of methane at these sites has brought forward an additional interest in identifying the microbial communities that can survive in the extreme environment of the ultra-basic, reducing fluids (Schrenk et al., 2004; Brazelton and Baross, 2008; Morrill et al., submitted). Previous microbial studies on sites of serpentinization include a marine location at the LCHF (Schrenk et al., 2004; Brazelton

and Baross, 2008; Konn, 2009), and continental locations including Cazedero, California (Morrill et al., submitted). Therefore the microbial communities and potential metabolisms that allow them to thrive at sites of serpentinization is still poorly understood. The Tablelands Ophiolite is a continental site exhibiting active serpentinization and it is a Mars analogue.

The first aim of this thesis was to geochemically characterize the springs at the Tablelands and determine the mechanisms for hydrocarbon synthesis within the fluids using both compositional and isotopic analysis. To meet the first objective of Chapter 2, ultra-basic springs discovered so far in the Tablelands Ophiolite (i.e., WHC1, WHC2, TLE, WB) were distinguished based on common geochemical characteristics of springs with other sites of serpentinization such as Cazadero, in California (Barnes et al., 1967; Morrill et al., submitted). Similar to the springs in Cazadero, the springs in the Tablelands are highly reducing; ultra-basic; and meteoric in origin; with high Ca^{2+}/Mg^{2+} ratios; and calcium-rich carbonate sediment and travertine deposits in and around the ultra-basic springs. Isotopic analyses of carbonates suggest that carbonate sediment and travertine were precipitated under non-equilibrium conditions with the atmosphere and fluids. ,

Additionally, large amounts of H_2 (g) and variable amounts of methane (CH_4) and low molecular weight hydrocarbon (C_2 to C_6) gases were detected in the springs. The second objective in Chapter Two was to determine the mechanisms responsible for their synthesis (microbial., thermogenic, or abiogenic) of aqueous hydroarbons trhough the bulk and stable carbon isotope analysis of methane and low molecular weight hydrocarbons. The results from this study showed that the primary source of methane in the ultra-basic springs is not microbial., but either thermogenic or abiogenic.

Additional work is needed to distinguish between the two possible sources of methane. One possible approach is to examine the stable isotope composition of hydrogen of the hydrocarbon gases to determine if they are abiogenic or thermogenic in origin. Hydrogen isotopes of thermogenic hydrocarbons have been determined to be more positive (>+250‰) relative to abiogenic hydrocarbons (<+250‰) for hydrocarbons with overlapping carbon isotope signatures (Sherwood Lollar et al., 2002). Therefore, a combination of carbon and hydrogen isotopes can help resolve between abiogenic and thermogenic hydrocarbons. In this study, dissolved concentrations of hydrocarbons were below detectable limits to measure hydrogen isotopes. To resolve the issue of low concentrations, larger sample sizes were collected but were not analyzed in this study.

A thermogenic origin for methane is possible mechanism at the Tablelands because it is likely that sedimentary organic matter is associated with the ultramafic complex that would have been exposed to high temperatures and pressures during the emplacement of the ophiolite. However, abiogenic synthesis of hydrocarbons has also been shown to occur at active sites of serpentinization (Sherwood Lollar et al., 2006; Proskurowski et al., 2008). Further isotopic and compositional analyses as well as biomarker, and other organic matter maturity analyses of the sedimentary organic matter beneath the Tablelands peridotite may help delineate the source of methane and hydrocarbon gases present in the ultra-basic springs.

Similar application of isotopes and composition of hydrocarbons used to delineate sources of methane at the serpentinization sites in the Tablelands can be used to analyze data from the Mars Sample Laboratory and source CH_4 detected in areas of serpentinization on Mars. Additionally, serpentinization at the Tablelands Ophiolite can

be used both as a mineralogical and a geochemical indicator to understand previous aqueous environment conditions and conditions suitable for methane production not only on Earth but also potentially on other ultramafic planetary bodies such as Mars.

Although the methane produced at the serpentinization sites in the Tablelands is non-microbial in origin, extant life was found in the ultra-basic springs. There are very few studies that report on microbial life that exists at sites of serpentinization. Understanding how microbial communities thrive in these present-day extreme environments could help in our interpretation of past or present life on Earth and other planets, as well as provide a window into microbial life in the deep subsurface where serpentinization is occurring not only at the Tablelands, but possibly at other continental sites of serpentinization.

The second aim of this thesis in Chapter 3 was to detect and identify the microbial community in the ultra-basic springs and determine their role in carbon cycling within the springs. Prior to this study, Brazelton et al. (2012) provided a metagenomic and phylogenic study of the ultra-basic springs at the Tablelands. This study is one of the first microbial studies at a continental site of serpentinization to examine microbial community structure using phospholipid biomarkers and isotopic analysis to determine possible substrate and metabolisms used by the ambient microbial community. The objectives of Chapter 3, to detect life and subsequently characterize the a microbial community, were met using life detection instrumentation including the LAL assay which determined the presence of gram-negative bacteria in the ultra-basic springs. Additionally, cell counts determined a large abundance of microbial life ($>10^6$) in the springs.

Using PLFA biomarker compounds, fungi, eukaryotes including algae, and bacteria (both gram positive and gram negative) groups were detected in the springs. The largest mol% abundace of total PLFA in the ultra-basic springs were monounsatured and cyclopropane unsaturated PLFA which are indicative of gram-negative bacteria. The dominance of gram-negative bacteria and lesser amounts of gram-positive bacteria supports the findings of Brazelton et al. (2012), who determined the presence of gram-negative proteobacteria as the dominant species and the presence of some gram-positive Firmicutes in the ultra-basic fluids.

Community structure was determined using compositional analysis of the biomass and phospholipid fatty acids (PLFA). Shifts in the community structure were identified in the groups of microorganism groups including fungi, algae, and bacteria (gram positive, gram negative) during June and August 2010, and June 2010.

No methanogenic PLFA signatures (16:1w8 and 18:1w8) were found in the ultra-basic springs, further confirming results from the second Chapter, which determined that the methane from ultra-basic springs was non-microbial. To meet the second objective of Chapter 3, to identify possible metabolisms in the ultra-basic springs, the stable carbon isotope composition ($\delta^{13}C$) of PLFA and biomass were identified and compared to the $\delta^{13}C$ value of dissolved inorganic and organic carbon pools. Differences in $\delta^{13}C$ of PLFA were observed between June and Aug 2010 and June 2011, with PLFA more enriched in ^{13}C in June 2011 relative to June and August 2010. This observation was consistent with the observed enrichment in $^{13}C_{OM}$ of the total biomass in 2011 relative to 2010 suggesting possible differences in the available substrates or metabolisms.

Variability in enrichment factors (ε) between fatty acids (FA) and biomass, FA and total inorganic carbon (TIC), and FA and dissolved organic carbon (DOC) suggests changes in the substrates used in combinations to changes in metabolic pathways.

Although it is difficult to resolve the exact metabolic pathways without knowing the specific carbon source, future labelled substrate and nutrient addition experiments on pure cultures with known metabolic pathways could help delineate the possible metabolic pathways (Zhang et al., 2004). Furthermore PLFA analysis on microbial isolates could identify distinct biomarkers that can be compared to the natural abundance biomarkers in order to identify specific microbes, their shifts within the community, and corresponding metabolisms *in situ*.

This study addresses the origin of methane in the Martian atmosphere and the potential for the existence of life on Mars. The discovery of a rich microbial community thriving in an extreme environment, could suggest the possibility of a similar microbial life is or was possible on Mars. However, this study has shown that microorganisms in the Tablelands springs do not produce methane, suggesting that Martian methane may not be the most indicative product of putative Martian metabolic activity. This is consistent with the recent findings by Keppler et al., (2012) that the Martian methane is produced when carbonaceous compounds are decomposed by high-energy UV radiation, rather than biological process. Further studies should aim at possible abiogenic sources that could be contributing to the Martian methane. Future work should aim at better constraining carbon sources of methane (abiogenic, thermogenic) and the carbon substrates and metabolic pathways used by the microbial community.

4.2 REFERENCES

Abrajano, T. A., N. Sturchio, B. M. Kennedy, G. L. Lyon, K. Muehlenbachs, and J. K. Bohlke, 1990, Geochemistry of reduced gas related to serpentinization of the Zambales ophiolite, Philippines: Applied Geochemistry, v. 5, p. 625-630.

Barnes, I., V. C. LaMarche, and H. G., 1967, Geochemical evidence of present-day serpentinization: Science, v. 156, p. 830-832.

Brazelton, W. J., and J. A. Baross, 2008, Biological methane cycling at the lost city hydrothermal field Astrobiology Science Conference.

Brazelton, W. J., B. Nelson, and M. O. Schrenk, 2012, Metagenomic evidence for H2 oxidation and H2 production by serpentinite-hosted subsurface microbial communities: Frontiers in Extreme Microbiology: Deep Subsurface Microbiology Special Issue v. 2.

Hosgormez, H., 2006, Origin of the natural gas seep of Cirali (Chimera), Turkey: Site of the first Olympic fire: Journal of Asian Earth Sciences, v. 30, p. 131-141.

Kelley, D. S., J. A. Karson, D. K. Blackman, G. L. Fruh-Green, D. A. Butterfield, M. D. Lilley, E. J. Olson, M. O. Schrenk, K. K. Roe, G. T. Lebon, and P. Rivizzigno, 2001, An off-axis hydrothermal vent field near the Mid-Atlantic Ridge at 30° N: Nature, v. 412, p. 145-149.

Keppler, F., I. Vigano, A. McLeod, U. Ott, M. Früchtl, and T. Röckmann, 2012, Ultraviolet-radiation-induced methane emissions from meteorites and the Martian atmosphere: Nature v. 486, p. 93-96.

Konn, C., 2009, Hydrocarbons and oxidized organic compounds in hydrothermal fluids from Rainbow and Lost City ultramafic-hosted vents: Chemical Geology, v. 258, p. 299-314.

Morrill, P. L., O. J. Johnson, J. Cotton, J. L. Eigenbrode, K. H. Nealson, B. Sherwood Lollar, and M. L. Fogel, submitted, Microbial hydrocarbon gases in ultrabasic reducing waters at a continental site of active serpentinization in N. California: Geochimica et Cosmochimica Acta.

Neal, C., and G. Stanger, 1983, Hydrogen generation from mantle source rocks in Oman: Earth and Planetary Science Letters, v. 66, p. 315-321.

Oze, C., 2005, Have olivine, will gas: Serpentinization and the abiogenic production of methane on Mars: Geophysical Research Letters, v. 32, p. 1-4.

Proskurowski, G., M. D. Lilley, J. S. Seewald, G. L. Früh-Green, E. J. Olson, L. J.E., S. P. Sylva, and D. S. Kelley, 2008, Abiogenic hydrocarbon production at Lost City Hydrothermal Field: Science, v. 319, p. 604-607.

Schrenk, M. O., D. S. Kelley, S. A. Bolton, and J. A. Baross, 2004, Low archaeal diversity linked to subseafloor geochemical processes at the Lost City Hydrothermal Field, Mid-Atlantic Ridge: Environmental Microbiology, v. 6, p. 1086-1095.

Schulte, M., D. Blake, T. Hoehler, and T. McMcCollom, 2006, Serpentinization and its implications for life on the early Earth and Mars: Astrobiology, v. 6, p. 364-376.

Sherwood Lollar, B., G. Lacrampe-Couloume, G. F. Slater, J. A. Ward, D. P. Moser, T. M. Gihring, L.-H. Lin, and T. C. Onstott, 2006, Unravelling abiogenic and biogenic sources of methane in the Earth's deep subsurface: Chemical Geology, v. 226, p. 328-339.

Sherwood Lollar, B., T. D. Westgate, J. A. Ward, G. F. Slater, and G. Lacrampe-Couloume, 2002, Abiogenic formation of gaseous alkanes in the Earth's crust as a minor source of global hydrocarbon reservoirs: Nature, v. 416, p. 522-524.

Zhang, C. L., B. W. Fouke, G. T. Bonheyo, A. Peacock, D. C. White, Y. Huang, and C. S. Romanek, 2004, Lipid Biomarkers and carbon-isotopes of modern travertine deposits (Yellowstone National Park, USA); Implications for biogeochemical dyamics in hot-spring systems: Geochemica et Cosmochimica Acta, v. 68, p. 3157-3169.

APPENDIX A: RAW DATA

A.1. Hydrogen and oxygen isotopes of fluids from Chapter 2, Figure 2.3 and 2.4

				Delta 18O and Delta 2H			
Location	Date Sampled	pH	Eh (mV)	Avg Delta 18O VSMOW	Stdev	Avg Delta 2H VSMOW	Stdev
WHC2a	Jul-09	11.64	-867				
	Jun-10	12.57	-847	**-11.13**	0.06	**-71.6**	0.24
	Aug-10	12.40	-842				
	Oct-10	12.50	-378				
WHC2b	Jul-09	11.62	-749	**-10.42**	0.08	**-68.31**	0.13
	Sep-09	12.2	-875	**-10.76**	0.05	**-67.53**	0.18
	Jun-10	12.63	-842	**-11.23**	0.09	**-72.74**	0.21
	Aug-10	12.06	-733				
	Oct-10	11.00	-123				
WHC01-pool 6	Sep-09	11	-90	**-9.48**	0.03	**-61.17**	0.25
	Jun-10	12.35	-63	**-9.46**	0.09	**-64.53**	0.18
	Aug-10	11.96	-85				
	Oct-10	12.31	-86				
WHC2c	Sep-09	10.3	-89	**-9.65**	0.13	**-62.88**	1
	Jun-10	13.11	-787	**-11.68**	0.05	**-77.66**	0.16
	Aug-10	12.31	-796				
	Oct-10	12	-306				
TLEb	Jul-09	10.19	-67	**-12.16**	0.25	**-79.88**	0.33
	Sep-09	10	-71	**-12.4**	0.05	**-80.57**	0.19
	Jun-10	10.5	24	**-12.34**	0.05	**-82.69**	0.2
	Aug-10	11.29	-7				
PIE	Jun-10	10.5	176	**-11.61**	0.06	**-79.61**	0.07
	Aug-10	10.91	128				
Rain water	Jun-10			**-12.57**	0.03	**-88.85**	0.32
Pond on top o	Jun-10			**-11.61**	0.06	**-79.61**	0.07
Snowmelt	Jun-10			**-11.95**	0.04	**-80.89**	0.16
WHBup	Jun-10	8.77	255	**-10.88**	0.09	**-78.7**	0.61
	Aug-10	7.29	223				
	Oct-10	7.51	172				
WHBdown	Jul-09	7.56	188	**-11.55**	0.09	**-74.02**	0.33
	Sep-09	8.5	239	**-9.86**	0.07	**-63.94**	0.4
	Aug-10	7.9	213				

A.2 Ion data from Chapter 2 and Figures 2.5 and 2.6 and extra Ion data from ICPMS

	Concentration (ppb)			
Sample ID	**Mg**	**Cl**	**Ca 43**	**Br**
Sep-13				
WHC-02-c	16522	12978	2087	37.32
WHC-02-c	16691	13588	2100	47.9
WHC-02-c	17215	13655	2104	43.13
WHC-01 (pool	52	457083	7879	1058.95
WHC-01 (pool	60	460188	8123	1077.51
WHC-01 (pool	51	441258	8019	1039.92
WHC-02b	592	369262	56655	843.98
WHC-02b	589	362133	55630	858.94
WHC-02b	770	369764	57708	878.79
TLE-b	869	6378	13963	24.05
TLE-b	869	6309	13690	12.57
TLE-b	855	5873	14179	13.74
Jun-14				
WHB inout 2	13305.17	7772.68	1076.03	15.39
WHC2a	604.64	403384.49	58474.56	892.52
WHC2b	1593.10	313576.33	43796.68	715.18
WHC2c	7570.45	165870.60	22516.27	373.46
WHC01 (poole	68.17	504843.83	9602.43	1141.93
PIE (1)	1503.85	93993.65	57004.49	564.74
PIE (2)	1427.78	7186.60	12916.60	8.54
TLEb	1347.30	90389.01	55993.42	563.13
TLEb	1402.21	94967.11	57369.29	579.83
WHB	9499	3507	653	<9.11
WHB	9453	3710	389	<9.41
WHB	9591	3972	503	9.21

Table A.3 Raw Total Inorganic Caron (TIC) Concentrations (mg/L) and stable carbon isotope values (permil) from Chapter 2 and 3 and Fig 3.5

						DIC Delta 13 C				DIC Concentration				
Location	Date Sampled	pH	avg	Eh (mV)	corrected +200mV	Delta Avg	Delta STDEV	Avg Delta of all Seasons	STDEV of all seasons	OI TIC Avg (ppm)	stdev	RSD%	Avg DIC conc of all seasons (ppm)	STDEV of all seasons
WHB	Jul-09	7.29	7.6	223	453	-1.5	1.1	-1.7	0.8	8.01	0.98	12.26	8.06	1.69
	Sep-09	7.56		188	418	-1.9	0.2			9.62	0.44	4.59		
	Jun-10	8.5		239	469	-1.1	0.0			7.47	0.20	2.72		
	Aug-10	7.9		213	443	-3.0	0.1			10.36	0.15	1.42		
	Oct-10	6.3		244	474	-0.8	0.2			5.76	0.13	2.19		
	Jun-11	7.82		182	412	-2.1	0.1			7.14	0.37	5.24		
WHC2a	Jul-09	11.64	12.3	-867	-637	-	-	-16.1	2.8	-	-	-	1.10	0.53
	Sep-09	-		-		-	-			-	-	-		
	Jun-10	12.5		-847	-617		0.1			0.39	0.05	11.89		
	Aug-10	12.4		-842	-612	-19.2	0.1			1.17	0.03	2.83		
	Oct-10	12.37		-600		-14.3	0.7			1.69	0.33	19.54		
	Jun-11	12.36		-890	-660	-14.7	0.9			1.13	0.40	35.36		
WHC2b	Jul-09	11.62	12.3	-749	-519	-	-	-16.2	3.0	-	-	-	4.45	6.27
	Sep-09	12.2		-875	-645	-19.8	1.2			1.48	0.31	20.97		
	Jun-10	12.63		-842	-612	-13.0	0.3			1.73	0.16	9.27		
	Aug-10	12.31		-796	-566	-17.3	1.5			2.16	0.41	18.76		
	Jun-11	12.28		-818	-588	-17.6	0.4			1.23	0.35	28.70		
WHC2c	Jul-09	10.3	11.3	-89	141	-	-	-12.5	0.8	-	-	-	14.94	2.58
	Sep-09	12.1		-787	-557	-13.0	0.2			18.54	0.64	3.44		
	Jun-10	12.31		-796	-566	-11.5	0.1			11.75	0.17	1.45		
	Aug-10	12		-306	-76	-12.6	0.2			14.78	0.45	3.03		
	Oct-10	8.77		255		-13.3	0.3			16.10	0.23	1.42		
	Jun-11	12.21		-658	-428	-11.8	0.0			13.52	0.61	4.51		
WHC01-pool 6	Jul-09	-	12.2	-		-	-	-29.4	1.7	-	-	-	27.25	14.82
	Sep-09	12		-90	140	-28.2	3.7			37.73	17.25	45.71		
	Jun-10	12.35		-63	167	-	-			-	-	-		
	Aug-10	11.96		-85	145	-30.6	0.2			16.78	0.30	1.79		
	Oct-10	12.31		-79	151	-	-			-	-	-		
	Jun-11	-		-		-	-			-	-	-		
TLE	Jul-09	10.19	10.6	-67	163		0.2	-11.8	2.6	0.31	0.03	8.25	0.83	0.49
	Sep-09	10		-71	159	-10.1	0.8			0.61	0.01	1.52		
	Jun-10	10.5		24	254	-10.0	0.3			1.49	0.22	15.05		
	Aug-10	11.29		-7	223	-11.5	8.6			0.55	0.03	5.50		
	Oct-10	-		-		-	-			-	-	-		
	Jun-11	10.81		53	283	-15.5	0.2			1.18	0.08	6.66		
WB	Jul-09	-	10.7	-		-	-	-18.6	3.0	-	-	-	0.80	0.34
	Sep-09	-		-		-	-			-	-	-		
	Jun-10	10.5		176	406		3.3			0.42	0.10	23.20		
	Aug-10	10.91		128	358	-16.5	0.0			1.07	0.01	0.72		
	Oct-10	-		-		-	-			-	-	-		
	Jun-11	10.76		50	280	-20.7	0.9			0.91	0.21	22.74		
WHC75	Jun-11	11.2	11.2	-803	-573	-11.7		-11.7		0.76	-	-	0.76	

A.4 Raw Dissolved Organic Carbon (DOC) concentration (mg/L) and stable carbon isotope values (‰) from Chapter 2,3, Figure 3.5

				DOC Delta 13 C				DOC Concentration					
Location	Date Sampled	pH	Eh (mV)	Delta Avg	Delta STDEV	Avg Delta of all Seasons	STDEV of all seasons	OI TOC Avg (ppm)	stdev	RSD%	Avg DOC conc of all seasons (ppm)	STDEV of all seasons	RSD% of all seasons
WHB	Jul-09	7.29	223	-26.6		-27.1	0.6	0.36	0.13	35.66	0.46	0.20	43.09
	Sep-09	7.56	188	BQL				0.45	0.00	0.16			
	Jun-10	8.5	239	BQL				0.44	0.02	3.58			
	Aug-10	7.9	213	BQL				0.35	0.01	3.41			
	Oct-10	6.3	244	-27.5	0.2			0.85	0.01	1.43			
	Jun-11	7.82	182	BQL				0.30	0.01	3.91			
WHC2a	Jul-09	11.64	-867	-	-	-16.8	0.5				1.62	0.97	59.82
	Sep-09	-	-	-	-								
	Jun-10	12.5	-847	-16.3	0.9			1.93	0.16	8.25			
	Aug-10	12.4	-842	-17.2	0.6			2.67	0.11	4.29			
	Oct-10	12.37	-600	-17.0	0.0			1.55	0.03	2.01			
	Jun-11	12.36	-890	BQL				0.35	0.20	57.40			
WHC2b	Jul-09	11.62	-749	-17.4	1.8	-20.1	4.6				0.96	0.62	64.57
	Sep-09	12.2	-875	-16.3	0.3			1.84	0.08	4.56			
	Jun-10	12.63	-842	BQL				0.44	0.08	17.56			
	Aug-10	12.31	-796	-26.5	0.7			1.15	0.14	12.24			
	Oct-10	12.46	-430	-20.3	0.3			1.09	0.03	2.33			
	Jun-11	12.28	-818	BQL				0.29	0.03	11.88			
WHC2c	Jul-09	10.3	-89	-	-	-23.7	1.5	1.51	0.22	14.73	1.24	0.44	35.18
	Sep-09	13.11	-787	-23.4	0.3			0.89	0.06	6.28			
	Jun-10	12.31	-796	-22.3	0.4			1.93	0.04	1.95			
	Aug-10	12	-306	-23.0	0.1			1.37	0.11	7.72			
	Oct-10	8.77	255	-26.2	1.5			0.91	0.07	7.95			
	Jun-11	12.21	-658	-23.7	0.0			0.84	0.01	1.52			
WHC01-pool 6	Jul-09	-	-	-	-	-18.2	1.1				2.04	0.65	31.75
	Sep-09	12	-90	-17.4	0.4			1.58	0.02	1.25			
	Jun-10	12.35	-63	-	-								
	Aug-10	11.96	-85	-19.0	0.2			2.50	0.08	3.34			
	Oct-10	12.31	-79	-	-								
	Jun-11	-	-	-	-								
TLE	Jul-09	10.19	-67	-23.3		-23.3	#DIV/0!	0.36	0.25	69.62	0.16	0.13	82.12
	Sep-09	10	-71	BQL				0.12	0.05	43.20			
	Jun-10	10.5	24	BQL				0.06	0.00	3.73			
	Aug-10	11.29	-7	BQL									
	Oct-10	-	-										
	Jun-11	10.81	53	BQL				0.12	0.00	2.62			
WB	Jul-09	-	-	-	-	#DIV/0!	#DIV/0!				0.19	0.11	60.59
	Sep-09	-	-	-	-								
	Jun-10	10.5	176	BQL				0.10	0.04	39.78			
	Aug-10	10.91	128	BQL				0.32	0.14	43.71			
	Oct-10	-	-	-	-								
	Jun-11	10.76	50	BQL				0.15	0.07	43.54			
WHC75	Jun-11	11.2	-803	-10.1	0.4	-10.1		1.54	0.03	2.19	1.54		

A.2 Ion data from Chapter 2 and Figures 2.5 and 2.6 and extra Ion data from ICPMS

	Concentration (ppb)			
Sample ID	**Mg**	**Cl**	**Ca 43**	**Br**
Sep-13				
WHC-02-c	16522	12978	2087	37.32
WHC-02-c	16691	13588	2100	47.9
WHC-02-c	17215	13655	2104	43.13
WHC-01 (pool	52	457083	7879	1058.95
WHC-01 (pool	60	460188	8123	1077.51
WHC-01 (pool	51	441258	8019	1039.92
WHC-02b	592	369262	56655	843.98
WHC-02b	589	362133	55630	858.94
WHC-02b	770	369764	57708	878.79
TLE-b	869	6378	13963	24.05
TLE-b	869	6309	13690	12.57
TLE-b	855	5873	14179	13.74
Jun-14				
WHB inout 2	13305.17	7772.68	1076.03	15.39
WHC2a	604.64	403384.49	58474.56	892.52
WHC2b	1593.10	313576.33	43796.68	715.18
WHC2c	7570.45	165870.60	22516.27	373.46
WHC01 (poole	68.17	504843.83	9602.43	1141.93
PIE (1)	1503.85	93993.65	57004.49	564.74
PIE (2)	1427.78	7186.60	12916.60	8.54
TLEb	1347.30	90389.01	55993.42	563.13
TLEb	1402.21	94967.11	57369.29	579.83
WHB	9499	3507	653	<9.11
WHB	9453	3710	389	<9.41
WHB	9591	3972	503	9.21

A.6. Hydrogen and Hydrocarbon gas concentrations from Figure 2.8

		H2 Concentration				CH4 concentration				C2 concentration				C3 concentration			
Location	Date Sampled	Avg Conc (mg/L)	Stdev	RSD%	Total Avg	Avg Conc (mg/L)	Stdev	RSD%	Total Avg	Avg Conc (mg/L)	Stdev	RSD%	Total Avg	Avg Conc (mg/L)	Stdev	RSD%	Total Avg
WHC2a	Jul-09	0.47			0.63	0.16			0.29	0.02	0.00	2.89	0.04	0.03	0.00	5.34	0.04
	Jun-10	0.75	0.06	7.43		0.25	0.00	0.70		0.03	0.00	12.08		0.04	0.00	5.00	
	Aug-10	0.69	0.15	21.29		0.31	0.01	4.39		0.04	0.01	17.61		0.05	0.01	17.49	
	Oct-10	0.07	0.01	18.29		0.38	0.00	0.93		0.04	0.00	6.41		0.05	0.00	9.26	
	Jun-11	1.18	0.05	4.34		0.32	0.01	2.42									
WHC2b	Jul-09	0.05	0.01	20.80	0.55	0.04	0.00	3.75	0.17	0.01	0.00	9.16	0.02	0.01	0.00	10.64	0.03
	Sep-09	0.47	0.04	7.45		0.16	0.01	3.78		0.02	0.00	7.88		0.02	0.00	10.64	
	Jun-10	0.73	0.03	4.22		0.25	0.00	1.67		0.03	0.00	6.13		0.04	0.00	6.24	
	Aug-10	0.47	0.07	14.50		0.26	0.00	0.90		0.03	0.00	3.14		0.04	0.00	1.58	
	Oct-10	ND				0.01	0.00	9.31		BDL				BDL			
	Jun-11	1.04	0.12	11.06		0.32	0.00	1.43									
WHC01-pool 6	Sep-09	0.03	0.00	11.90	0.05	0.03	0.00	0.83	0.04	0.00	0.00	1.85	0.01	0.00	0.00	0.59	0.01
	Aug-10	ND				0.04	0.00	1.76		0.01	0.00	17.26		0.01	0.00	28.73	
	Oct-10	0.06				0.06				0.01	0.00	0.96		0.01	0.00	11.02	
WHC2c	Sep-09	0.00	0.00	0.00	0.21	0.05	0.00	0.65	0.03	0.03	0.01	29.30	0.01	0.03	0.01	27.08	0.02
	Jun-10	0.57	0.22	37.99		0.03	0.00	0.16		0.00				0.01	0.00	13.85	
	Aug-10	ND				0.01	0.00	5.50		BDL				BDL			
	Jun-11	0.07	0.01	12.98		0.03	0.00	3.08									
TLE	Jul-09	0.36			0.25												
	Sep-09	0.13	0.07	49.45													

		nC4 concentration				nC5 concentration				nC6 concentration			
Location	Date Sampled	Avg Conc (mg/L)	Stdev	RSD%	Total Avg	Avg Conc (mg/L)	Stdev	RSD%	Total Avg	Avg Conc (mg/L)	Stdev	RSD%	Total Avg
WHC2a	Jul-09	0.01	0.00	0.89	0.02	0.01	0.00	16.25	0.01	0.04	0.00	5.26	0.02
	Jun-10	0.01	0.00	8.96		0.01	0.00	19.46		0.02	0.00	18.23	
	Aug-10	0.02	0.00	23.91		0.01	0.00	22.23		0.02	0.00	23.08	
	Oct-10	0.02	0.00	7.80		0.02	0.00	3.86		0.02	0.01	27.84	
	Jun-11												
WHC2b	Jul-09	BDL			0.02	BDL			0.01	0.01	0.00	6.77	0.01
	Sep-09	0.01	0.00	2.29		0.01	0.00	18.97		0.02	0.01	47.85	
	Jun-10	0.02	0.00	5.90		0.01	0.00	14.43		BDL			
	Aug-10	0.02	0.00	3.59		0.01	0.00	8.64		0.01	0.00	21.74	
	Oct-10	BDL				BDL				BDL			
	Jun-11												
WHC01-pool 6	Sep-09	BDL			0.00	BDL			0.00	0.01	0.00	26.10	0.01
	Aug-10	BDL				BDL							
	Oct-10	0.00	0.00	7.49		0.00	0.00	9.26		0.00	0.00	8.09	
WHC2c	Sep-09	0.01	0.00	16.00	0.01	0.01	0.00	20.06	0.01	0.01	0.00	23.49	0.01
	Jun-10	BDL				BDL				0.00	0.00	12.69	
	Aug-10	BDL				BDL				BDL			
	Jun-11												

A.7. Stable carbon isotope data of hydrocarbon gases from Figure 2.8, and 2.9

	WHC2a		WHC2b	WHC2c	WHC75
Carbon #	Jun-10	Jun-11	Jun-11	Jun-11	Jun-11
C1	-27.2	-26.4	-26.4	-26.4	-20.7
C2	-29.1	-29.1	-28.9	-28.2	-28.9
C3	-30.9	-31.3	-31.1	-30.4	-30.8
iC4	-30.2	-29.9	-30.5		
nC4	-30.2	-30.5	-30.4	-30.1	-29.4
nC5	-30.2	-30.7	-30.5	<d.l	-30.9
nC6	-32.9	-32.4	-31.4	-32.9	-31.5

Error +/ 0.5 permil

A.8. Phospholipid mol% from Figures 3.1, 3.2, 3.3 and 3.4

	WHC 2a		WHC 2b		WHC2c			
	Jun-10	Jun-11	Jun-10	Aug-10	Jun-10	Aug-10	Jun-11	Jun-10
PLFA I.D.	% Moles	% Moles	% Moles	% Moles	% Moles	% Moles	% Moles	% Moles
a-15:0	0.00	2.50	4.09	0.00	2.13	3.27	2.24	2.2
i-15:0	4.10	2.73	3.81	2.42	2.11	4.73	2.06	2.1
i-16:0	0.00	1.34	0.00	0.00	1.10	1.32	0.85	1.5
i-17:0	0.00	1.03	0.00	0.00	0.86	1.00	0.61	0.8
Δ 17:0	0.00	1.41	0.00	0.00	0.97	1.12	0.76	0.8
16:1w7	12.38	15.20	17.69	7.27	14.74	12.97	17.12	14.3
18:1w4trans	0.00	0.85	0.00	0.00	1.52	0.00	0.81	1.6
18:1w9cis	10.76	14.11	13.54	36.74	20.13	23.55	17.01	21.4
18:1w9trans	8.62	4.42	6.33	12.45	5.51	6.24	4.11	5.2
16:2w6	0.00	1.94	0.00	0.00	1.31	0.00	1.81	1.1
18:2w5	0.00	0.95	0.00	0.00	1.73	3.67	1.15	1.8
18:2w6	4.02	3.48	3.79	3.55	4.52	4.26	3.86	4.2
18:3w3	0.00	3.20	0.00	0.00	2.28	1.24	3.30	2.2
18:3w6	5.42	3.34	4.38	10.13	3.17	4.46	1.82	3.3
18:4w3	0.00	2.11	0.00	0.00	1.02	0.00	1.36	0.9
20:4w6	0.00	1.49	2.40	2.02	1.68	1.32	1.05	1.7
20:5w3	0.00	8.26	3.57	5.67	4.89	2.38	9.00	4.9
22:5w6	3.67	0.91	0.00	0.00	0.80	0.84	0.65	0.7
22:6w6	0.00	1.08	0.00	0.00	0.75	0.00	0.97	0.9
14:0	5.66	3.82	4.72	2.30	3.01	2.87	3.53	3.3
15:0	0.00	0.95	0.00	0.00	0.85	0.00	0.72	0.9
16:0	19.91	15.77	16.96	7.06	14.26	16.17	18.17	14.2
17:0	0.00	0.00	0.00	0.00	0.75	1.01	0.56	0.6
18:0	10.77	3.54	7.56	5.40	3.94	4.51	2.63	3.4
20:0	5.88	1.48	4.12	3.20	1.30	1.27	0.80	1.1
22:0	4.75	1.17	3.43	1.79	0.97	0.96	0.63	0.9
24:0	4.05	1.11	3.63	0.00	0.95	0.84	0.73	0.9
Unknown	0.00	1.80	0.00	0.00	2.76	0.00	1.70	2.90

PLFA I.D.	FAME	M.W.	# Of Carbons	Calibration	Slope (m)	Intercept (b)
14:0	C15H30O2	242	15	C14	14.9316347	-9.69060749
i-15:0	C16H32O2	256	16	C15	16.04597	-11.776019
a-15:0	C16H32O2	256	16	C15	16.04597	-11.776019
15:0	C16H32O2	256	16	C15	16.04597	-11.776019
i-16:0	C17H34O2	270	17	C16	16.3464868	-13.6805684
16:0	C17H34O2	270	17	C16	16.3464868	-13.6805684
16:1w7	C17H32O2	268	17	C16	16.3464868	-13.6805684
i-17:0	C18H36O2	284	18	C17	16.6864433	-15.25174
16:1w9?	C17H32O2	268	17	C17	16.6864433	-15.25174
17:0	C18H36O2	284	18	C17	16.6864433	-15.25174
16:2w6	C17H30O2	266	17	C17	16.6864433	-15.25174
Δ 17:0	C18H34O2	282	18	C17	16.6864433	-15.25174
18:0	C19H38O2	298	19	C18	15.8805747	-15.0552301
18:1w9^{trans}	C19H36O2	296	19	C18	15.8805747	-15.0552301
18:1w9^{cis}	C19H36O2	296	19	C18	15.8805747	-15.0552301
18:1w4^{trans}	C19H36O2	296	19	C18	15.8805747	-15.0552301
18:2w5	C19H34O2	294	19	C18	15.8805747	-15.0552301
18:2w6	C19H34O2	294	19	C19	16.1125979	-15.8136731
18:3w6	C19H32O2	292	19	C19	16.1125979	-15.8136731
18:3w3	C19H32O2	292	19	C19	16.1125979	-15.8136731
20:0	C21H42O2	326	21	C20	16.779843	-12.635538
18:4w3	C19H30O2	290	19	C20	16.779843	-12.635538
20:4w6	C21H34O2	318	21	C20	16.779843	-12.635538
22:0	C23H46O2	354	23	C22	13.5374775	-11.3278734
20:5w3	C21H32O2	316	21	C22	13.5374775	-11.3278734
24:0	C25H50O2	344	23	C22	13.5374775	-11.3278734
22:5w6	C23H36O2	344	23	C22	13.5374775	-11.3278734
22:6w6	C23H34O2	342	23	C22	13.5374775	-11.3278734

A.9. Stable carbon isotope values of phospholipid fatty acids from Figure 3.1, 3.2, and 3.3

		WHC 2a June 2010						WHC2a June 2011					
PLFA I.D.	Cabon #	measured delta 13C (0)	measured delta 13C (1)	measured delta 13C (2)	Avg	corrected delta 13 C	STDEV	measured delta 13C (0)	measured delta 13C (1)	measured delta 13C (2)	Average	corrected delta 13 C	STDEV
14:0	14							-25.9	-22.9		-24.4	-22.4	2.1
i-15:0	15							-26.4	-23.6		-25.0	-23.1	2.0
a-15:0	15							-25.8	-20.7		-23.3	-21.3	3.6
16:0	16	-33.8		-34.7	-34.3	-33.1	0.6	-25.2	-24.8	-24.6	-24.9	-23.1	0.3
16:1w7	16	-32.2		-33	-32.6	-31.3	0.6	-24.3	-23.5	-23.7	-23.8	-22.0	0.4
18:0	18	-30.8	-31.7	-32	-31.5	-30.3	0.6	-29.7	-29.1		-29.4	-28.1	0.4
18:1w9^{trans}	18	-30	-30.9	-32.9	-31.3	-30.1	1.5	-26.1	-26.4	-25.7	-26.1	-24.6	0.4
18:1w9^{cis}	18	-31.6	-25.6	-30.2	-29.1	-27.8	3.1		-26.6	-26.1	-26.4	-24.9	0.4
18:1	18		-30.2	-31.2	-30.7	-29.5	0.7		-26.3	-25.9	-26.1	-24.6	0.3
18:2w6	18							-29.2	-26.8		-28.0	-26.6	1.7
18:3w6	18							-29.5	-28.7		-29.1	-27.8	0.6
18:3w3	18							-31.2			-31.2	-30.0	#DIV/0!
20:4w6	20												
20:5w3	20							-26.5	-27.5	-26.5	-26.8	-25.5	0.6
22:6w6	22												

		WHCb Aug 2010						WHCc June 2010						
PLFA I.D.	Cabon #	measured delta 13C (0)	measured delta 13C (1)	measured delta 13C (2)	Average	corrected delta 13 C	STDEV	measured delta 13C (0)	measured delta 13C (1)	measured delta 13C (2)	measured delta 13C (3)	Average	corrected delta 13 C	STDEV
14:0	14							-34.0		-33.3	-33.6	-33.6	-32.3	0.4
i-15:0	15	-28.8			-28.8	-27.4	#DIV/0!	-30.0		-27.5	-27.5	-28.3	-26.7	1.4
a-15:0	15	-28.6			-28.6	-27.2	#DIV/0!	-29.5		-27.5	-28.3	-28.4	-26.8	1.0
16:0	16	-32.8	-32.3	-32.4	-32.5	-31.4	0.3	-32.4	-33.8	-34.0	-34.1	-33.6	-32.4	0.8
16:1w7	16	-33.0	-30.1	-29.9	-31.0	-29.8	1.7	-33.6	-31.6	-31.1	-30.9	-31.8	-30.5	1.2
18:0	18	-32.8	-31.1	-31.4	-31.8	-30.8	0.9	-32.6	-31.5	-32.8	-31.8	-32.2	-31.0	0.6
18:1w9^{trans}	18	-31.6	-29	-29.0	-29.9	-28.7	1.5	-33.5	-31.4	-32.2	-32.3	-32.4	-31.2	0.9
18:1w9^{cis}	18	-30.0	-28.9	-29.3	-29.4	-28.3	0.6	-31.3	-30.4	-30.6	-30.6	-30.7	-29.5	0.4
18:1	18		-28.9	-29.3	-29.1	-27.9	0.3		-30.6	-31.1	-30.9	-30.9	-29.6	0.3
18:2w6	18								-34.4	-35.1	-35.1	-34.9	-33.9	0.4
18:3w6	18	-31.8	-32	-32.5	-32.1	-31.1	0.4	-32.7	-33.7	-33.1	-32.7	-33.1	-32.0	0.5
18:3w3	18												2.9	#DIV/0!
20:4w6	20	-31.2			-31.2	-30.3	#DIV/0!	-34.2				-34.2	-33.3	#DIV/0!
20:5w3	20	-38.0			-38.0	-37.4	#DIV/0!	-38.9	-40.7	-40.2	-39.3	-39.8	-39.1	0.8
22:6w6	22	-33.0			-33.0	-32.2	#DIV/0!	-33.3				-33.3	-32.4	#DIV/0!

		WHCb June 2010						WHC2c Aug 2010						WHC2c June 2011					
PLFA I.D.	Cabon #	measured delta 13C (0)	measured delta 13C (1)	measured delta 13C (2)	Average	corrected delta 13 C	STDEV	measured delta 13C (0)	measured delta 13C (1)	measured delta 13C (2)	Average	corrected delta 13 C	STDEV	measured delta 13C (0)	measured delta 13C (1)	measured delta 13C (2)	Average	corrected delta 13 C	STDEV
14:0	14													-26.4	-25.2	-24.7	-25.4	-23.5	0.9
i-15:0	15													-27.0	-26.8	-27.3	-27.0	-25.3	0.3
a-15:0	15													-26.2	-26	-25.2	-25.8	-24.0	0.5
16:0	16	-30.4	-32.2	-32.4	-31.7	-30.3	1.1	-32.7	-33.9	-32.7	-33.1	-32.0	0.7	-26.2	-27.1	-26.9	-26.7	-25.1	0.5
16:1w7	16	-30.4	-30.1	-29.9	-30.1	-28.7	0.3							-25.5	-25.4	-24.6	-25.2	-23.4	0.5
18:0	18	-31.8	-31.3	-31.4	-31.5	-30.3	0.3	-31.7	-31.4	-31.2	-31.4	-30.4	0.3	-30.6	-28.7	-29.1	-29.5	-28.2	1.0
18:1w9^{trans}	18	-33.0	-29.0	-29	-30.3	-29.1	2.3	-30.9	-29.7	-29.1	-29.9	-28.8	0.9	-29.3	-29.1	-29	-29.1	-27.8	0.2
18:1w9^{cis}	18	-27.5	-28.9	-29.3	-28.6	-27.2	0.9	-30.3	-29.1	-28.9	-29.4	-28.3	0.8	-27.4	-27.1	-27.5	-27.3	-25.9	0.2
18:1	18		-28.9	-29.3	-29.1	-27.8	0.3		-29.6	-29.7	-29.7	-28.5	0.1		-27.5	-27.6	-27.6	-26.1	0.1
18:2w6	18													-33.2	-31.4	-31.1	-31.9	-30.7	1.1
18:3w6	18		-32.0	-32.5	-32.3	-31.1	0.4	-32.7	-31.4	-32.7	-32.3	-31.3	0.8	-35.6	-32.6	-32.3	-33.5	-32.4	1.8
18:3w3	18														-33.9	-33.9	-33.6	-32.5	0.4
20:4w6	20							-34.2			-34.2	-33.4	#DIV/0!	-29.2					
20:5w3	20														-29	-29.2	-29.1	-27.9	0.1
22:6w6	22																		

APPENDIX B: STATISTICS

B.1 Delta 13 C of organic matter (OM) statistical tests

OM delta 13C

Location	Jun-10	Jun-11	Aug-10
WHC2a	-26.7	-25.9	-27.4
WHC2b	-27.1	-25.8	-27.6
WHC2c	-26.7	-25.6	

Normality Tests

Variable #1 (Jun-10)

Sample size	2	*Mean*	-26.8975
Standard Deviation	0.32173	*Median*	-26.8975
Skewness	0.E+0	*Kurtosis*	1.
Alternative Skewness (Fishe	#N/A	*Alternative I*	#N/A

	Test Statistic	p-level	Conclusion: (5%)
Kolmogorov-Smirnow/Lillief	0.26025	#N/A	*No evidence against norm*
Shapiro-Wilk W	1.	1.	*Accept Normality*
D'Agostino Skewness	#N/A	#N/A	*Reject Normality*
D'Agostino Kurtosis	#N/A	#N/A	*Reject Normality*
D'Agostino Omnibus	#N/A	#N/A	*Reject Normality*

Variable #2 (Aug-10)

Sample size	1	*Mean*	-27.58
Standard Deviation	#N/A	*Median*	-27.58
Skewness	#N/A	*Kurtosis*	#N/A
Alternative Skewness (Fishe	#N/A	*Alternative I*	#N/A

	Test Statistic	p-level	Conclusion: (5%)
Kolmogorov-Smirnow/Lillief	#N/A	#N/A	*No evidence against norm*
Shapiro-Wilk W	1.	1.	*Accept Normality*
D'Agostino Skewness	#N/A	#N/A	*Reject Normality*
D'Agostino Kurtosis	#N/A	#N/A	*Reject Normality*
D'Agostino Omnibus	#N/A	#N/A	*Reject Normality*

Variable #3 (Jun-11)

Sample size	2	*Mean*	-25.665
Standard Deviation	0.13435	*Median*	-25.665
Skewness	0.E+0	*Kurtosis*	1.
Alternative Skewness (Fishe	#N/A	*Alternative I*	#N/A

	Test Statistic	p-level	Conclusion: (5%)
Kolmogorov-Smirnow/Lillief	0.26025	#N/A	*No evidence against norm*
Shapiro-Wilk W	1.	1.	*Accept Normality*
D'Agostino Skewness	#N/A	#N/A	*Reject Normality*
D'Agostino Kurtosis	#N/A	#N/A	*Reject Normality*
D'Agostino Omnibus	#N/A	#N/A	*Reject Normality*

Comparing Multiple Independent Samples

	Sample size	Sum of Ranks
WHC2a	3	12.
WHC2b	3	11.
WHC2c	2	13.

Kruskal-Wallis ANOVA

H	1.81	*N*	8
Degrees Of Freedom	2	*p-level*	0.41
H (corrected)	1.81		

Median Test

Overall Median	-26.68	*Chi-square*	2.67
p-level	0.26		

	Variable #1	*Variable #2*	*Variable #3*	*Total*
<= Median (observed)	2.	2.	0.E+0	4.
<= Median (excepted)	1.5	1.5	1.	
observed-excepted	0.5	0.5	-1.	
> Median (observed)	1.	1.	2	4.
> Median (excepted)	1.5	1.5	1.	
observed-excepted	-0.5	-0.5	1.	
Total:observed	3	3	2	8

Normality Tests

Variable #1 (WHC2a)

Sample size	3	*Mean*	-26.66
Standard Deviation	0.78	*Median*	-26.68
Skewness	0.04	*Kurtosis*	1.5
Alternative Skewness (F	0.1	*Alternative Kurtosis (Fis*	#N/A

	Test Statistics	p-level	Conclusion: (5%)
Kolmogorov-Smirnow/La	0.38	#N/A	*Suggestive evidence against normality*
Shapiro-Wilk W	0.77	0.05	*Accept Normality*
D'Agostino Skewness	#N/A	#N/A	*Reject Normality*
D'Agostino Kurtosis	#N/A	#N/A	*Reject Normality*
D'Agostino Omnibus	#N/A	#N/A	*Reject Normality*

Variable #2 (WHC2b)

Sample size	3	*Mean*	-26.82
Standard Deviation	0.95	*Median*	-27.13
Skewness	0.53	*Kurtosis*	1.5
Alternative Skewness (F	1.29	*Alternative Kurtosis (Fis*	#N/A

	Test Statistics	p-level	Conclusion: (5%)
Kolmogorov-Smirnow/La	0.32	#N/A	*No evidence against normality*
Shapiro-Wilk W	0.88	0.33	*Accept Normality*
D'Agostino Skewness	#N/A	#N/A	*Reject Normality*
D'Agostino Kurtosis	#N/A	#N/A	*Reject Normality*
D'Agostino Omnibus	#N/A	#N/A	*Reject Normality*

Variable #3 (WHC2c)

Sample size	2	*Mean*	-26.12
Standard Deviation	0.78	*Median*	-26.12
Skewness	0.E+0	*Kurtosis*	1.
Alternative Skewness (F	#N/A	*Alternative Kurtosis (Fis*	#N/A

	Test Statistics	p-level	Conclusion: (5%)
Kolmogorov-Smirnow/La	0.26	#N/A	*No evidence against normality*
Shapiro-Wilk W	1.	1.	*Accept Normality*
D'Agostino Skewness	#N/A	#N/A	*Reject Normality*
D'Agostino Kurtosis	#N/A	#N/A	*Reject Normality*
D'Agostino Omnibus	#N/A	#N/A	*Reject Normality*

Comparing Multiple Independent Samples

	Sample size	Sum of Ranks
10-Jun	3	12.
11-Jun	3	21.
10-Aug	2	3.

Kruskal-Wallis ANOVA

H	6.25	*N*	8
Degrees Of Freed	2	*p-level*	0.04
H (corrected)	6.25		

Median Test

Overall Median	-26.68	*Chi-square*	5.33
p-level	0.07		

	Variable #1	*Variable #2*	*Variable #3*
<= Median (obs	2.	0.E+0	2.
<= Median (exc	1.5	1.5	1.
observed-excepte	0.5	-1.5	1.
> Median (obser	1.	3.	0.E+0
> Median (excep	1.5	1.5	1.
observed-excepte	-0.5	1.5	-1.
Total:observed	3	3	2

B.2. C:N ratios on Organic Matter statistical tests

Location	OM C:N Jun-10	Aug-10	Jun-11
WHC2a	16	16	12
WHC2b	14	15	12
WHC2c	14		12

Normality Tests

Variable #1 (Jun-10)

Sample size	2	*Mean*	13.81715
Standard Deviation	0.08181	*Median*	13.81715
Skewness	0.E+0	*Kurtosis*	1.
Alternative Skewness (Fisher	#N/A	*Alternative I*	#N/A

	Test Statistic	p-level	Conclusion: (5%)
Kolmogorov-Smirnow/Lilliefc	0.26025	#N/A	*No evidence against norm*
Shapiro-Wilk W	1.	1.	*Accept Normality*
D'Agostino Skewness	#N/A	#N/A	*Reject Normality*
D'Agostino Kurtosis	#N/A	#N/A	*Reject Normality*
D'Agostino Omnibus	#N/A	#N/A	*Reject Normality*

Variable #2 (Aug-10)

Sample size	1	*Mean*	15.43956
Standard Deviation	#N/A	*Median*	15.43956
Skewness	#N/A	*Kurtosis*	#N/A
Alternative Skewness (Fisher	#N/A	*Alternative I*	#N/A

	Test Statistic	p-level	Conclusion: (5%)
Kolmogorov-Smirnow/Lilliefc	#N/A	#N/A	*No evidence against norm*
Shapiro-Wilk W	1.	1.	*Accept Normality*
D'Agostino Skewness	#N/A	#N/A	*Reject Normality*
D'Agostino Kurtosis	#N/A	#N/A	*Reject Normality*
D'Agostino Omnibus	#N/A	#N/A	*Reject Normality*

Variable #3 (Jun-11)

Sample size	2	*Mean*	12.03979
Standard Deviation	0.24745	*Median*	12.03979
Skewness	0.E+0	*Kurtosis*	1.
Alternative Skewness (Fisher	#N/A	*Alternative I*	#N/A

	Test Statistic	p-level	Conclusion: (5%)
Kolmogorov-Smirnow/Lilliefc	0.26025	#N/A	*No evidence against norm*
Shapiro-Wilk W	1.	1.	*Accept Normality*
D'Agostino Skewness	#N/A	#N/A	*Reject Normality*
D'Agostino Kurtosis	#N/A	#N/A	*Reject Normality*
D'Agostino Omnibus	#N/A	#N/A	*Reject Normality*

Normality Tests

Variable #1 (WHC2a)

Sample size	3	*Mean*	14.67891
Standard De	2.07054	*Median*	15.52166
Skewness	-0.62387	*Kurtosis*	1.5
Alternative S	-1.52816	*Alternative I*	#N/A

	Test Statistic	p-level	Conclusion: (5%)
Kolmogorov	0.23199	#N/A	*No evidence against normality*
Shapiro-Wil	0.87575	0.31201	*Accept Normality*
D'Agostino S	#N/A	#N/A	*Reject Normality*
D'Agostino I	#N/A	#N/A	*Reject Normality*
D'Agostino (	#N/A	#N/A	*Reject Normality*

Variable #2 (WHC2b)

Sample size	3	*Mean*	13.84311
Standard De	1.61263	*Median*	13.875
Skewness	-0.03631	*Kurtosis*	1.5
Alternative S	-0.08895	*Alternative I*	#N/A

	Test Statistic	p-level	Conclusion: (5%)
Kolmogorov	0.17702	#N/A	*No evidence against normality*
Shapiro-Wil	0.99971	0.96729	*Accept Normality*
D'Agostino S	#N/A	#N/A	*Reject Normality*
D'Agostino I	#N/A	#N/A	*Reject Normality*
D'Agostino (	#N/A	#N/A	*Reject Normality*

Variable #3 (WHC2c)

Sample size	2	*Mean*	12.81205
Standard De	1.3396	*Median*	12.81205
Skewness	0.E+0	*Kurtosis*	1
Alternative S	#N/A	*Alternative I*	#N/A

	Test Statistic	p-level	Conclusion: (5%)
Kolmogorov	0.26025	#N/A	*No evidence against normality*
Shapiro-Wil	1.	1.	*Accept Normality*
D'Agostino S	#N/A	#N/A	*Reject Normality*
D'Agostino I	#N/A	#N/A	*Reject Normality*
D'Agostino (	#N/A	#N/A	*Reject Normality*

Comparing Multiple Independent Samples

	Sample size	Sum of Ranks
WHC2a	3	18.
WHC2b	3	13.
WHC2c	2	5.

Kruskal-Wallis ANOVA

H	2.47	*N*	8
Degrees Of Freedom	2	*p-level*	0.29
H (corrected)	2.47		

Median Test

Overall Median	13.82	*Chi-square*	2.67
p-level	0.26		

	Variable #1	*Variable #2*	*Variable #3*	*Total*
<= Median (observed)	1.	1.	2.	4.
<= Median (excepted)	1.5	1.5	1.	
observed-excepted	-0.5	-0.5	1.	
> Median (observed)	2.	2.	0.E+0	4.
> Median (excepted)	1.5	1.5	1.	
observed-excepted	0.5	0.5	-1.	
Total:observed	3	3	2	8

Comparing Multiple Independent Samples

	Sample size	Sum of Ranks
10-Jun	3	17
10-Aug	2	13.
11-Jun	3	6.

Kruskal-Wallis ANOVA

H	5.14	*N*	8
Degrees Of	2	*p-level*	0.08
H (correcte	5.14		

Median Test

Overall Mea	13.82	*Chi-square*	5.33
p-level	0.07		

	Variable #1	*Variable #2*	*Variable #3*	*Total*
<= Median	1.	0.E+0	3.	4.
<= Median	1.5	1.	1.5	
observed-ex	-0.5	-1.	1.5	
> Median (o	2.	2.	0.E+0	4.
> Median (e	1.5	1.	1.5	
observed-ex	0.5	1.	-1.5	
Total:observ	3	2	3	8

B.3. Dissolved organic matter concetration statistical tests

	Avg DOC conc ug/L		
Location	**Jun-10**	**Aug-10**	**Jun-11**
WHC2a	1.93	2.67	0.35
WHC2b	0.44	1.09	0.29
WHC2c	1.93	1.37	0.84
WHB	0.44	0.35	0.30

Normality Tests

Variable #1 (jun-10)

Sample size	3	*Mean*	1.43206
Standard Deviation	0.86117	*Median*	1.9285
Skewness	-0.7071	*Kurtosis*	1.5
Alternative Skewness (Fish	-1.73204	*Alternative I*	#N/A

	Test Statistic	p-level	Conclusion: (5%)
Kolmogorov-Smirnov/Lilli	0.28156	#N/A	*No evidence against norm*
Shapiro-Wilk W	0.75075	0.00166	*Reject Normality*
D'Agostino Skewness	#N/A	#N/A	*Reject Normality*
D'Agostino Kurtosis	#N/A	#N/A	*Reject Normality*
D'Agostino Omnibus	#N/A	#N/A	*Reject Normality*

Variable #2 (aug-10)

Sample size	3	*Mean*	1.71289
Standard Deviation	0.84397	*Median*	1.37
Skewness	0.62319	*Kurtosis*	1.5
Alternative Skewness (Fish	1.52649	*Alternative I*	#N/A

	Test Statistic	p-level	Conclusion: (5%)
Kolmogorov-Smirnov/Lilli	0.3244	#N/A	*No evidence against norm*
Shapiro-Wilk W	0.8762	0.31331	*Accept Normality*
D'Agostino Skewness	#N/A	#N/A	*Reject Normality*
D'Agostino Kurtosis	#N/A	#N/A	*Reject Normality*
D'Agostino Omnibus	#N/A	#N/A	*Reject Normality*

Variable #3 (Jun-11)

Sample size	3	*Mean*	0.49389
Standard Deviation	0.30091	*Median*	0.34733
Skewness	0.68251	*Kurtosis*	1.5
Alternative Skewness (Fish	1.6718	*Alternative I*	#N/A

	Test Statistic	p-level	Conclusion: (5%)
Kolmogorov-Smirnov/Lilli	0.35355	#N/A	*Little evidence against no*
Shapiro-Wilk W	0.82209	0.16841	*Accept Normality*
D'Agostino Skewness	#N/A	#N/A	*Reject Normality*
D'Agostino Kurtosis	#N/A	#N/A	*Reject Normality*
D'Agostino Omnibus	#N/A	#N/A	*Reject Normality*

Normality Tests

Variable #1 (WHB)

Sample size	3	*Mean*	0.36
Standard De	0.07	*Median*	0.35
Skewness	0.26	*Kurtosis*	1.5
Alternative S	0.64	*Alternative I*	#N/A

	Test Statistic	p-level	Conclusion: (5%)
Kolmogorov	0.22	#N/A	*No evidence against normality*
Shapiro-Will	0.98	0.76	*Accept Normality*
D'Agostino S	#N/A	#N/A	*Reject Normality*
D'Agostino I	#N/A	#N/A	*Reject Normality*
D'Agostino C	#N/A	#N/A	*Reject Normality*

Variable #2 (WHC2a)

Sample size	3	*Mean*	1.65
Standard De	1.19	*Median*	1.93
Skewness	-0.41	*Kurtosis*	1.5
Alternative S	-1.	*Alternative I*	#N/A

	Test Statistic	p-level	Conclusion: (5%)
Kolmogorov	0.2	#N/A	*No evidence against normality*
Shapiro-Will	0.96	0.61	*Accept Normality*
D'Agostino S	#N/A	#N/A	*Reject Normality*
D'Agostino I	#N/A	#N/A	*Reject Normality*
D'Agostino C	#N/A	#N/A	*Reject Normality*

Variable #3 (WHC2b)

Sample size	3	*Mean*	0.61
Standard De	0.43	*Median*	0.44
Skewness	0.62	*Kurtosis*	1.5
Alternative S	1.51	*Alternative I*	#N/A

	Test Statistic	p-level	Conclusion: (5%)
Kolmogorov	0.32	#N/A	*No evidence against normality*
Shapiro-Will	0.88	0.32	*Accept Normality*
D'Agostino S	#N/A	#N/A	*Reject Normality*
D'Agostino I	#N/A	#N/A	*Reject Normality*
D'Agostino C	#N/A	#N/A	*Reject Normality*

Variable #4 (WHC2c)

Sample size	3	*Mean*	1.38
Standard De	0.55	*Median*	1.37
Skewness	0.03	*Kurtosis*	1.5
Alternative S	0.08	*Alternative I*	#N/A

	Test Statistic	p-level	Conclusion: (5%)
Kolmogorov	0.17	#N/A	*No evidence against normality*
Shapiro-Will	1.	0.97	*Accept Normality*
D'Agostino S	#N/A	#N/A	*Reject Normality*
D'Agostino I	#N/A	#N/A	*Reject Normality*
D'Agostino C	#N/A	#N/A	*Reject Normality*

B.3. Dissolved organic matter concetration statistical tests continuted

Comparing Multiple Independent Samples

Sample size	ium of Ranks	
WHB	3	11.
WHC2a	3	25.
WHC2b	3	15.
WHC2c	3	27.

Kruskal-Wallis ANOVA			
H	4.59	*N*	12
Degrees Of	3	*p-level*	0.2
H (correctea	4.59		

Median Test			
Overall Mea	0.64	*Chi-square*	6.67
p-level	0.08		

	Variable #1	*Variable #2*	*Variable #3*	*Variable #4*	*Total*
<= Median	3.	1.	2.	0.E+0	6.
<= Median	1.5	1.5	1.5	1.5	
observed-ex	1.5	-0.5	0.5	-1.5	
> Median (o	0.E+0	2.	1.	3.	6.
> Median (e	1.5	1.5	1.5	1.5	
observed-ex	-1.5	0.5	-0.5	1.5	
Total:observ	3	3	3	3	12

Comparing Multiple Independent Samples

Sample size	ium of Ranks	
10-Jun	4	32.
10-Aug	4	33.
11-Jun	4	13.

Kruskal-Wallis ANOVA			
H	4.88	*N*	12
Degrees Of	2	*p-level*	0.09
H (correctea	4.88		

Median Test			
Overall Mea	0.64	*Chi-square*	2.
p-level	0.37		

	Variable #1	*Variable #2*	*Variable #3*	*Total*
<= Median	2.	1.	3.	6.
<= Median	2.	2.	2.	
observed-ex	0.E+0	-1.	1.	
> Median (o	2.	3.	1.	6.
> Median (e	2.	2.	2.	
observed-ex	0.E+0	1.	-1.	
Total:observ	4	4	4	12

Comparing Multiple Independent Samples

Sample size	ium of Ranks	
WHC2a	3	18.
WHC2b	3	9.
WHC2c	3	18.

Kruskal-Wallis ANOVA			
H	2.4	*N*	9
Degrees Of	2	*p-level*	0.3
H (correctea	2.4		

Median Test			
Overall Mea	1.09	*Chi-square*	3.67
p-level	0.16		

	Variable #1	*Variable #2*	*Variable #3*	*Total*
<= Median	1.	3.	1.	5.
<= Median	1.5	1.5	1.5	
observed-ex	-0.5	1.5	-0.5	
> Median (o	2.	0.E+0	2.	4.
> Median (e	1.5	1.5	1.5	
observed-ex	0.5	-1.5	0.5	
Total:observ	3	3	3	9

ONLY SPRI

Comparing Multiple Independent Samples

Sample size	ium of Ranks	
10-Jun	3	18.
10-Aug	3	20.
11-Jun	3	7.

Kruskal-Wallis ANOVA			
H	4.36	*N*	9
Degrees Of	2	*p-level*	0.11
H (correctea	4.36		

Median Test			
Overall Mea	1.09	*Chi-square*	3.67
p-level	0.16		

	Variable #1	*Variable #2*	*Variable #3*	*Total*
<= Median	1.	1.	3.	5.
<= Median	1.5	1.5	1.5	
observed-ex	-0.5	-0.5	1.5	
> Median (o	2.	2.	0.E+0	4.
> Median (e	1.5	1.5	1.5	
observed-ex	0.5	0.5	-1.5	
Total:observ	3	3	3	9

B.4. Delta 13 C of organic matter concetration statistical tests

DOC Avg Delta 13C

Location	Jun-10	Aug-10	Jun-11
WHC2c	-22.3	-23.0	-23.7
WHC2a	-16.3	-17.2	
WHC2b		-20.3	

Normality Tests

Variable #1 (WHC2a)			
Sample size	2	*Mean*	-16.74
Standard Deviation	0.66	*Median*	-16.74
Skewness	0.E+0	*Kurtosis*	1.
Alternative Skewness (Fi	#N/A	*Alternative I*	#N/A

	Test Statistic	p-level	Conclusion: (5%)
Kolmogorov-Smirnov/Li	0.26	#N/A	*No evidence against norm*
Shapiro-Wilk W	1.	1.	*Accept Normality*
D'Agostino Skewness	#N/A	#N/A	*Reject Normality*
D'Agostino Kurtosis	#N/A	#N/A	*Reject Normality*
D'Agostino Omnibus	#N/A	#N/A	*Reject Normality*

Variable #2 (WHC2b)			
Sample size	1	*Mean*	-20.32
Standard Deviation	#N/A	*Median*	-20.32
Skewness	#N/A	*Kurtosis*	#N/A
Alternotive Skewness (Fi	#N/A	*Alternative I*	#N/A

	Test Statistic	p-level	Conclusion: (5%)
Kolmogorov-Smirnov/Li	#N/A	#N/A	*No evidence against norm*
Shapiro-Wilk W	1.	1.	*Accept Normality*
D'Agostino Skewness	#N/A	#N/A	*Reject Normality*
D'Agostino Kurtosis	#N/A	#N/A	*Reject Normality*
D'Agostino Omnibus	#N/A	#N/A	*Reject Normality*

Variable #3 (WHC2c)			
Sample size	3	*Mean*	-22.97
Standard Deviation	0.68	*Median*	-22.97
Skewness	-0.01	*Kurtosis*	1.5
Alternative Skewness (Fi	-0.03	*Alternative I*	#N/A

	Test Statistic	p-level	Conclusion: (5%)
Kolmogorov-Smirnov/Li	0.29	#N/A	*No evidence against norm*
Shapiro-Wilk W	0.93	0.47	*Accept Normality*
D'Agostino Skewness	#N/A	#N/A	*Reject Normality*
D'Agostino Kurtosis	#N/A	#N/A	*Reject Normality*
D'Agostino Omnibus	#N/A	#N/A	*Reject Normality*

Normality Tests

Variable #1 (Jun-10)			
Sample size	2	*Mean*	-19.28
Standard De	4.26	*Median*	-19.28
Skewness	0.E+0	*Kurtosis*	1.
Alternative S	#N/A	*Alternative I*	#N/A

	Test Statistic	p-level	Conclusion: (5%)
Kolmogorov	0.26	#N/A	*No evidence against normality*
Shapiro-Wilk	1.	1.	*Accept Normality*
D'Agostino S	#N/A	#N/A	*Reject Normality*
D'Agostino I	#N/A	#N/A	*Reject Normality*
D'Agostino (	#N/A	#N/A	*Reject Normality*

Variable #2 (Aug-10)			
Sample size	3	*Mean*	-20.17
Standard De	2.88	*Median*	-20.32
Skewness	0.1	*Kurtosis*	1.5
Alternative S	0.24	*Alternative I*	#N/A

	Test Statistic	p-level	Conclusion: (5%)
Kolmogorov	0.23	#N/A	*No evidence against normality*
Shapiro-Wilk	0.98	0.75	*Accept Normality*
D'Agostino S	#N/A	#N/A	*Reject Normality*
D'Agostino I	#N/A	#N/A	*Reject Normality*
D'Agostino (	#N/A	#N/A	*Reject Normality*

Variable #3 (Jun-11)			
Sample size	1	*Mean*	-23.65
Standard De	#N/A	*Median*	-23.65
Skewness	#N/A	*Kurtosis*	#N/A
Alternative S	#N/A	*Alternative I*	#N/A

	Test Statistic	p-level	Conclusion: (5%)
Kolmogorov	#N/A	#N/A	*No evidence against normality*
Shapiro-Wilk	1.	1.	*Accept Normality*
D'Agostino S	#N/A	#N/A	*Reject Normality*
D'Agostino I	#N/A	#N/A	*Reject Normality*
D'Agostino (	#N/A	#N/A	*Reject Normality*

Comparing Multiple Independent Samples

	Sample size	Sum of Ranks
WHC2a	2	11.
WHC2b	1	4.
WHC2c	3	6.

Kruskal-Wallis ANOVA			
H	4.29	*N*	6
Degrees Of Freedom	2	*p-level*	0.12
H (corrected)	4.29		

Comparing Multiple Independent Samples (springs only)

	Sample size	Sum of Ranks
10-Jun	2	9.
10-Aug	3	11.
11-Jun	1	1.

Kruskal-Wallis ANOVA			
H	2.38	*N*	6
Degrees Of	2	*p-level*	0.3
H (correcte	2.38		

Median Test			
Overall Median	-21.31	*Chi-square*	6.
p-level	0.05		

	Variable #1	*Variable #2*	*Variable #3*	*Total*
<= Median (observed)	0.E+0	0.E+0	3.	3.
<= Median (excepted)	1.	0.5	1.5	
observed-excepted	-1	-0.5	1.5	
> Median (observed)	2.	1.	0.E+0	3
> Median (excepted)	1	0.5	1.5	
observed-excepted	1.	0.5	-1.5	
Total:observed	2	1	3	6

Median Test			
Overall Mea	-21.31	*Chi-square*	1.33
p-level	0.51		

	Variable #1	*Variable #2*	*Variable #3*	*Total*
<= Median	1.	1.	1.	3.
<= Median	1.	1.5	0.5	
observed-ex	0.E+0	-0.5	0.5	
> Median (o	1.	2.	0.E+0	3.
> Median (e	1.	1.5	0.5	
observed-ex	0.E+0	0.5	-0.5	
Total:observ	2	3	1	6

B.5. Total inorganic matter concetration statistical tests

	Av. TIC conc (ug/L)		
Location	**Jun-10**	**Aug-10**	**Jun-11**
WHC2a	0.39	1.17	1.13
WHC2b	1.73	2.16	1.2
WHC2c	11.75	14.7	13.5
WHB	7.47	10.36	7.1

Normality Tests

Variable #1 (Jun-10)

Sample size	3	*Mean*	4.62333
Standard Deviation	6.20813	*Median*	1.73
Skewness	0.67023	*Kurtosis*	1.5
Alternative Skewness (Fish	1.64171	*Alternative I*	#N/A

	Test Statistic	p-level	Conclusion: (5%)
Kolmogorov-Smirnov/Lillie	0.34608	#N/A	*No evidence against norm*
Shapiro-Wilk W	0.83709	0.20652	*Accept Normality*
D'Agostino Skewness	#N/A	#N/A	*Reject Normality*
D'Agostino Kurtosis	#N/A	#N/A	*Reject Normality*
D'Agostino Omnibus	#N/A	#N/A	*Reject Normality*

Variable #2 (Aug-10)

Sample size	3	*Mean*	6.01111
Standard Deviation	7.54095	*Median*	2.16
Skewness	0.69351	*Kurtosis*	1.5
Alternative Skewness (Fish	1.69875	*Alternative I*	#N/A

	Test Statistic	p-level	Conclusion: (5%)
Kolmogorov-Smirnov/Lillie	0.36188	#N/A	*Little evidence against no*
Shapiro-Wilk W	0.80439	0.12503	*Accept Normality*
D'Agostino Skewness	#N/A	#N/A	*Reject Normality*
D'Agostino Kurtosis	#N/A	#N/A	*Reject Normality*
D'Agostino Omnibus	#N/A	#N/A	*Reject Normality*

Variable #3 (june-11)

Sample size	3	*Mean*	5.28733
Standard Deviation	7.11256	*Median*	1.232
Skewness	0.70694	*Kurtosis*	1.5
Alternative Skewness (Fish	1.73165	*Alternative I*	#N/A

	Test Statistic	p-level	Conclusion: (5%)
Kolmogorov-Smirnov/Lillie	0.38238	#N/A	*Suggestive evidence agai*
Shapiro-Wilk W	0.75618	0.01369	*Reject Normality*
D'Agostino Skewness	#N/A	#N/A	*Reject Normality*
D'Agostino Kurtosis	#N/A	#N/A	*Reject Normality*
D'Agostino Omnibus	#N/A	#N/A	*Reject Normality*

Normality Tests

Variable #1 (WHB)

Sample size	3	*Mean*	8.32
Standard De	1.77	*Median*	7.47
Skewness	0.68	*Kurtosis*	1.5
Alternative S	1.66	*Alternative I*	#N/A

	Test Statistic	p-level	Conclusion: (5%)
Kolmogorov	0.35	#N/A	*Little evidence against norm*
Shapiro-Will	0.83	0.18	*Accept Normality*
D'Agostino S	#N/A	#N/A	*Reject Normality*
D'Agostino I	#N/A	#N/A	*Reject Normality*
D'Agostino (	#N/A	#N/A	*Reject Normality*

Variable #2 (WHC2a)

Sample size	3	*Mean*	0.9
Standard De	0.44	*Median*	1.13
Skewness	-0.7	*Kurtosis*	1.5
Alternative S	-1.71	*Alternative I*	#N/A

	Test Statistic	p-level	Conclusion: (5%)
Kolmogorov	0.27	#N/A	*No evidence against normali*
Shapiro-Will	0.79	0.09	*Accept Normality*
D'Agostino S	#N/A	#N/A	*Reject Normality*
D'Agostino I	#N/A	#N/A	*Reject Normality*
D'Agostino (	#N/A	#N/A	*Reject Normality*

Variable #3 (WHC2b)

Sample size	3	*Mean*	1.71
Standard De	0.46	*Median*	1.73
Skewness	-0.09	*Kurtosis*	1.5
Alternative S	-0.22	*Alternative I*	#N/A

	Test Statistic	p-level	Conclusion: (5%)
Kolmogorov	0.18	#N/A	*No evidence against normali*
Shapiro-Will	1.	0.92	*Accept Normality*
D'Agostino S	#N/A	#N/A	*Reject Normality*
D'Agostino I	#N/A	#N/A	*Reject Normality*
D'Agostino (	#N/A	#N/A	*Reject Normality*

Variable #4 (WHC2c)

Sample size	3	*Mean*	13.32
Standard De	1.48	*Median*	13.5
Skewness	-0.22	*Kurtosis*	1.5
Alternative S	-0.55	*Alternative I*	#N/A

	Test Statistic	p-level	Conclusion: (5%)
Kolmogorov	0.19	#N/A	*No evidence against normali*
Shapiro-Will	0.99	0.8	*Accept Normality*
D'Agostino S	#N/A	#N/A	*Reject Normality*
D'Agostino I	#N/A	#N/A	*Reject Normality*
D'Agostino (	#N/A	#N/A	*Reject Normality*

B.5. Total inorganic matter concetration statistical tests continued

Comparing Multiple Independent Samples		
Sample size	um of Ranks	
WHB	3	24.
WHC2a	3	6.
WHC2b	3	15.
WHC2c	3	33.

Kruskal-Wallis ANOVA			
H	10.38	N	12
Degrees Of	3	p-level	0.02
H (correctea	10.38		

Median Test			
Overall Mea	4.65	Chi-square	12.
p-level	0.01		

	Variable #1	Variable #2	Variable #3	Variable #4	Total
<= Median	0.E+0	3.	3.	0.E+0	6.
<= Median	1.5	1.5	1.5	1.5	
observed-exc	-1.5	1.5	1.5	-1.5	
> Median (o	3.	0.E+0	0.E+0	3.	6.
> Median (e	1.5	1.5	1.5	1.5	
observed-exc	1.5	-1.5	-1.5	1.5	
Total:observ	3	3	3	3	12

Comparing Multiple Independent Samples		
Sample size	um of Ranks	
WHC2a	3	6.
WHC2b	3	15.
WHC2c	3	24.

Kruskal-Wallis ANOVA			
H	7.2	N	9
Degrees Of	2	p-level	0.03
H (correctea	7.2		

Median Test			
Overall Mea	1.73	Chi-square	6.33
p-level	0.04		

	Variable #1	Variable #2	Variable #3	Total
<= Median	3.	2.	0.E+0	5.
<= Median	1.5	1.5	1.5	
observed-exc	1.5	0.5	-1.5	
> Median (o	0.E+0	1.	3.	4.
> Median (e	1.5	1.5	1.5	
observed-exc	-1.5	-0.5	1.5	
Total:observ	3	3	3	9

Comparing Multiple Independent Samples		
Sample size	um of Ranks	
10-Jun	4	24.
10-Aug	4	30.
11-Jun	4	24.

Kruskal-Wallis ANOVA			
H	0.46	N	12
Degrees Of	2	p-level	0.79
H (correctea	0.46		

Median Test			
Overall Mea	4.65	Chi-square	0.E+0
p-level	#N/A		

	Variable #1	Variable #2	Variable #3	Total
<= Median	2.	2.	2.	6.
<= Median	2.	2.	2.	
observed-exc	0.E+0	0.E+0	0.E+0	
> Median (o	2.	2.	2.	6.
> Median (e	2.	2.	2.	
observed-exc	0.E+0	0.E+0	0.E+0	
Total:observ	4	4	4	12

nparing Multiple Independent Samples (springs o		
Sample size	um of Ranks	
10-Jun	3	13.
10-Aug	3	18.
11-Jun	3	14.

Kruskal-Wallis ANOVA			
H	0.62	N	9
Degrees Of	2	p-level	0.73
H (correctea	0.62		

Median Test			
Overall Mea	1.73	Chi-square	1.
p-level	0.61		

	Variable #1	Variable #2	Variable #3	Total
<= Median	2.	1.	2.	5.
<= Median	1.5	1.5	1.5	
observed-exc	0.5	-0.5	0.5	
> Median (o	1.	2.	1.	4.
> Median (e	1.5	1.5	1.5	
observed-exc	-0.5	0.5	-0.5	
Total:observ	3	3	3	9

B.6. Delta 13 C of Total Inorganic matter statistical tests

TIC Avg delta13C

Location	Jun-10	Aug-10	Jun-11
WHC2a	-12.5	-19.2	-14.7
WHC2b	-13.0	-17.3	-17.6
WHC2c	-11.5	-12.6	-11.8
WHB	-1.1	-3.0	-2.1

Normality Tests

Variable #1 (June 10)

Sample size	3	*Mean*	-12.32889
Standard Deviation	0.72865	*Median*	-12.47
Skewness	0.34243	*Kurtosis*	1.5
Alternative Skewness (Fish	0.83879	*Alternative I*	#N/A

	Test Statistic	p-level	Conclusion: (5%)
Kolmogorov-Smirnov/Lillie	0.36133	#N/A	*Little evidence against normality*
Shapiro-Wilk W	0.8056	0.12794	*Accept Normality*
D'Agostino Skewness	#N/A	#N/A	*Reject Normality*
D'Agostino Kurtosis	#N/A	#N/A	*Reject Normality*
D'Agostino Omnibus	#N/A	#N/A	*Reject Normality*

Variable #2 (Aug-10)

Sample size	3	*Mean*	-16.38222
Standard Deviation	3.39195	*Median*	-17.26333
Skewness	0.44502	*Kurtosis*	1.5
Alternative Skewness (Fish	1.09007	*Alternative I*	#N/A

	Test Statistic	p-level	Conclusion: (5%)
Kolmogorov-Smirnov/Lillie	0.26043	#N/A	*No evidence against normality*
Shapiro-Wilk W	0.8048	0.126	*Accept Normality*
D'Agostino Skewness	#N/A	#N/A	*Reject Normality*
D'Agostino Kurtosis	#N/A	#N/A	*Reject Normality*
D'Agostino Omnibus	#N/A	#N/A	*Reject Normality*

Variable #3 (June-11)

Sample size	3	*Mean*	-14.72222
Standard Deviation	2.91003	*Median*	-14.70667
Skewness	-0.00982	*Kurtosis*	1.5
Alternative Skewness (Fish	-0.02405	*Alternative I*	#N/A

	Test Statistic	p-level	Conclusion: (5%)
Kolmogorov-Smirnov/Lillie	0.17532	#N/A	*No evidence against normality*
Shapiro-Wilk W	0.99998	0.99116	*Accept Normality*
D'Agostino Skewness	#N/A	#N/A	*Reject Normality*
D'Agostino Kurtosis	#N/A	#N/A	*Reject Normality*
D'Agostino Omnibus	#N/A	#N/A	*Reject Normality*

Normality Tests

Variable #1 (WHB)

Sample size	3	*Mean*	-2.07
Standard De	0.96	*Median*	-2.14
Skewness	0.13	*Kurtosis*	1.5
Alternative S	0.32	*Alternative Kurtosis (Fisher's)*	#N/A

	Test Statistic	p-level	Conclusion: (5%)
Kolmogorov	0.17	#N/A	*No evidence against norm*
Shapiro-Wil	1	0.99	*Accept Normality*
D'Agostino S	#N/A	#N/A	*Reject Normality*
D'Agostino I	#N/A	#N/A	*Reject Normality*
D'Agostino (	#N/A	#N/A	*Reject Normality*

Variable #2 (WHC2a)

Sample size	3	*Mean*	-15.47
Standard De	3.45	*Median*	-14.71
Skewness	-0.39	*Kurtosis*	1.5
Alternative S	-0.95	*Alternative Kurtosis (Fisher's)*	#N/A

	Test Statistic	p-level	Conclusion: (5%)
Kolmogorov	0.32	#N/A	*No evidence against norm*
Shapiro-Wil	0.89	0.35	*Accept Normality*
D'Agostino S	#N/A	#N/A	*Reject Normality*
D'Agostino I	#N/A	#N/A	*Reject Normality*
D'Agostino (	#N/A	#N/A	*Reject Normality*

Variable #3 (WHC2b)

Sample size	3	*Mean*	-15.96
Standard De	2.59	*Median*	-17.26
Skewness	0.69	*Kurtosis*	1.5
Alternative S	1.69	*Alternative Kurtosis (Fisher's)*	#N/A

	Test Statistic	p-level	Conclusion: (5%)
Kolmogorov	0.36	#N/A	*Little evidence against no*
Shapiro-Wil	0.81	0.14	*Accept Normality*
D'Agostino S	#N/A	#N/A	*Reject Normality*
D'Agostino I	#N/A	#N/A	*Reject Normality*
D'Agostino (	#N/A	#N/A	*Reject Normality*

Variable #4 (WHC2c)

Sample size	3	*Mean*	-12.
Standard De	0.57	*Median*	-11.82
Skewness	-0.52	*Kurtosis*	1.5
Alternative S	-1.27	*Alternative Kurtosis (Fisher's)*	#N/A

	Test Statistic	p-level	Conclusion: (5%)
Kolmogorov	0.21	#N/A	*No evidence against norm*
Shapiro-Wil	0.93	0.47	*Accept Normality*
D'Agostino S	#N/A	#N/A	*Reject Normality*
D'Agostino I	#N/A	#N/A	*Reject Normality*
D'Agostino (	#N/A	#N/A	*Reject Normality*

B.6. Delta 13 C of Total inorganic matter statistical tests continued

Comparing Multiple Independent Samples

Sample size	sum of Ranks
WHB	3 33.
WHC2a	3 12.
WHC2b	3 10.
WHC2c	3 23.

Kruskal-Wallis ANOVA

H	8.74	*N*	12
Degrees Of Freedom	3	*p-level*	**0.03**
H (corrected)	8.74		

Median Test

Overall Median	-12.55	*Chi-square*	6.67
p-level	0.08		

	Variable #1	*Variable #2*	*Variable #3*	*Variable #4*	*Total*
<= Median (observed)	0.E+0	2.	3.	1.	6.
<= Median (excepted)	1.5	1.5	1.5	1.5	
observed-excepted	-1.5	0.5	1.5	-0.5	
> Median (observed)	3.	1.	0.E+0	2.	6.
> Median (excepted)	1.5	1.5	1.5	1.5	
observed-excepted	1.5	-0.5	-1.5	0.5	
Total:observed	3	3	3	3	12

Comparing Multiple Independent Samples

Sample size	sum of Ranks
10-Jun	4 33
10-Aug	4 20
11-Jun	4 25.

Kruskal-Wallis ANOVA

H	1.65	*N*	12
Degrees Of Freedom	2	*p-level*	0.44
H (corrected)	1.65		

Median Test

Overall Median	-12.55	*Chi-square*	2.
p-level	0.37		

	Variable #1	*Variable #2*	*Variable #3*	*Total*
<= Median (observed)	1.	3.	2.	6.
<= Median (excepted)	2.	2.	2.	
observed-excepted	-1.	1.	0.E+0	
> Median (observed)	3.	1.	2.	6.
> Median (excepted)	2.	2.	2.	
observed-excepted	1	-1.	0.E+0	
Total:observed	4	4	4	12

Comparing Two Independent Samples (June 2010 and 2011)

Sample size #1	3	*Sample size*	3
Mann-Whitney U Test			
W1 Sum of Ranks (series	13.	*U (larger)*	2.
W2 Sum of Ranks (series	8.	*U*	7.
Mean W1	10.5	*Mean W2*	10.5
Standard Deviation W	2.29	*Multiplicity .*	0.E+0
Z	1.09	*p-level*	0.28

Kolmogorov-Smirnov Test

Maximal Difference	0.33	*p-level*	0.98

Wald-Wolfowitz Runs Test

Runs count R	6	*Z*	0.68
p-level	0.49		

Rosenbaum Criterion

Rosenbaum Q	3	*Critical valu*	#N/A

Comparing Multiple Independent Samples

Sample size	sum of Ranks
WHC2a	3 12
WHC2b	3 10
WHC2c	3 23.

Kruskal-Wallis ANOVA

H	4.36	*N*	9
Degrees Of	2	*p-level*	0.11
H (correcte	4.36		

Median Test

Overall Mea	-12.98	*Chi-square*	6.33
p-level	0.04		

	Variable #1	*Variable #2*	*Variable #3*	*Total*
<= Median	2.	3	0.E+0	5.
<= Median	1.5	1.5	1.5	
observed-ex	0.5	1.5	-1.5	
> Median (o	1.	0.E+0	3.	4.
> Median (e	1.5	1.5	1.5	
observed-ex	-0.5	-1.5	1.5	
Total:observ	3	3	3	9

Comparing Multiple Independent Samples (springs only)

Sample size	sum of Ranks
10-Jun	3 21
10-Aug	3 10
11-Jun	3 14.

Kruskal-Wallis ANOVA

H	2.76	*N*	9
Degrees Of	2	*p-level*	0.25
H (correcte	2.76		

Median Test

Overall Mea	-12.98	*Chi-square*	1
p-level	0.61		

	Variable #1	*Variable #2*	*Variable #3*	*Total*
<= Median	1.	2.	2.	5.
<= Median	1.5	1.5	1.5	
observed-ex	-0.5	0.5	0.5	
> Median (o	2.	1	1.	4.
> Median (e	1.5	1.5	1.5	
observed-ex	0.5	-0.5	-0.5	
Total:observ	3	3	3	9

B.7. Phospholipid fatty acid (PLFA) mol% statistical test

Mol%

Sampling Time	Branched	Polyunsaturated FA	Saturated (<20C)	Saturated (>20C	cyclic	Mono recalc
WHC2a June 2010	4.1	13.1	36.3	14.7	0.0	31.8
WHC2a June 2011	7.6	26.8	24.1	3.8	1.4	36.3
WHC2b June 2010	7.9	14.1	29.2	11.2	0.0	37.6
WHC2b Aug 2010	2.4	21.4	14.8	4.9	0.0	56.5
WHC2c June 2010	6.2	22.1	22.8	3.2	1.0	44.7
WHC2c Aug 2010	10.2	18.2	24.6	3.1	1.1	42.8
WHC2c June 2011	5.8	25.0	25.6	2.2	0.8	40.6

Normality Tests

Variable #1 (Branched)

Sample size	7	*Mean*	6.31
Standard Deviation	2.57	*Median*	6.2
Skewness	-0.07	*Kurtosis*	2.19
Alternative Skewness (Fish	-0.08	*Alternative Kurtosis (I*	-0.13

	Test Statistics	p-level	Conclusion: (5%)
Kolmogorov-Smirnov/Lillie,	0.13	0.98	*No evidence against normality*
Shapiro-Wilk W	0.99	0.99	*Accept Normality*
D'Agostino Skewness	#N/A	#N/A	*Reject Normality*
D'Agostino Kurtosis	0.06	0.95	*Accept Normality*
D'Agostino Omnibus	#N/A	#N/A	*Reject Normality*

Variable #2 (Polyunsaturated FA)

Sample size	7	*Mean*	20.1
Standard Deviation	5.21	*Median*	21.4
Skewness	-0.17	*Kurtosis*	1.66
Alternative Skewness (Fish	-0.22	*Alternative Kurtosis (I*	-1.42

	Test Statistics	p-level	Conclusion: (5%)
Kolmogorov-Smirnov/Lillie,	0.16	0.84	*No evidence against normality*
Shapiro-Wilk W	0.94	0.64	*Accept Normality*
D'Agostino Skewness	#N/A	#N/A	*Reject Normality*
D'Agostino Kurtosis	-0.92	0.36	*Accept Normality*
D'Agostino Omnibus	#N/A	#N/A	*Reject Normality*

Variable #3 (Saturated (<20C))

Sample size	7	*Mean*	25.35
Standard Deviation	6.52	*Median*	24.6
Skewness	0.12	*Kurtosis*	2.92
Alternative Skewness (Fish	0.16	*Alternative Kurtosis (I*	1.6

	Test Statistics	p-level	Conclusion: (5%)
Kolmogorov-Smirnov/Lillie,	0.2	0.55	*No evidence against normality*
Shapiro-Wilk W	0.95	0.72	*Accept Normality*
D'Agostino Skewness	#N/A	#N/A	*Reject Normality*
D'Agostino Kurtosis	1.06	0.29	*Accept Normality*
D'Agostino Omnibus	#N/A	#N/A	*Reject Normality*

Variable #4 (Saturated (>20C))

Sample size	7	*Mean*	6.15
Standard Devia	4.81	*Median*	3.8
Skewness	1.	*Kurtosis*	2.31
Alternative Ske	1.29	*Alternative Kur*	0.15

	Test Statistics	p-level	Conclusion: (5%)
Kolmogorov-Sn	0.32	0.03	*Sufficient evidence against norm*
Shapiro-Wilk W	0.79	0.03	*Reject Normality*
D'Agostino Ske	#N/A	#N/A	*Reject Normality*
D'Agostino Kur	0.24	0.81	*Accept Normality*
D'Agostino Om	#N/A	#N/A	*Reject Normality*

Variable #5 (cyclic)

Sample size	7	*Mean*	0.61
Standard Devia	0.6	*Median*	0.8
Skewness	-0.03	*Kurtosis*	1.32
Alternative Ske	-0.03	*Alternative Kur*	-2.23

	Test Statistics	p-level	Conclusion: (5%)
Kolmogorov-Sn	0.26	0.17	*No evidence against normality*
Shapiro-Wilk W	0.84	0.09	*Accept Normality*
D'Agostino Ske	#N/A	#N/A	*Reject Normality*
D'Agostino Kur	-1.73	0.08	*Accept Normality*
D'Agostino Om	#N/A	#N/A	*Reject Normality*

Variable #6 (Mono recalc)

Sample size	7	*Mean*	41.47
Standard Devia	7.9	*Median*	40.6
Skewness	0.85	*Kurtosis*	3.04
Alternative Ske	1.1	*Alternative Kur*	1.9

	Test Statistics	p-level	Conclusion: (5%)
Kolmogorov-Sn	0.2	0.55	*No evidence against normality*
Shapiro-Wilk W	0.93	0.57	*Accept Normality*
D'Agostino Ske	#N/A	#N/A	*Reject Normality*
D'Agostino Kur	1.2	0.23	*Accept Normality*
D'Agostino Om	#N/A	#N/A	*Reject Normality*

aring Two Independent Samples

Sample size #1	6	*Sample size #2*	6
Mann-Whitney U Test			
W1 Sum of Ranks (series 1)	40.	*U (larger)*	17.
W2 Sum of Ranks (series 2)	38.	*U*	19.
Mean W1	39.	*Mean W2*	39.
Standard Deviation W	6.24	*Multiplicity Factor*	0.E+0
Z	0.16	*p-level*	0.87
Kolmogorov-Smirnov Test			
Maximal Difference	0.17	*p-level*	1.
Wald-Wolfowitz Runs Test			
Runs count R	12	*Z*	1.36
p-level	0.17		
Rosenbaum Criterion			
Rosenbaum Q	1	*Critical value (5%)*	#N/A

Comparing Two Independent Samples (June 2010 and 2011)

Sample size #1	6	*Sample size #2*	6
Mann-Whitney U Test			
W1 Sum of Ranks (series 1)	39.	*U (larger)*	18.
W2 Sum of Ranks (series 2)	39.	*U*	18.
Mean W1	39.	*Mean W2*	39.
Standard Deviation W	6.24	*Multiplicity Factor*	0.E+0
Z	0.E+0	*p-level*	1.
Kolmogorov-Smirnov Test			
Maximal Difference	-0.33	*p-level*	0.81
Wald-Wolfowitz Runs Test			
Runs count R	12	*Z*	1.36
p-level	0.17		
Rosenbaum Criterion			
Rosenbaum Q	2	*Critical value (5%)*	#N/A

Comparing Two Independent Samples (WHC2b June '10 and '11)

Sample size #1	6	*Sample size #2*	6
Mann-Whitney U Test			
W1 Sum of Ran	37.5	*U (larger)*	19.5
W2 Sum of Ran	40.5	*U*	16.5
Mean W1	39.	*Mean W2*	39.
Standard Devia	6.24	*Multiplicity Fa*	6.
Z	0.24	*p-level*	0.81
Kolmogorov-Smirnov Test			
Maximal Differ	-0.33	*p-level*	0.81
Wald-Wolfowitz Runs Test			
Runs count R	11	*Z*	1.06
p-level	0.29		
Rosenbaum Criterion			
Rosenbaum Q	1	*Critical value (.*	#N/A

B.9. Phospholipid fatty acid (PLFA) delta 13C statistical test

		delta 13 C FA				
		Bacteria (n.s)	Gm -ve	Fungi	Gm +ve	ME. algal
Jun-10	WHC2c	-31.9	-30.4	-32.9	-26.8	-39.1
Aug-10	WHC2b	-31.1	-28.9	-31.1	-27.4	-37.4
Jun-11	WHC2a	-24.5	-23.8	-27.2	-22.2	-27.8
Jun-11	WHC2c	-25.6	-25.7	-31.6	-24.7	-30.2
Jun-10	WHC2b	-30.3	-28.3	-31.1		
Aug-10	WHC2c	-31.2	-28.5	-31.3		
Jun-10	WHC2a	-31.7	-29.7			

Normality Tests

Variable #1 (Bacteria (n.s))

Sample size	7	*Mean*	-29.48
Standard Deviation	3.08	*Median*	-31.08
Skewness	0.9	*Kurtosis*	1.96
Alternative Skewness (Fisher's)	1.16	*Alternative Kur*	-0.69

Test Statistics		p-level	'onclusion: (5%)
Kolmogorov-Smirnov/Lilliefor	0.34	0.01	*Strong evidence against normal*
Shapiro-Wilk W	0.66	0.	*Reject Normality*
D'Agostino Skewness	#N/A	#N/A	*Reject Normality*
D'Agostino Kurtosis	-0.33	0.74	*Accept Normality*
D'Agostino Omnibus	#N/A	#N/A	*Reject Normality*

Variable #2 (Gm -ve)

Sample size	7	*Mean*	-27.93
Standard Deviation	2.33	*Median*	-28.54
Skewness	0.81	*Kurtosis*	2.34
Alternative Skewness (Fisher's)	1.06	*Alternative Kur*	0.22

Test Statistics		p-level	'onclusion: (5%)
Kolmogorov-Smirnov/Lilliefor	0.28	0.09	*Suggestive evidence against nor*
Shapiro-Wilk W	0.89	0.29	*Accept Normality*
D'Agostino Skewness	#N/A	#N/A	*Reject Normality*
D'Agostino Kurtosis	0.29	0.77	*Accept Normality*
D'Agostino Omnibus	#N/A	#N/A	*Reject Normality*

Variable #3 (Fungi)

Sample size	6	*Mean*	-30.87
Standard Deviation	1.92	*Median*	-31.19
Skewness	1.24	*Kurtosis*	3.5
Alternative Skewness (Fisher's)	1.7	*Alternative Kur*	3.97

Test Statistics		p-level	'onclusion: (5%)
Kolmogorov-Smirnov/Lilliefor	0.43	0.	*Strong evidence against normality*
Shapiro-Wilk W	0.66	0.	*Reject Normality*
D'Agostino Skewness	#N/A	#N/A	*Reject Normality*
D'Agostino Kurtosis	1.97	0.05	*Reject Normality*
D'Agostino Omnibus	#N/A	#N/A	*Reject Normality*

Variable #4 (Gm +ve)

Sample size	4	*Mean*	-25.25
Standard Deviation	2.34	*Median*	-25.71
Skewness	0.46	*Kurtosis*	1.66
Alternative Skewness (Fisher's)	0.79	*Alternative Kur*	-1.09

Test Statistics		p-level	'onclusion: (5%)
Kolmogorov-Smirnov/Lilliefor	0.24	#N/A	*No evidence against normality*
Shapiro-Wilk W	0.93	0.59	*Accept Normality*
D'Agostino Skewness	#N/A	#N/A	*Reject Normality*
D'Agostino Kurtosis	#N/A	#N/A	*Reject Normality*
D'Agostino Omnibus	#N/A	#N/A	*Reject Normality*

Variable #5 (ME. algal)

Sample size	4	*Mean*	-33.63
Standard Deviation	5.49	*Median*	-33.81
Skewness	0.05	*Kurtosis*	1.19
Alternative Skewness (Fisher's)	0.09	*Alternative Kur*	-4.58

Test Statistics		p-level	'onclusion: (5%)
Kolmogorov-Smirnov/Lilliefor	0.15	#N/A	*No evidence against normality*
Shapiro-Wilk W	0.98	0.89	*Accept Normality*
D'Agostino Skewness	#N/A	#N/A	*Reject Normality*
D'Agostino Kurtosis	#N/A	#N/A	*Reject Normality*
D'Agostino Omnibus	#N/A	#N/A	*Reject Normality*

Comparing Multiple Independent Samples

	Sample size	Sum of Ranks
Bacteria (n.s)	7	91.
Gm -ve	7	128.
Fungi	6	56.
Gm +ve	4	95.
ME. algal	4	36.

Kruskal-Wallis ANOVA			
H	10.93	*N*	28
Degrees Of Fre	4	*p-level*	0.03
H (corrected)	10.93		

Median Test

Overall Media	-29.98	*Chi-square*	12.52
p-level	0.01		

	Variable #1	*Variable #2*	*Variable #3*	*Variable #4*	*Variable #5*	*Total*
<= Median (ob	5.	1.	5.	0.E+0	3.	14.
<= Median (ex	3.5	3.5	3.	2.	2.	
observed-excep	1.5	-2.5	2.	-2.	1.	
> Median (obse	2.	6.	1.	4.	1.	14.
> Median (exc	3.5	3.5	3.	2.	2.	
observed-excep	-1.5	2.5	-2.	2.	-1.	
Total:observed	7	7	6	4	4	28

Comparing Two Independent Samples(WHC2a June 2010 and 2011)

Sample size #1	3	*Sample size #2*	6

Mann-Whitney U Test

W1 Sum of Ran	6.	*U (larger)*	18.
W2 Sum of Ran	39.	*U*	0.E+0
Mean W1	15.	*Mean W2*	30.
Standard Devia	3.87	*Multiplicity Fa*	0.E+0
Z	2.32	*p-level*	0.02

Kolmogorov-Smirnov Test

Maximal Differ	-0.67	*p-level*	0.2

Wald-Wolfowitz Runs Test

Runs count R	9	*Z*	1.43
p-level	0.15		

Rosenbaum Criterion

Rosenbaum Q	9	*Critical value (*	#N/A

Comparing Two Independent Samples (WHC2c June 2010 and 2011)

Sample size #1	6	*Sample size #2*	6

Mann-Whitney U Test

W1 Sum of Ran	27.	*U (larger)*	30.
W2 Sum of Ran	51.	*U*	6.
Mean W1	39.	*Mean W2*	39.
Standard Devia	6.24	*Multiplicity Fa*	0.E+0
Z	1.92	*p-level*	0.05

Kolmogorov-Smirnov Test

Maximal Differ	-0.67	*p-level*	0.08

Wald-Wolfowitz Runs Test

Runs count R	12	*Z*	1.36
p-level	0.17		

Rosenbaum Criterion

Rosenbaum Q	7	*Critical value (*	#N/A

Comparing Two Independent Samples (WHC 2b June 2010 and 2011)

Sample size #1	6	*Sample size #2*	4

Mann-Whitney U Test

W1 Sum of Ran	30.	*U (larger)*	9.
W2 Sum of Ran	25.	*U*	15.
Mean W1	33.	*Mean W2*	22.
Standard Devia	4.69	*Multiplicity Fa*	0.E+0
Z	0.64	*p-level*	0.52

Kolmogorov-Smirnov Test

Maximal Differ	-0.42	*p-level*	0.67

Wald-Wolfowitz Runs Test

Runs count R	10	*Z*	1.3
p-level	0.19		

Rosenbaum Criterion

Rosenbaum Q	2	*Critical value (*	#N/A

B.9. Model II regression for determining relationship between fractionation of PLFA to TIC and PLFA to DOM

Time	Site	Eh (mV)	E Fa-TIC	std	E FA-DOC	std
Jun-10	WHC2a	-647	-19.5	-0.04	-15.7	-0.05
	WHC2b	-642	-17.6	-0.01		
	WHC2c	-468	-20.6	-0.01	-9.8	0.00
	WHC2b	-642	-18.4	-0.01		
	WHC2c	-468	-21.6	0.00	-10.9	0.00
	WHC2a	-647	-17.5	-0.03	-13.7	-0.05
	WHC2b	-642	-15.6	-0.01		
	WHC2c	-468	-19.1	-0.01	-8.3	0.00
	WHC2c	-468	-15.4	0.00	-4.6	0.00
	WHC2c	-468	-27.9	-0.01	-17.2	-0.01
Aug-10	WHC2a	-642	-10.0	-0.10		
	WHC2c	-106	-13.9	-0.06	-2.0	-0.01
	WHC2a	-642	-12.7	-0.03		
	WHC2c	-106	-20.0	0.00	-8.1	0.00
	WHC2a	-642	-9.3	-0.04		
	WHC2c	-106	-14.1	-0.05	-2.1	-0.01
	WHC2a	-642	-7.6	-0.03		
	WHC2c	-106	-13.0	0.00	-1.0	0.00
	WHC2a	-642	-13.3	-0.11		
	WHC2c	-106	-18.6	-0.11	-6.7	-0.04
Jun-11	WHC2b	-596	-14.1	-0.05	-11.0	0.00
	WHC2c	-458	-18.8	-0.01	-8.5	-0.01
	WHC2b	-596	-14.1	-0.06	-11.0	0.00
	WHC2c	-458	-18.9	0.00	-8.5	0.00
	WHC2b	-596	-11.9	-0.05	-8.8	0.00
	WHC2c	-458	-16.1	0.00	-5.7	0.00
	WHC2b	-596	-10.3	-0.04	-7.2	0.00
	WHC2b	-596	-20.5	-0.08	-17.4	0.00

MODEL II For graph fractionation FA-TIC vs fractionation FA-DOC for individual fatty acid groups

bacteria		**fungi**		**GM-ve**	
Beta	0.6235374	Beta	0.682726	Beta	0.7
Intercept	-12.171293	Intercept	-13.22988	Intercept	-11.2
SDBeta	0.1912034	SDBeta	0.2560787	SDBeta	0.2
SDIntercept	1.8341245	SDIntercept	2.2699	SDIntercept	1.7
Mean X Vari	-6.7013511	Mean X Vari	-6.4161582	Mean X Varia	-5.5
Mean Y Vari	-16.349836	Mean Y Vari	-17.610358	Mean Y Varia	-14.8
R	**0.585**	**R**	**0.395**	**R**	**0.516**
R^2	**0.342**	**R^2**	**0.156**	**R^2**	**0.267**

GM +ve		**algea**	
Beta	1.9	Beta	1.1945249
Intercept	-4.5	Intercept	-6.1749043
SDBeta	0.7	SDBeta	0.3021216
SDIntercept	3.2	SDIntercept	3.718801
Mean X Vari	-2.6	Mean X Vari	-8.2746889
Mean Y Vari	-9.3	Mean Y Vari	-16.059226
R	**0.516**	**R**	**0.825**
R^2	**0.266**	**R^2**	**0.680**

MODEL II For graph fractionation FA-TIC vs fractionation FA-DOC for all fatty acid groups

ALL

Beta	1.4692579
Intercept	-4.8307757
SDBeta	0.1647753
SDIntercept	1.2491088
Mean X Vari	-4.5688046
Mean Y Vari	-11.543528
R	**0.714**
R^2	**0.509**